Appendix Part 2. Precipitation-Runoff Model Development and Calibration

Figures

Tables

Appendix Part 2. Precipitation-Runoff Model Development and Calibration

By Phillip J. Zarriello

Precipitation-Runoff Model

The effects of water withdrawals and land-use change on streamflow in the Pawcatuck River Basin were simulated with the Hydrological Simulation Program-FORTRAN (Bicknell and others, 2000), hereafter referred to as HSPF. The HSPF model was chosen because its capabilities make it an appropriate management tool for the continuous simulation of hydrology and complex water-withdrawal patterns in the basin, and the model has been a successful management tool for similar basins with similar water issues in New England (Zarriello and Ries, 2000; Zarriello and Bent, 2004). The computer code for HSPF and its companion programs are public domain and freely available. In general terms, the model was developed by (1) compiling, collecting, and processing needed data; (2) creating a model structure that represents the basin; (3) calibrating the model; and (4) evaluating its performance. The calibrated model was then used to simulate alternative withdrawals and land-use change in the basin.

Functional Description of Hydrologic Simulation Program-FORTRAN (HSPF)

HSPF is a mathematical model designed to simulate the hydrology and movement of contaminants in a basin, but only the hydrologic simulation capability was developed and used in this study. Runoff from a basin is quantified by the continuous simulation of the hydrologic response to climatic and human stresses on the basis of the principle of conservation of water mass—that is, inflow equals outflow plus or minus any change in storage. In HSPF, a basin is represented by a collection of hydrologically similar areas referred to as hydrologic response units (HRUs) that drain to a network of stream or lake segments (RCHRESs). For each HRU and RCHRES, the model computes a water budget (inflows, outflows, and changes in storage) for each time step. A complete description of the processes involved in computing water budgets and the required input model variables are given in the "HSPF User's Manual" (Bicknell and others, 2000).

HRUs reflect areas of similar land use, soil, subsurface geology, and other factors deemed important in producing a similar hydrologic response to precipitation and potential evapotransipiration. HRUs are divided into pervious-area land elements (PERLNDs) and impervious-area land elements (IMPLNDs). Within these elements are zones that define storages and processes between zones. PERLNDs and IMPLNDs have zones that retain precipitation at the surface as interception storage or snowpack storage. All water that is not evaporated from the surface produces runoff from IMPLNDs, but PERLNDs allow precipitation to infiltrate into the subsurface, where storages and processes are represented by upper, lower, and groundwater zones. Processes that control the rate of infiltration and change in subsurface storage make simulation of PERLNDs considerably more complex than the water-budget calculations for IMPLNDs. Surface runoff from PERLNDs and IMPLNDs and subsurface discharge from PERLNDs are typically directed into reaches (RCHRESs); however, water can be directed elsewhere if desired.

RCHRESs are model elements that represent a length of stream channel or reservoir. The downstream end of each RCHRES is referred to as a node. Nodes are typically placed to define channel segments with similar physical properties, such as reach segments with similar slope and width, stream junctions, lakes and reservoirs, and locations of data-collection sites. Nodes can be placed at other locations where estimates of streamflow are desired, such as upstream and downstream from municipal well fields, water diversions, or points of contaminant discharge. The storage-discharge properties of a RCHRES used to route water by the kinematic-wave method are specified in the FTABLE of the model input.

The SCHEMATIC block, the NETWORK block, or both are used to represent the physical layout of the basin. The area of each IMPLND and PERLND that drains to a RCHRES is defined in this section of the model to formulate subbasins. The SCHEMATIC or NETWORK blocks are also used to define the linkage of one RCHRES to another. The MASSLINK associated with a SCHEMATIC block or the specifications of the NETWORK block control the linkage of flow components between model elements. Typically, this linkage involves routing (1) surface runoff from PERLNDs and IMPLNDs, (2) interflow and baseflow from PERLNDs to reaches, and (3) streamflow from reach to reach.

The inflows to and outflows from a stream reach are illustrated in figure A2–1. Surface runoff can discharge to a reach from impervious surfaces (SURI) and pervious surfaces (SURO). Infiltrated water can discharge to the reach through the subsurface as interflow (IFWO)—a fast-responding shallow subsurface flow, or from active groundwater (AGWO)—a slow-responding baseflow component, or, optionally, exit from an HRU as deep groundwater flow that discharges outside of the basin. Inflow to a reach can also come from upstream reaches (IVOL), direct precipitation, and other user-specified sources such as treated wastewater. Typically, one or two

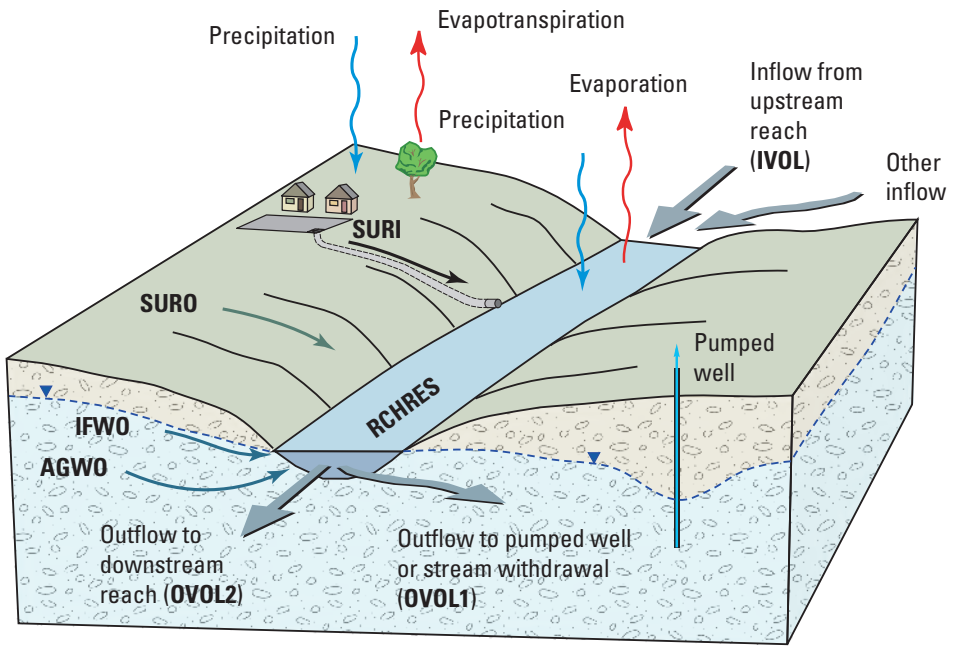

EXPLANATION

SURI–Surface runoff from impervious areas

SURO–Surface runoff from pervious areas

IFWO–Interflow (subsurface flow that responds rapidly to precipitation)

AGWO–Active groundwater flow (base flow)

RCHRES–Stream reach or reservoir segment

IVOL–Inflow volume

OVOLx–Outflow volume through individual exits (x). Reach can have up to five exits.

Figure A2–1. Simplified schematic representation of the Hydrologic Simulation Program-FORTRAN (HSPF) inflows and outflows to a stream.

outflow exits (or gates) were designated for each reach in this study as illustrated in figure A2–1 (a reach can have up to five exits). When two outflow gates are specified (OVOL 1), the volume time series of water withdrawals (OUTDGT 1) for each reach is read from the EXT SOURCES block (external sources). Specifying the first outflow gate for water withdrawals requires that the specified withdrawals are satisfied before water is routed through successive outflow gates. In the Pawcatuck River Basin model, water was routed downstream through the second outflow gate (OVOL 2) in reaches with withdrawals. In reaches with no withdrawals, a single outflow gate was generally specified.

HSPF requires two primary input files for its operation, the User Control Input (uci) file and the Watershed Data Management (WDM) file. The uci file directs the model-process algorithms and sets user-specified input variables. The WDM file is a binary file that efficiently stores large amounts of data. The three primary model elements—PERLNDs, IMPLNDs, and RCHRESs—are organized by blocks in the uci file. Within each block are modules and submodules that define model variables that control the movement of water and changes in storage between zones. Some modules are mandatory for simulations and others are optional. For example, the PERLND block requires PWATER modules to simulate hydrology, but the SNOW module is optional for simulating snowpack buildup and melt. A number of other blocks are required for administrative functions, such as controlling the operational sequence of the program, directing the model to external sources, controlling the output of time-series data, and defining the linkage between model elements. Other blocks are available for data manipulation, displaying and reporting model results, and other optional model features.

Database

The WDM file stores time-series data required for simulations or generated by the HSPF model. Precipitation and evapotranspiration are required time series; air temperature, dew-point temperature, solar radiation, and wind speed are required if snowpack buildup and melt are simulated. These data are typically entered into the WDM database by use of the software IOWDM (Lumb and others, 1990) or WDMUtil. The EXT SOURCES block (external sources) of the uci file reads data from the WDM file and model-generated time series are passed to the WDM file through the EXT TARGETS block (external targets) of the uci file. Output time series can be generated for any component in the simulation process defined in the "Time Series Catalog" section of the user's manual (for example, the active groundwater outflow from a PERLND—AGWO can be output directly), but streamflow time series are typically the primary output. Time-series data in WDM can be accessed, displayed, transformed, and plotted by use of ANNIE (Flynn and others, 1995), GenScn (Kittle and others, 1998), or WDMUtil software.

Dataset numbers (DSNs) and attribute information must exist in the WDM file to pass time-series data between the WDM file and the model. The WDM file is organized by DSNs and relational attribute information. The organization of the WDM file developed for the Pawcatuck River Basin is summarized in table A2–1. Attributes describe the data type, time step, location, and other important features of the data. The data type is defined by the constituent attribute IDCONS, which are defined for the Pawcatuck Basin in table A2–2.

Irrigation withdrawals for long-term simulations (1960–2004) were simplified by creating two WDM data sets; DSN 1003 reflects the pattern of daily irrigation on turf farms, and DSN 1002 reflects the pattern of daily irrigation on golf courses. For days in which the logistic-regression equation predicted irrigation, these distribution patterns were expressed as hourly irrigation rates defined in cubic feet per second per acre. On days of no irrigation, hourly values were set equal to zero. For each reach with irrigation withdrawals, hourly withdrawals were read into the HSPF model by multiplying the irrigated area applicable to that reach, in acres, by the irrigation rate per acre. Irrigation withdrawals were assumed to be lost to evapotranspiration.

Representation of the Basin

The physical and spatial representation of the basin in the model is defined by the combination of HRUs (PERLNDs and IMPLNDs), their contributing area to a reach, and the linkage of one reach to another. The process of defining HRUs, their linkage to reaches, and the linkage of reaches to each other often is referred to as the schematization or discretization of a basin. A geographic information system (GIS) was used to aid in this process. Basin and subbasin boundaries in the study area were obtained from available USGS, RIGIS, and MAGIC sources or digitized from 1:24,000-scale USGS topographic maps when necessary. Other digital data layers used in the discretization process included surficial geology, land use, hydrography, wetlands, and soils. The spatial data were simplified and grouped to obtain categories that were considered important to the basin hydrology. The surficial-geology data layer was simplified from seven types of material into two types on the basis of permeability and storage characteristics; (1) sand and gravel and (2) till. The land-use data layer was combined with the wetland data layer and then simplified from 56 to 10 categories; (1) forest, (2) open (3) irrigated crop, (4) turf farm, (5) golf course, (6) forested wetland, (7) nonforested wetland, (8) low-density residential, (9) moderate- to high-density residential, and (10) commercial-industrial-transportation (fig. 2–9). Preliminary calibration results indicated that an additional HRU type was needed to better define the hydrologic response in the western part of the basin. This HRU was defined on the basis of two soil categories (1) those classified as bedrock outcrops or rocky soils on steep slopes, and (2) all other soils.

Development of Hydrologic Response Units (HRUs)

HRUs were obtained by combining the simplified land-use, surficial geology and soils data layers, which resulted in 40 unique combinations of land use, surficial-geology types, and soils. Unique HRUs with areas less than about 1 percent of the basin area were grouped into the HRU with the most similar characteristics. For example, open space in commercial and industrial areas which accounted for about 1 percent of the basin area, was combined with the open space in high-density residential areas. From the 40 possible combinations of HRU types, 17 pervious-area (PERLNDs) and 2 impervious-area (IMPLNDs) HRUs were established for the Pawcatuck Basin (fig. A2–2). The area of each HRU for each subbasin was computed with a GIS macro program that intersects the HRU types with the subbasin boundaries.

Impervious Areas (IMPLNDs)

Impervious areas that drain directly to streams (hydrologically effective impervious areas) are simulated as impervious areas (IMPLNDs). Impervious areas that drain to pervious areas (hydrologically ineffective impervious areas) are incorporated into the PERLNDs representing developed areas. Initial estimates of effective impervious area were determined as a percentage of the area for various developed land-use classes (table A2–3) as assigned in the 1995 land-use cover. The land-use classes in table A2–3 are more detailed than the land-use classes used to develop the model HRUs as indicated in fig. A2–2. These percentages of effective impervious area by land-use type are similar to the values used in the Usquepaug-Queen Basin HSPF model (Zarriello and Bent, 2004) and appear to be representative of the overall responsiveness

Table A2–1. Organization and description of Data Set Numbers (DSNs) in the Watershed Data Management (WDM) database developed for the Hydrologic Simulation Program-FORTRAN (HSPF) model of the Pawcatuck River Basin, southeastern Rhode Island and southwestern Connecticut.

DSN	Purpose
	Model input
20–90	Measured or computed climate data.
101–179	Measured or estimated streamflow data.
307–380	Combined estimated 2000–04 total withdrawals from a reach (current conditions).
407–465	Combined estimated total withdrawals from a reach (1960–04) when selected withdrawals are converted from surface-water to groundwater sources.
1021–1203	Measured (1999–04) individual surface-water withdrawals or calculated streamflow depletion from groundwater withdrawals, where
1xx1–1xx3	xx, identifies the reach number, and
102x–120x	x, identifies individual withdrawal points.
2021–2801	Long-term (1960–04) estimated and measured surface-water withdrawals or calculated streamflow depletion from groundwater withdrawals, where
2xx1–2xx3	xx, identifies the reach number, and
201x–280x	x, identifies individual withdrawal points.
3321–3803	Measured (1999–04) pump rates from individual groundwater withdrawals, where
3xx1–3xx3	xx, identifies the reach number, and
332x–380x	x, identifies individual withdrawal points.
4071–4432	Calculated (1960–04) streamflow depletion rates for irrigation withdrawals converted from surface-water to groundwater sources, where
4xx1–4xx2	xx, identifies the reach number, and
407x–443x	x, identifies individual withdrawal points.
1002	Hourly (1960–04) golf-course irrigation rate determined from logistic regression.
1003	Hourly (1960–04) turf-farm irrigation rate determined from logistic regression.
	Model output
201–284	Simulated streamflow by reach (base scenario).
5001–5219	Simulated flow components by hydrologic response unit (HRU), where
5xx1–5xx9	xx, identifies the reach, and
500x–5210x	x, identifies individual flow component.
6x01–6x84	Scenario simulation results, where
6x01–6x84	x, identifies a unique scenario, and
60xx–67xx	xx, identifies the reach number.

Table A2–2. Constituent attribute (IDCONS) values used in the Watershed Data Management (WDM) system for the Hydrologic Simulation Program-FORTRAN (HSPF) model of the Pawcatuck River Basin, southeastern Rhode Island and southwestern Connecticut.

[ft^3/s, cubic feet per second; °C, degrees Celsius; °F, degrees Fahrenheit; mi/hr, miles per hour; mi/d, miles per day]

IDCONS	Purpose (units)
FLOW	Measured or simulated streamflow (ft^3/s)
	Climate data
AIRT	Measured air temperature (°C or °F)
DEWP	Measured dew-point temperature (°C or °F)
WIND	Measured wind speed (mi/hr)
TWND	Computed total wind movement (mi/hr or mi/d)
PREC	Measured precipitation (inch)
PET	Computed potential evapotranspiration (inch)
SOLR	Measured solar radiation (Langley)
	Water-use data
ExDemand	Total water withdrawal from reach (ft^3/s)
SWDL	Reported surface-water withdrawal (ft^3/s)
STRMDEPL	Calculated streamflow depletion from a pumped well (ft^3/s)
PUMP	Reported groundwater withdrawal (ft^3/s)
WSPD	Water-supply demand (ft^3/s)
	Flow or storage components from PERLNDs and IMPLNDs
PERO	Total runoff (inch)
SURO	Surface runoff (inch)
IFWO	Interflow (inch)
AGWO	Active groundwater flow (inch)
UZSN	Upper-zone storage (inch)
LZSN	Lower-zone storage (inch)
AGWET	Active groundwater evapotranspiration (inch)

of the hydrograph to precipitation and water budgets. Two IMPLND types were used in the model: (1) commercial-industrial-transportation, and (2) residential. Hydrologically, these two IMPLNDs are similar, but they were given unique HRUs for possible future water-quality applications.

About 10 percent of the basin is classified as developed (areas classified as residential, commercial, industrial, and transportation), but the effective impervious area was estimated to be about 1.6 percent of the basin area. Subbasin impervious area, as a percentage of the total subbasin area has a median value of 0.7 percent and ranged from 0 to 12 percent of subbasin areas. The highest concentrations of impervious area are found in the lower part of the Pawcatuck Basin in the City of Westerly. In several subbasins along the U.S. Interstate 95 corridor, about 5 percent of the basin area is effective impervious area. The distribution of effective impervious area is shown in figure A2–3.

Pervious Areas (PERLNDs)

Nonirrigated pervious areas (PERLNDs) in the basin are represented by five HRUs overlying sand and gravel and five HRUs of similar land use overlying till (fig. A2–2). For each of these ten HRUs, six represent open space in developed areas (PERLNDs 1, 2, 3, 11, 12, and 13), two represent open space in undeveloped areas (PERLNDs 4 and 14), and two represent forested areas (PERLNDs 5 and 15). PERLND 16 was created to represent areas where soils were classified as rock outcrop or very rocky soils with steep slopes. Other PERLNDs represent the three irrigated HRUs—golf courses, turf farms, and agriculture (PERLNDs 6, 7, and 8, respectively); open water, which represents small surface-water features not associated with a river reach (PERLND 17); and the two wetland HRUs—nonforested and forested (PERLNDs 18 and 19, respectively). Open water and wetland PERLNDs were not differentiated by underlying surficial material.

Open space in undeveloped areas (PERLNDs 4 and 14) compose about 9.7 percent of the total basin area and is about evenly divided between areas overlying sand and gravel and till (averages are 5.2 and 4.4 percent, respectively). Open space in developed areas compose about 8.1 percent of the total basin area. Open space associated with development represents the combined area of green space between buildings and the adjacent impervious area that contributes runoff to the pervious area. The additional runoff from impervious areas causes these areas to respond more rapidly to precipitation than similar undisturbed HRUs; therefore, infiltration and soil-water storage were decreased relative to undeveloped open space for similar types of surficial geology.

The dominant HRU in the Pawcatuck River Basin (fig. A2–2) is forest. Collectively, forested areas overlying sand and gravel, till, and forested wetlands (PERLNDs 5, 15, and 19, respectively) compose about 63 percent of the basin area. Forested areas mostly overlie till (PERLND 15), which composes about 36 percent of the total basin area, but also include substantial areas overlying sand and gravel (16 percent) and forested wetlands (11 percent). Forest overlying till compose as much as 68 percent of the area in headwater subbasins; this HRU is less common in the subbasins along the lower reaches of the mainstem (as little as 1 percent of the subbasin area). Forest overlying sand and gravel composes as much as 50 percent of the area in valley subbasins and generally little, if any, area in the headwater subbasins. Forested wetlands compose between 3.5 and 37 percent of subbasin areas and are generally more common in valley subbasins then in headwater subbasins.

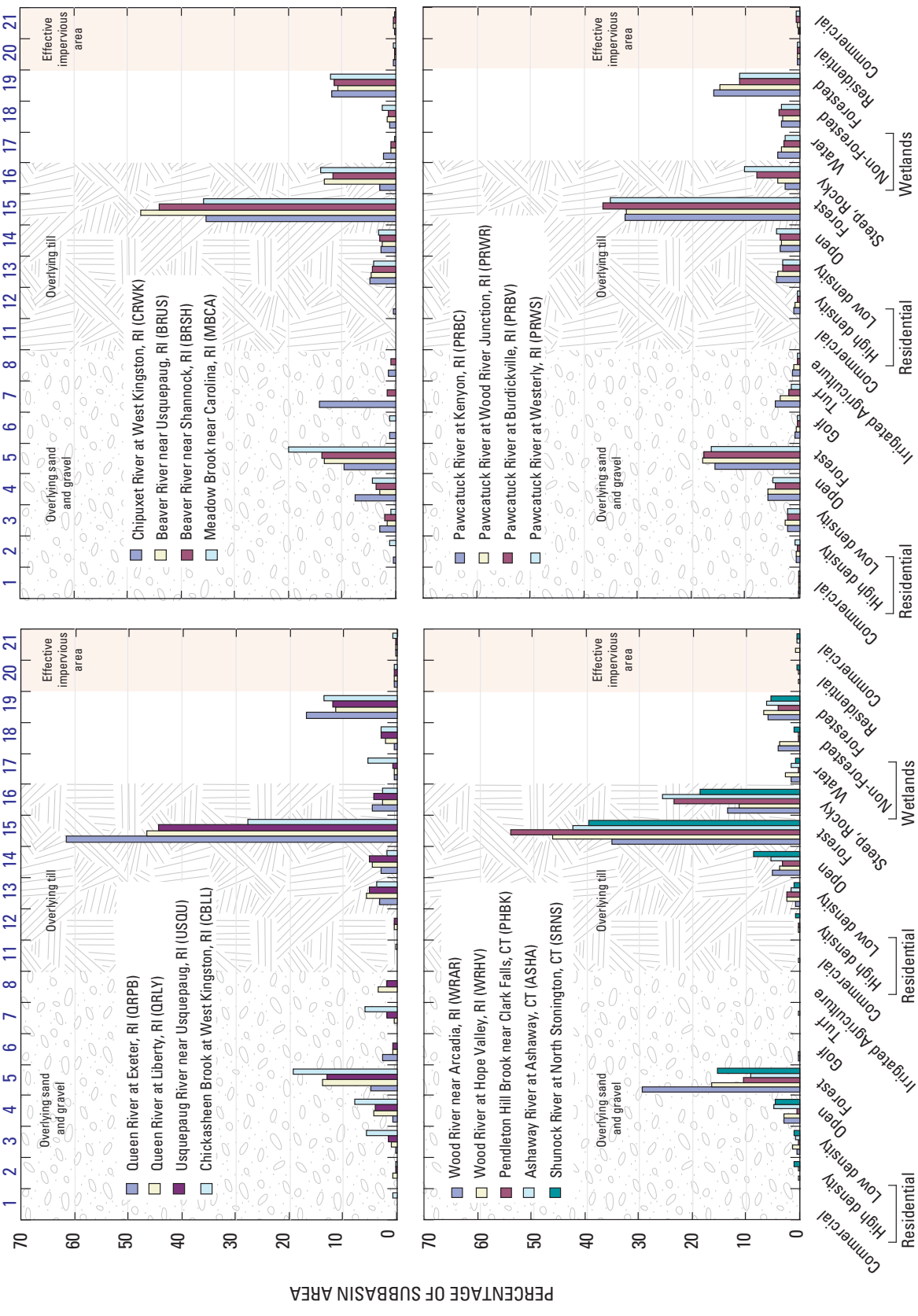

Figure A2–2. Percentages of the Hydrologic Simulation Program-FORTRAN (HSPF) model hydrologic response unit (HRU) area contributing to the continuous streamflow-gaging stations in the Pawcatuck River Basin, southwestern Rhode Island and southeastern Connecticut. (Site locations shown in figure A2–4 and described in table A2–4).)

Table A2–3. Estimated effective impervious area as a percentage of developed land-use categories used in the development of the Hydrologic Simulation Program-FORTRAN (HSPF) model of the Pawcatuck River Basin, southeastern Rhode Island and southwestern Connecticut.

[>, greater than]

Land-use classification	Total area (acres)	Percent impervious[1]	Effective impervious area	
			Total (acres)	Percent of total basin area
High-density residential lot size 0.125 or less	1,391	20	278	0.14
Medium- to high-density residential lot size >0.125 to 0.25 acre	2,262	15	339	0.18
Low- to medium-density residential lot size >0.25 to 1 acre	10,077	5	504	0.26
Low-density residential lot size >1 acre	2,535	2	51	0.03
Light urban and transportation facilities	136	10	14	0.01
Commercial, industrial, and transportation	2,402	80	1,922	0.99
Total	18,803	132	3,108	1.61

[1] Percent of total area estimated as effective imperious area.

Three HRUs were established for areas that receive irrigation (fig. A2–2)—golf courses (PERLND 6), turf farms (PERLND 7), and irrigated agriculture (PERLND 8). The 1995 digital land cover indicates 1,161 acres in the basin are classified as golf courses; however, field investigations indicated that about 29 percent (74 acres) of the 258 acres in the Queen-Usquepaug subbasin classified as golf course was not irrigated. Areas of golf courses that were not irrigated were reclassified as open space overlying sand and gravel (PERLND 4). Although the underlying surficial material is not defined for the irrigated HRUs, about 80 percent of areas classified as golf course and nearly all the area classified as turf farm or other irrigated agriculture are underlain by sand and gravel. For this reason, these HRUs were assigned similar model-variable values as the HRU representing open space overlying sand and gravel. Collectively, irrigated HRUs represent about 2.4 percent of the total basin area, which is unevenly distributed; irrigated areas can compose as much as 20 percent of a subbasin area, but most subbasins contain little or no irrigated area.

Two HRUs were established to represent wetland areas (fig. A2–2)—nonforested wetland (PERLND 18) and forested wetland (PERLND 19). Collectively, nonforested and forested wetlands compose about 14 percent of the Pawcatuck River Basin. As a percentage of the subbasin area, the total wetland area range from 4.0 to 40 percent; nonforested wetland area range from 3.5 to 37 percent, and forested wetland area range from 0 to 24 percent. The wetland HRUs were not distinguished by their underlying surficial material because this was considered secondary to the soil properties and evaporation potential of wetlands. About 68 percent of nonforested and forested wetlands overlie sand and gravel deposits, however. Area classified as open water composes about 2.8 percent of the Pawcatuck River Basin and range from 0 to 18 percent of the subbasin area.

An alternative model of the Pawcatuck River Basin was developed in which additional wetlands and open water were simulated as virtual RCHRESs. Virtual RCHRES allowed more evaporation than their corresponding HRUs because evapotranspiration was not limited to the available moisture supply from direct precipitation. To maintain a consistent model area, the area of the virtual RCHRESs was set equal to the area of wetlands and open water. The area of the virtual RCHRES was defined in its corresponding FTABLE over which direct precipitation and evaporation were applied.

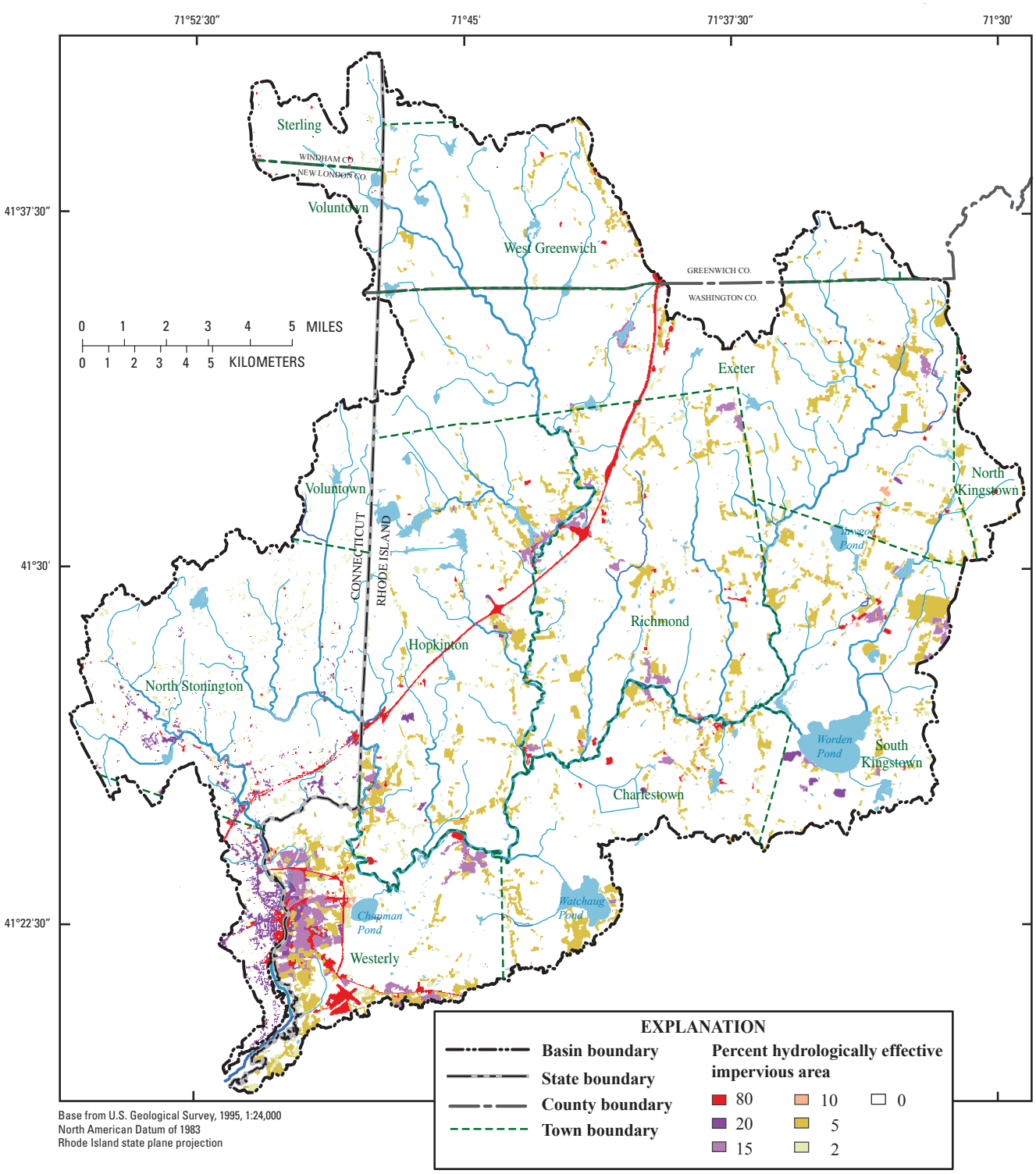

Figure A2–3. Hydrologically effective impervious area represented in the Hydrologic Simulation Program-FORTRAN (HSPF) model of the Pawcatuck River Basin, southwestern Rhode Island and southeastern Connecticut.

Stream Reaches (RCHRES)

The Pawcatuck River Basin was segmented into 70 stream reaches (fig. A2–4; table A2–4). The reach segmentation was based on hydrologic characteristics and the availability of streamflow information. In general, RCHRES are numbered in downstream order; however, the number jumps to the next nearest increment of 10 for a new major subbasin. For example, RCHRESs 1 through 20 define the Usquepaug-Queen subbasin as was done previously by Zarriello and Bent (2004); then the numbering jumps to RCHRESs 31 through 37 to define the Chipuxet and Chickasheen subbasins. RCHRESs 41 through 43 define the Beaver River subbasin, RCHRESs 51 through 66 defines the Wood River subbasin, RCHRESs 73 through 77 define the Ashaway River subbasin, and RCHRESs 81 through 83 define the Shunock River subbasin. The Pawcatuck River is defined by RCHRES 37, 46, 50, 69, 71, 72, 80, and ends at RCHRES 84, the mouth of the river.

The linkage of reaches in the SCHEMATIC block to one another, in most cases, is easily identified in figure A2–4. For example, RCHRES 1 flows into RCHRES 2, which flows into RCHRES 3. Linkages between some tributaries and the main stem are less obvious where the confluence does not coincide with a reach junction (node). In general, flow in a reach is routed into the closest node to provide the most realistic flow. If streamflow is monitored at the downstream end of a reach, but a major tributary flows into the reach just above that gage, this scheme would not include the flow from the tributary because its discharge is not accounted for by the model until the end of the next RCHRES. In this situation, the COPY feature of HSPF was used to account for all flow at the streamflow-gaging stations prior to writing simulation results to the WDM file. COPY operations were used to combine flows in RCHRESs 9 and 10; RCHRESs 34 and 374; RCHRESs 53, 54, and 55; RCHRESs 50, 65, and 66; RCHRESs 59 and 62; and RCHRESs 80 and 83 prior to outputting simulated flows. Output from these COPY operations correspond to streamflow-gaging stations at Queen River at Liberty (QRLY, 01117370), Pawcatuck River at Kenyon (PRBC, 01117430), Wood River near Arcadia (WRAR, 011178000); Pawcatuck River at Burdickville (PRBV, 01118010), Wood River at Hope Valley (WRHV, 01118000), and Pawcatuck River at Westerly (PRWS, 01118500). The italicized numbers in the column labeled "Upstream RCHRES number" in table A2–4 identify RCHRES that are directed to the next downstream RCHRES in the model, but are included in the flows output at that station through the COPY operation.

Reaches typically have one or two exit gates depending on the presence of withdrawals from the reach. In reaches that do not have simulated withdrawals, water is generally routed to the next downstream reach though a single exit gate. In the Pawcatuck River Basin HSPF model, 24 of the 70 reaches have only one outflow gate. In reaches with specified withdrawals, the first exit gate is used to satisfy the withdrawal demand and the second exit gate was used to route water to the next downstream reach. In the Pawcatuck River Basin HSPF model, 45 reaches have two outflow gates. Exceptions to this rule apply to subbasins where the groundwater divide does not coincide with the surface-water divide. This condition is known to occur in two subbasins in the Pawcatuck River Basin—the upper Queens Fort Brook (RCHRES 7) and the upper Meadow Brook (RCHRES 47). Diversions through exit gates in these subbasins were treated differently.

The upper Queens Fort Brook reach (RCHRES 7) is specialized to account for subsurface discharge from this subbasin that is reported to drain to the Hunt-Annequatucket-Pettaquamscutt (HAP) Basin (Dickerman and others, 1997; Barlow and Dickerman, 2001). In this subbasin, all active groundwater outflow, and 80 percent of interflow, is directed out of the subbasin as described by Zarriello and Bent (2004). These flow components are not routed to other areas in the model and, therefore lost from the system.

In the upper Meadow Brook subbasin (RCHRES 47), the water-table gradient reported by Allen and others (1966) indicates that groundwater in the sand and gravel deposits in the center of RCHRES 47 flows south-southeast toward the Pawcatuck River at RCHRES 46 (fig. A2–4). Initial simulations indicated that low flows were oversimulated in RCHRES 47 compared to the measured flows (MBCA, 01117600), which supports the possibility of groundwater flow toward RCHRES 46. To simulate groundwater diversion to RCHRES 46, a third outflow gate was added to RCHRES 47. The first exit gate is used for water withdrawals in RCHRES 47, the second exit gate diverts water to RCHRES 46, and the third exit gate routes water downstream to RCHRES 48. The groundwater diversion specified by the second exit gate is controlled by a second discharge column in the RCHRES 47 FTABLE. Discharges from the second exit gate were determined by minimizing the difference between measured and simulated flows in the reach and are specified as a constant 2.0 ft^3/s except at the lowest storage-to-discharge values, which are slightly less.

Alternatively, a percentage of the PERLND active groundwater flow component (AGWO) can be diverted from RCHRES 47 to RCHRES 46 (similar to the diversion of groundwater in the upper Queens Fort Brook subbasin). The diversion fluctuates and can be a large percentage of the total flow to the RCHRES at times. Specifying a diversion through a RCHRES exit gate is controlled by the values specified in the FTABLE. The fixed-rate diversion specified by the second exit gate in RCHRES 47 appears to represent the diversion of groundwater from the basin better than the variable rate diversion. In principle, a fixed-rate diversion better represents a relatively constant or uniform transmissivity and head gradient.

Subbasins in which the stream channel is largely dominated by open water are simulated with direct precipitation and evaporation to the RCHRES. These include RCHRES 34 (Worden Pond), RCHRES 35 (Yawgoo and Barber Ponds), RCHRES 62 (Locustville Pond) and RCHRES 68 (Watchaug Pond). The area of these ponds is not included in the HRU area for water (PERLND 17) in the corresponding SCHEMATIC BLOCK for these subbasins.

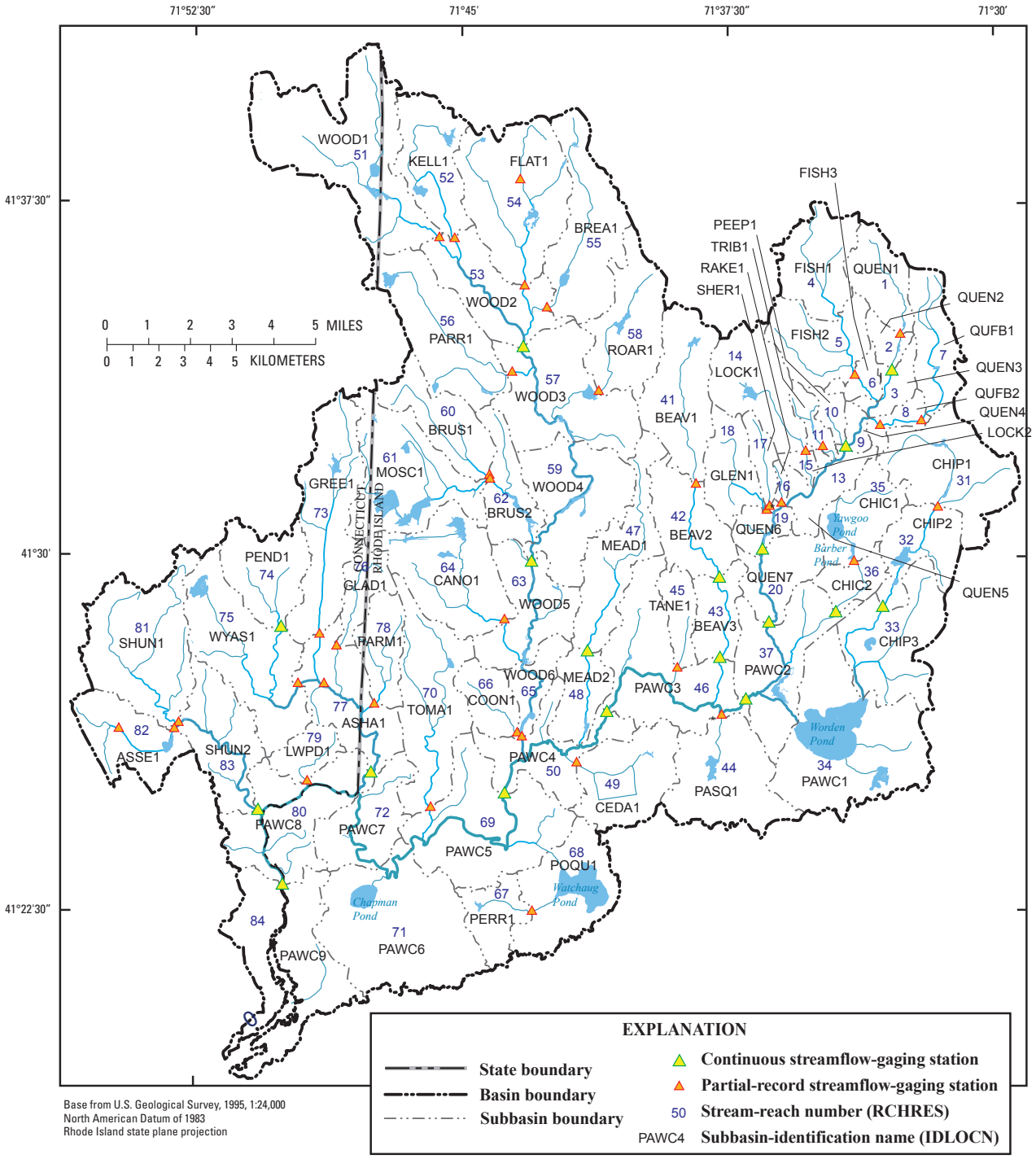

Figure A2–4. Reaches and subbasin boundaries defined for the Hydrologic Simulation Program-FORTRAN (HSPF) model of the Pawcatuck River Basin, southwestern Rhode Island and southeastern Connecticut. (Names of reaches associated with the model-reach number and name are given in table A2–4).

Table A2–4. Stream reaches (RCHRES) in the Hydrological Simulation Program-FORTRAN (HSPF) model of the Pawcatuck River Basin, southwestern Rhode Island and southeastern Connecticut.

[Site locations shown in figure A2–4; USGS stations described in table 1–3; no(s)., number(s); IDLOCN, identification attribute in the Watershed Data Management (WDM) database; mi^2, square miles; --, not applicable; upsteam reach numbers in bold-italics contribute flow to the streamflow-gaging station only, not the model reach]

Stream reach no. (RCHRES)	Subbasin IDLOCN	Stream name	IDLOCN of streamflow-gaging station (p indicates partial record)	Direct drainage area (mi^2)	Total drainage area (mi^2)	Upstream reach nos. (RCHRES)	USGS station no.
1	QUEN1	Queen River	(QECC-p)	2.77	2.77	--	01117354
2	QUEN2	Queen River	(QRPB)	0.87	3.64	1	011173545
3	QUEN3	Queen River	(QREX-p)	1.27	4.91	2	01117355
4	FISH1	Fisherville Brook		3.94	3.94	--	--
5	FISH2	Fisherville Brook	(FBEX-p)	4.02	7.97	4	01117360
6	FISH3	Fisherville Brook		0.91	8.87	5	--
7	QUFB1	Queens Fort Brook		3.19	3.19	--	--
8	QUFB2	Queens Fort Brook	(QFBK-p)	0.99	4.18	7	01117367
9	QUEN4	Queen River	(QRLY)	0.63	19.3	3,6,8,***10***	01117370
10	PEEP1	Peeper Pond Brook		0.74	0.74	--	--
11	TRIB1	Unnamed tributary	(UTLY-p)	0.95	0.95	--	01117375
13	QUEN5	Queen River		2.33	22.6	9,11	--
14	LOCK1	Locke Brook	(LBLY-p)	4.47	4.47	--	01117380
15	LOCK2	Locke Brook		0.45	4.92	14	--
16	RAKE1	Rake Factory Brook	(RFBK-p)	0.26	0.26	--	01117385
17	SHER1	Sherman Brook	(SBGR-p)	1.06	1.06	--	01117400
18	GLEN1	Glen Rock Brook	(GRGR-p)	2.80	2.80	--	01117390
19	QUEN6	Queen River	(URUS)	1.36	33.0	13,15,16,17,18	01117410
20	QUEN7	Usquepaug River	(USQU)	2.96	35.4	19	01117420
31	CHIP1	Chipuxet River	(CRWK-p)	6.35	6.35	--	01117336
32	CHIP2	Chipuxet River	(CRWK)	3.33	9.69	31	01117350
33	CHIP3	Chipuxet River		5.77	15.4	32	--
34	PAWC1	Pawcatuck/Chipuxet River		10.4	25.8	33	--
35	CHIC1	Chickasheen Brook	(CBLL-p)	3.34	3.34	--	01117421
36	CHIC2	Chickasheen Brook	(CBLL)	1.56	4.89	35	01117424
37	PAWC2	Pawcatuck River	(PRBC)	5.91	72.0	20,***34***,36	01117430
41	BEAV1	Beaver River	(BRWY-p)	5.42	5.42	--	01117465
42	BEAV2	Beaver River	(BRUS)	3.97	9.39	41	01117468
43	BEAV3	Beaver River	(BRSH)	2.36	11.8	42	01117471
44	PASQ1	Pasquiset Brook	(PBWY-p)	6.05	6.05	--	01117450
45	TANE1	Taney Brook	(TBCA-p)	1.61	1.61	--	01117480
46	PAWC3	Pawcatuck River	(PRWR)	7.62	99.1	37,43,44,45	01117500
47	MEAD1	Meadow Brook	(MBCA)	4.95	4.95	--	01117600
48	MEAD2	Meadow Brook		2.41	7.36	47	--

Table A2–4. Stream reaches (RCHRES) in the Hydrological Simulation Program-FORTRAN (HSPF) model of the Pawcatuck River Basin, southwestern Rhode Island and southeastern Connecticut.—Continued

[Site locations shown in figure A2–4; USGS stations described in table 1–3; no(s)., number(s); IDLOCN, identification attribute in the Watershed Data Management (WDM) database; mi², square miles; --, not applicable; upsteam reach numbers in bold-italics contribute flow to the streamflow-gaging station only, not the model reach]

Stream reach no. (RCHRES)	Subbasin IDLOCN	Stream name	IDLOCN of streamflow-gaging station (p indicates partial record)	Direct drainage area (mi²)	Total drainage area (mi²)	Upstream reach nos. (RCHRES)	USGS station no.
49	CEDA1	Cedar Swamp Brook	(CSBK-p)	4.82	4.82	--	01117700
50	PAWC4	Pawcatuck River	(PRBV)	4.32	205	46,48,49,***65***,***66***	01118010
51	WOOD1	Wood River	(WREH-p)	11.1	11.1	--	01117720
52	KELL1	Kelly Brook	(KBEH-p)	4.41	4.41	--	01117740
53	WOOD2	Wood River	(WRAR)	4.79	34.9	51,52,***54***,***55***	01117800
54	FLAT1	Flat River	(FRAR-p)	8.23	8.23	--	01117760
55	BREA1	Breakheart Brook	(BBAR-p)	6.41	6.41	--	01117780
56	PARR1	Parris Brook	(PBAR-p)	6.54	6.54	--	01117840
57	WOOD3	Wood River		7.60	46.5	53,56,58	--
58	ROAR1	Roaring Brook	(RBAR-p)	5.07	5.07	--	01117860
59	WOOD4	Wood River	(WRHV)	6.43	71.5	57,58,***62***	01118000
60	BRUS1	Brushy Brook	(BBHV-p)	3.66	3.66	--	01117900
61	MOSC1	Moscow Brook	(MBHV-p)	6.91	6.91	--	01117950
62	BRUS2	Brushy Brook		2.93	13.5	60,61	--
63	WOOD5	Wood River	(WRHV)	4.50	76.0	59	--
64	CANO1	Canonchet Brook	(CBHV-p)	6.59	6.59	--	01118006
65	WOOD6	Wood River	(WRAL-p)	1.77	86.4	63,64,***66***	01118009
66	COON1	Coon Hill tributary	(CHAL-p)	2.05	2.05	--	01118008
67	PERR1	Perry Healy Brook	(PHBB-p)	2.37	2.37	--	01118022
68	POQU1	Poquiant Brook		5.38	7.75	67	--
69	PAW5	Pawcatuck River		8.62	221	50,68	--
70	TOMA1	Tomaquag Brook	(TBBF-p)	6.68	6.68	--	01118055
71	PAWC6	Pawcatuck River		10.3	238	69,70	--
72	PAWC7	Pawcatuck River		3.87	242	71	--
73	GREE1	Green Fall River	(GRLG-p)	6.74	6.74	--	01118255
74	PEND1	Pendleton Hill Brook	(PHBK)	4.00	4.00	--	01118300
75	WYAS1	Wyassup Brook	(WBCF-p)	7.44	7.44	--	01118340
76	GLAD1	Glade Brook	(GBLG-p)	1.85	1.85	--	01118352
77	ASHA1	Ashaway River	(ARAS)	4.96	27.5	73,74,75,76,78	01118360
78	PARM1	Paramenter Brook	(PBHK-p)	2.50	2.50	--	01118355
79	LWPD1	Lewis Pond Outlet	(LPPH-p)	1.59	1.59	--	01118365
80	PAWC8	Pawcatuck River	(PRWS)	6.48	294	72,77,79,***83***	01118500
81	SHUN1	Shunock River	(SRPH-p)	7.80	7.80	--	01118373
82	ASSE1	Assekonk Brook	(ABNS-p)	3.89	3.89	--	01118375
83	SHUN2	Shunock River	(SRNS)	4.62	16.3	81,82	01118400
84	PAWC9	Pawcatuck River	(PRWS)	8.39	302	80	--

Hydraulic Characteristics (FTABLES)

Stage-storage-discharge characteristics (FTABLES) were developed for the outflow gate used to route water from each of the 84 reaches. The FTABLE characterizes the hydraulic properties of the reach by defining the relation between depth, storage, and discharge. This relation is usually defined by the hydraulic properties at the downstream end of the reach, but the discharge-volume relation is a function of the properties of the entire reach.

The channel-geometry analysis program (CGAP) by Regan and Schaffranek (1985) was used to define the relations among depth, surface area, and volume. A supplemental program, GENFTBL, reads the channel-geometry output from CGAP to calculate the stage-storage-discharge relation by solving Manning's equation for open-channel flow. CGAP requires data on the cross-section channel geometry; these data were obtained from discharge-measurement notes for each of the continuous and partial-record streamflow-gaging stations, and from USGS 1:24,000-scale digital topographic maps. A minimum of three cross-sections were used to define the storage-discharge relations for each reach. GENFTBL requires Manning's roughness coefficients for each cross section; these coefficients were estimated from field observations and guidelines by Coon (1998) and Arcement and Schneider (1989).

Model Calibration

The HSPF model was calibrated by comparing simulated and measured streamflows at numerous locations in the basin for the period January 1, 2000, to September 30, 2004. Streamflow is simulated by using an hourly time step and data collected at the FBWR climate station. Variables were initially assigned values similar to those used for comparable HRUs in the Usquepaug-Queen River Basin HSPF model (Zarriello and Bent, 2004). An iterative process then was used to adjust these values to minimize the difference between simulated and observed flows. Discharges measured at 17 continuous record streamflow-gaging stations (fig. A2–4; table A2–4) provided the main model-calibration points. In addition to these sites, 34 partial-record stations were used to evaluate the model fit. Hence, the model performance reflects a wide range of basin characteristics and sizes.

The model was calibrated in accordance with guidelines by Donigian and others (1984) and Lumb and others (1994). Calibration generally entailed adjusting the variable values to fit the model output to total and seasonal water budgets; then values were further adjusted to improve the model fit for daily flows while maintaining the total and seasonal water budgets. The model was calibrated by first adjusting variable values as a group for PERLNDs overlying sand and gravel, till, and wetlands. Once reasonable simulation results were obtained, further adjustments were made to variable values for PERLNDs representing different land-use types within each of these groups. Storm runoff and snowmelt were not given detailed consideration because the primary purpose of the model is to simulate the effects of withdrawals during low-flow periods. Snow rarely remains on the ground for appreciable periods; thus, the snow-buildup and melt processes were included primarily to adjust precipitation data (by a factor of 1.30) to compensate for inefficiencies in precipitation-gage measurements during periods of snow.

The model fit was examined by visual inspection of the simulated and observed hydrographs, flow-duration curves, and scatterplots, and by mathematical summary statistics provided by the GenScn utility "compare two time series". Two of the primary statistics used to evaluate the model fit were the coefficient of determination (R^2) and the model-fit efficiency (also referred to as the Nash-Sutcliffe coefficient and herein abbreviated as MFE), both of which provide a measure of the variation in the simulated value explained by the observed value. The MFE is sensitive to differences between the observed and simulated means and variances providing a more rigorous evaluation of the fit quality than the R^2, which measures the differences between mean values only (Legates and McCabe, 1999). In cases where the observed values and model residuals are normally distributed, the value of R^2 and MFE should be equal (Duncker and Melching, 1998).

Automated Parameter Estimation (PEST)

Once a reasonable empirical fit was obtained, the model-independent parameter estimation (PEST) program (Doherty, 2004) was used to refine selected parameter values and to evaluate correlated parameter sensitivities. PEST is designed to search for parameter values that minimize a user-defined objective function. An objective function is typically defined as the sum of the squared differences between simulated and observed values that, when minimized generally, improve the overall performance of the model. To accomplish this, PEST has three principal components that (1) define the parameters and the excitation (change) of those parameters used in the estimation process, (2) define the observed data that are measured against simulated values in the computation of the objective function, and (3) perform a nonlinear search by a Gauss-Marquardt-Levenberg algorithm to find the optimal parameter values being tested. Surface-water utility programs developed by Doherty (2003) facilitate input requirements for PEST, perform parameter transformations, and provide data management and filters for reading and writing data in PEST. Many of these utilities are designed specifically to facilitate the use of PEST with HSPF.

The surface-water utility TSPROC was used to build PEST control files and to process time-series data for use in the optimization process. The control file specifies (1) variable values that regulate the nonlinear-search algorithm, (2) information on the HSPF parameters to be optimized, and (3) the observation data, groups, and weights. One of the main functions of the PEST control variables is to direct the magnitude and direction of parameter change

by searching through a Jacobian matrix that PEST creates to define the change in the objective function relative to the change (excitation) of a parameter value (derivatives). PEST therefore requires at least one model run for each excitation of each parameter being optimized (two parameter-observation pairs), but the search algorithm often resorts to two model runs to define derivatives by the method of "central differences" according to criteria supplied in the control file (three parameter-observation pairs). The three-point-derivatives calculation improves the optimization performance particularly as parameter values move closer to their optimum value. PEST then uses this information to upgrade the direction and magnitude of the parameter-change vector for the next excitation iteration. PEST also has the ability to temporarily hold insensitive parameters at their current value to determine a suitable update for other parameters. PEST stops when further parameter excitations fail to produce further improvements in the objective function.

When PEST is run the number of model runs can be potentially large. Because of this, and because many HSPF parameters are correlated, HSPF parameters were parsimoniously selected for optimization on the basis of their influence in the model-calibration process observed in previously developed HSPF models and in the calibration of the Pawcatuck HSPF model. Initial PEST runs included the optimization of infiltration (INFILT), active groundwater-recession constant (AGWRC) and its modifier for non-exponential decay (KVARY), lower-zone nominal storage (LZSN), upper-zone nominal storage (UZSN), active groundwater evapotranspiration (AGWET), and lower-zone evapotranspiration index (LZET). UZSN was later removed from optimization because it was found to be insensitive. In addition, parameter estimation was restricted to the two dominant HRUs in the Pawcatuck River Basin, forested areas overlying sand and gravel (PERLND 5) and forested areas overlying till (PERLND 15).

The objective function (explained below) was computed at four locations representing different parts of the Pawcatuck River Basin-Usquepaug River near Usquepaug (USQU, 01117420), Beaver River near Usquepaug (BRUS, 01117468), Pawcatuck River at Wood River Junction (PRWR, 01117500), and Wood River at Hope Valley (WRHV, 01118000). A subsequent PEST run was made with these parameters for soils classified as steep and rocky or bedrock (PERLND 16) using an objective function determined at three locations where this HRU is prevalent—Pendleton Hill Brook near Clarks Falls (PHBK, 01118300), Ashaway River at Ashaway (ARAS, 01118360), and Shunock River near North Stonington (SRNS 01118400).

The role of PEST is to minimize the objective function, which is the sum of the square difference between simulated and observed values. The values used to compute the objective function can be defined in many different ways or combination of ways. The success of PEST is often affected by how well the objective function responds to parameter excitations that is facilitated by the surface-water utilities developed for PEST (Doherty, 2003). Initial PEST runs were made by minimizing an objective function that included weighted hourly time-series values, total monthly runoff volumes, and flows at various flow-duration intervals. Observations were weighted so that these three components at each of the observation sites had about equal influence in the computation of the objective function. The hourly time-series data also were weighted so that the influence of the observations decreased as the discharge increased.

Early in the formulation of the optimization problem, it was found that the hourly time-series data in the objective function produced erratic and often poor results. These results were believed to be caused by differences between the timing of simulated and observed hourly values that can be affected by a number of factors unrelated to the HSPF parameters being optimized. These factors include spatial precipitation distribution, RCHRES storage-discharge relation, and the land-surface roughness and flow-plane length. Thus, when PEST was tasked with optimizing HSPF parameters that have little effect on the timing of flow, the search algorithm performed poorly, often selecting parameter values at the outer allowed limit or parameters insensitive in the optimization, or both. The time-series component of the objective function was subsequently computed with daily mean flows, which improved PEST performance because it minimized problems associated with the short-term differences in the timing of flow. Therefore, all subsequent PEST runs were made with an objective function computed from daily mean flows, total monthly runoff volumes, and flows at various flow durations weighted in the same manner as previously described.

PEST requires information about the parameters used in the optimization process. This includes identification of the parameters, initial values and allowed limits, relations to other parameters, and mathematical transformations in the excitation process. Initial parameter values were set to the manually calibrated values. In subsequent parameter-estimation runs, the optimal parameter values determined previously were used as initial values or fixed when optimizing other parameters. All parameters were set to switch to a three-point derivative calculation as needed for a more precise computation of the Jacobian matrix.

Par2par, an auxiliary program included in the PEST Surface-Water Utilities, provides an unlimited ability to transform parameter values for parameter estimation. The transformed parameters are used by PEST, but are transformed back to allowable parameter values for use by HSPF. Par2par made changes in the AGWRC and IRC parameter values relatively linear with respect to changes in the model output compared to the response of the non-transformed parameters values. Monthly LZET parameter (MON–LZET) values were calculated by a sinusoidal function and two estimated parameters in par2par as indicated in figure A2–5. No transformations were made for excitations of INFILT, KVARY, AGWET, and UZSN. Excitations of LZSN were log-transformed to improve the derivative linearity. For the same reason, AGWRC,

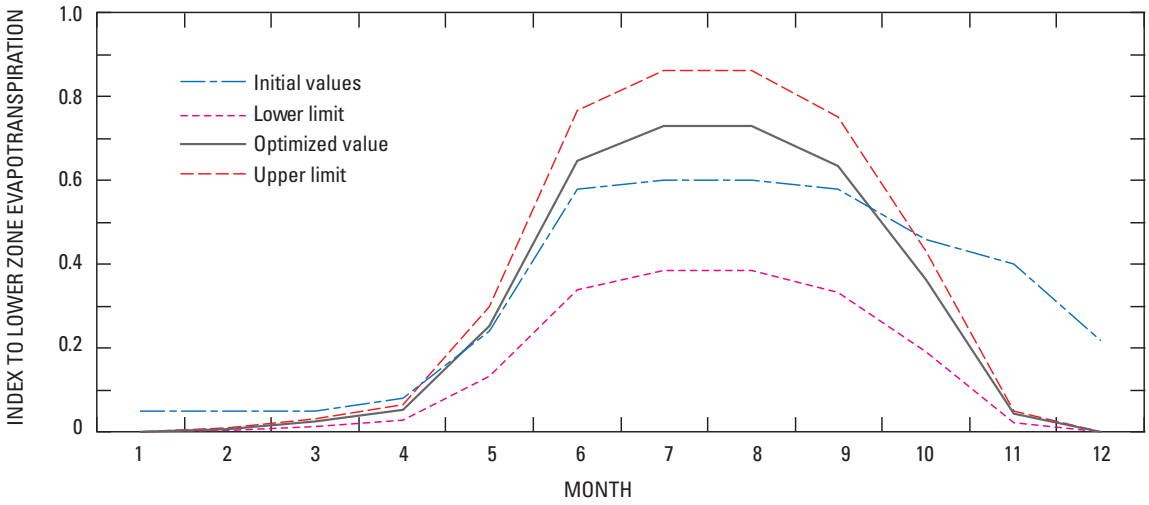

Figure A2–5. Sinusoidal function used to optimize the Lower Zone Evapotranspiration (LZET) parameter in the Hydrologic Simulation Program-FORTRAN (HSPF) of the Pawcatuck River Basin, southwestern Rhode Island and southeastern Connecticut.

IRC, and LZET parameter values were excited by use of the customized parameter transformation utility par2par.

The optimization process also was improved by separating baseflow from non-baseflow by using the PEST digital filter surface-water utility. Baseflow separation was performed by using a single parameter filter with an recession coefficient (alpha value) of 0.95. Filtering simulated and observed values prior to the computation of the objective function allows the optimization to be targeted to different flow components and the parameters that affect those components.

HSPF parameters LZSN, INFILT, AGWRC, KVARY, AGWET, and LZET, which are associated with the simulation of baseflow, were optimized with baseflow estimated from observed and simulated data at USQU, BRSH, PRWR, and WRHV. In a subsequent PEST run, the nonbaseflow runoff was used to optimize upper-zone storage (UZSN), interflow inflow (INTFW), and interflow recession (IRC) at the same four locations in the basin. These HSPF parameters are associated with the simulation of interflow and surface runoff.

The final model calibration was the outcome of the last four PEST optimization runs, herein referred to as CASE 5 through CASE 8. CASEs 5, 6, and 8 were used to perturb variables LZSN, INFILT, KVARY, AGWRC, AGWET, UZSN, and MON–LZETP. CASEs 5 and 8 perturbed these variables for HRUs representing forested areas overlying sand and gravel (PERLND 5) and forested areas overlying till (PERLND 15), which are the dominant HRU types in the basin (about 16 and 36 percent of the entire basin area, respectively). Variable values specific to an HRU were assigned unique identifiers in PEST and are denoted here by the variable abbreviation followed by the HRU number it is associated with. For example, INFILT in forested areas overlying till (PERLND 15) is identified as INFILT-15.

For CASE 5, the objective function was calculated for the entire flow hydrograph at USQU, BRSH, PRWR, WRHV, whereas CASE 8 limited the objective-function calculation to baseflow at the same sites plus PHBK. For CASE 6, the same variables were perturbed for the HRU representing steep-rocky soils (PERLND 16), and the objective function was computed at PHBK, ARAS, and SRNS in the northwestern part of the basin where this HRU is most dominant (24, 24, and 19 percent the total subbasin areas, respectively). CASE 7 perturbed the interflow (INTFW) and interflow-recession-rate (IRC) variables for HRUs representing forested areas overlying sand and gravel (PERLND 5) and till (PERLND 15), but limited the objective-function computation to non-baseflow runoff (surface runoff and interflow) at the same sites used in CASE 8. Key variable values at the start of the optimization process (obtained from manual calibration), their optimized values, and their confidence limits are summarized in table A2–5. Additional information on model-variable optimization is presented in the sensitivity section of this chapter.

Table A2–5. Starting and optimized variable values and their 95-percent confidence range calculated by PEST in order of ranked influence in the optimization of the Hydrologic Simulation Program-FORTRAN (HSPF) model of the Pawcatuck Basin Pawcatuck River Basin, southeastern Rhode Island and southwestern Connecticut. (Sites shown in figure A2–4 and described in table A2–4)

[ND, not determined; No., number]

Adjusted model variable[1]	Starting value	Optimized value	95-percent confidence limits	
			Lower	Upper
CASE 5—Forest over sand and gravel (5) and over till (15)				
INFILT–15	0.200	0.117	0.107	0.127
AGWET–15	.300	.291	.244	.338
LZET	.380	.380	.357	.403
AGWRCTRANS–15	211	192	165	223
(transformed)	(.995)	(.995)	(.994)	(.996)
KVARY–5	.268	.209	.141	.278
AGWET–5	.300	.162	.090	.235
KVARY–15	.791	.800	.705	.895
AGWRCTRANS–5	189	140	108	182
(transformed)	(.995)	(.993)	(.991)	(.995)
LZSN–15	5.74	4.65	3.96	5.46
INFILT–5	.428	.400	.253	.547
UZSN–15	.150	.900	.743	1.06
LZSN–5	11.6	7.24	5.03	10.4
UZSN–5	.200	.437	.143	1.02
CASE 6—Steep-rocky soil (16)				
INFILT–16	0.020	0.063	0.046	0.079
UZSN–16	.090	.900	.483	1.32
AGWET–16	.020	.300	.012	.588
LZET–16	.220	.380	.166	.594
AGWRCTRANS–16	3.0	59.6	7.7	460
(transformed)	(.750)	(.983)	(.885)	(.998)
LZSN–16	3.70	3.82	2.74	5.32
KVARY–16	.610	.800	-1.37	2.97
CASE 7—Non-baseflow				
INTFW–5	3.22	ND	ND	ND
INTFW–15	1.92	2.70	ND	ND
INTFW–16	1.72	1.90	ND	ND
IRC–5	.850	.950	ND	ND
IRC–15	.750	.701	ND	ND
IRC–16	.600	.500	ND	ND
CASE 8—Baseflow				
AGWET–15	0.300	0.300	0.279	.321
INFILT–15	.193	.179	0.173	.184
LZET	.380	.380	0.369	.391
AGWRCTRANS–15	213	142	120	167
(transformed)	(.995)	(.993)	(.992)	(.994)
KVARY–5	.286	.200	.132	.268
AGWRCTRANS–5	188	83.8	68.5	103
(transformed)	(.995)	(.988)	(.986)	(.990)
AGWET–5	.300	.300	.265	.335
KVARY–15	.801	.800	.644	.956
LZSN–15	6.16	8.85	8.17	9.58
LZSN–5	11.3	7.23	5.65	9.24
INFILT–5	.402	.449	.307	.592

[1] Number following the dash indicates the number of the Hydrologic Response Unit (HRU) for which the variable was perturbed.

CASE 5
Sites: USQU, BRSH, PRWR, WRHV
RCHRES: 20, 43, 46, 59

Objective function
Start: 487
End: 414
Percent change: -15
No. observations: 7080
No. parameters: 13
No. model runs: 237

CASE 6
Sites: PHBK, ARAS, SRNS
RCHRES: 74, 77, 83

Objective function
Start: 4624
End: 2805
Percent change: -39
No. observations: 5310
No. parameters: 7
No. model runs: 204

CASE 7
Sites: USQU, BRSH, PRWR, WRHV, PHBK
RCHRES: 20, 43, 46, 59, 74

Objective function
Start: 3.96E+11
End: 3.78E+11
Percent change: -5
No. observations: 8520
No. parameters: 6
No. model runs: 109

CASE 8
Sites: USQU, BRSH, PRWR, WRHV, PHBK
RCHRES: 20, 43, 46, 59, 74

Objective function
Start: 3099
End: 1506
Percent change: -51
No. observations: 7080
No. parameters: 11
No. model runs: 174

Model Fit

In general, flows simulated by the calibrated model matched the observed flows over a wide range of conditions and subbasin characteristics within an acceptable range of error. The median R^2 value for the simulated and observed daily mean flows for the 17 continuous streamflow-gaging stations is 0.81 and ranged between 0.66 and 0.87; the median MFE is 0.79 and ranged between 0.59 and 0.86 (table A2–6). Simulated and observed monthly mean flows for the 17 continuous streamflow-gaging stations has a median R^2 of 0.93 and ranged between 0.86 and 0.95; the MFE is 0.90 and ranged between 0.80 and 0.94 (table A2–7). These and other calibration statistics for each continuous streamflow-gaging station are summarized in tables A2–6 and A2–7.

Statistical measures do not adequately describe all aspects of a model fit; visual inspection of the hydrographs, flow-duration curves, and scatterplots of simulated and observed discharges provide additional information to assess model performance. Observed and simulated flow hydrographs, scatterplots, and flow-duration curves are shown for the 17 continuous streamflow-gaging stations in figures A2–6 through A2–22. These graphs generally indicate a close match between simulated and observed flows over about five orders of magnitude.

Differences between the mean observed and simulated flows, as indicated by the percent error, is generally largest for stations at which flows were estimated for part of the calibration period. These stations include Chickasheen Brook at West Kingston (CBLL, RCHRES 36; fig. A2–10), Pawcatuck River at Kenyon (PRBC, RCHRES 37; fig. A2–11), Beaver River near Shannock (BRSH, RCHRES 43; fig. A2–13), Meadow Brook near Carolina (MBCA, RCHRES 47; fig. A2–15), Pawcatuck River at Burdickville (PRBV, RCHRES 50; fig. A2–18), Ashaway River at Ashaway (ARAS, RCHRES 77; fig. A2–20), and Shunock River near North Stonington (SRSN, RCHRES 83; fig. A2–21). Continuous flow monitoring at these sites began in the late summer and early fall of 2002; thus, daily mean flows had to be estimated for about the first half of the calibration period. When model-fit statistics were computed for these stations from the period of actual record (October 1, 2002, through September 30, 2004), the percent error between the mean simulated and observed discharge generally decreased by about half; however, the overall R^2 and MFE values did not change appreciably.

Another source of model error can result from inaccurate withdrawal information, particularly in small headwater subbasins during periods of low flow when withdrawals can compose a large percentage of the total flow. Under this condition, error in measured or estimated withdrawals can translate into large model errors. Inaccurate withdrawal information is believed to have contributed to the model error (particularly at low flows) for the Queen River at Exeter (QRPB, RCHRES 2; fig. A2–6), Chipuxet River at West Kingston (CRWK, RCHRES 32; fig. A2–9), Chickasheen Brook at West Kingston (CBLL, RCHRES 36; fig. A2–10), Beaver River near Usquepaug (BRUS, RCHRES 42; fig. A2–12), Beaver River near Shannock (BRSH, RCHRES 43; fig. A2–13), and Meadow Brook near Carolina (MBCA, RCHRES 47; fig. A2–15).

Regulation of in-stream ponds (for example, the placement or removal of flash boards) also affects the relation between simulated and observed flows because these types of operations are not explicitly simulated. Sudden changes in observed flow, such as those in the late summers of 2001 through 2004 in the Chipuxet River at West Kingston (CRWK, RCHRES 32; fig. A2–9), could have been caused by this type of alteration. These unexplained changes in observed flow could also reflect unknown or inaccurate withdrawal information.

Precipitation spatial variability and measurement error can affect simulation results. The Pawcatuck River Basin model was calibrated with precipitation data from the FBWR station (fig. 1–1). The precipitation measured at this station is uniformly distributed across the entire 303-mi^2 basin. Often, the largest model error, as measured by the percent difference between the observed and simulated monthly mean flow, is associated with the largest variation in total monthly precipitation (fig. A2–23). Precipitation variation was measured by the deviation in the monthly precipitation at the FBWR station from the monthly mean precipitation measured at PROVID, URI, FBWR, NIC, and WESTERLY stations (fig. 1–1) as a percentage of the monthly precipitation at FBWR.

Large precipitation variability, as indicated by the shaded area on figure A2–23, can be an appreciable source of model error, although the error is not always large. Generally, the largest model error was during low flows months when the absolute differences between simulated and observed flows are small, but the percent differences can be large. The largest model error associated with small precipitation variation (near the zero line on the y axis; fig. A2–23) mostly correspond to small subbasins in the western part of the Pawcatuck River Basin when precipitation differences at FBWR and Westerly (the westernmost precipitation gage; fig. 1–1) were greatest. Other months with relatively large model error were most common during periods of low flow and in reaches where upstream withdrawals account for a large percentage of the total flow; this error could reflect uncertainty in the withdrawal information.

At several locations, particularly at stations below extensive wetlands, the mean simulated flow is appreciably greater than the mean observed flow. For example, at Pawcatuck River at Kenyon, R.I. (PRBC, RCHRES 37), the subbasin with the largest wetland, the simulated mean flow is about 10 percent greater than the observed mean flow. This difference is attributed to the evapotranspiration (ET) losses from wetlands simulated as PERLNDs; wetland PERLNDs are believed to undersimulate ET losses because the available moisture supply is limited to precipitation held in storage, which caps the potential ET loss. ET loss from a natural wetland in Wisconsin was shown to exceed potential evapotranspiration (PET) during the height of the growing season

Table A2–6. Summary of model-fit statistics for daily mean discharge, January 2000 through September 2004, simulated by the Hydrologic Simulation Program-FORTRAN (HSPF) and observed at 17 continuous-record streamflow-gaging stations, Pawcatuck River Basin, southwestern Rhode Island and southeastern Connecticut.

[Site locations shown in figure A2–4; see table A2–4 for reach names; No, number; RCHRES, model reach; IDLOCN, attribute name for reaches and gages; ft^3/s, cubic feet per second; RMS, Root mean square. Shaded cells indicate stations for which part of the flow record was estimated]

RCHRES		Gage IDLOCN	Daily discharge (ft^3/s)		Correlation coefficient	Coefficient of determination (R^2)	Mean error (ft^3/s)	Percent mean error	RMS error (ft^3/s)	Model fit efficiency (MFE)
No.	IDLOCN		Observed	Simulated						
2	QUEN2	QRPB	7.43	7.67	0.91	0.83	-0.24	-3.19	3.4	0.79
9	QUEN4	QRLY	36.1	34.9	0.91	0.82	1.14	3.17	15.1	0.74
20	QUEN7	USQU	71.9	70.9	0.92	0.85	0.99	1.37	24.8	0.82
32	CHIP2	CRWK	21.5	20.3	0.84	0.71	1.18	5.49	9.59	0.64
36	CHIC2	CBLL	8.76	10.4	0.90	0.80	-1.67	-19.1	3.96	0.73
37	PAWC2	PRBC	131	144	0.93	0.86	-12.7	-9.72	44.3	0.82
42	BEAV2	BRUS	20.0	19.6	0.93	0.86	0.40	2.00	6.41	0.85
43	BEAV3	BRSH	23.2	24.7	0.93	0.87	-1.55	-6.68	7.59	0.86
46	PAWC3	PRWR	197	203	0.92	0.85	-5.75	-2.92	59.0	0.84
47	MEAD1	MBCA	9.75	8.89	0.82	0.68	0.86	8.80	5.96	0.64
53	WOOD2	WRAR	68.5	74.4	0.84	0.71	-5.85	-8.54	36.3	0.71
59	WOOD4	WRHV	150	159	0.90	0.81	-9.38	-6.26	63.7	0.80
50	PAWC4	PRBV	401	430	0.92	0.84	-28.5	-7.11	138	0.84
74	PEND1	PHBK	8.42	8.68	0.81	0.66	-0.27	-3.17	6.12	0.59
77	ASHA1	ARAS	53.5	60.9	0.82	0.67	-7.39	-13.8	39.2	0.63
83	SHUN2	SRNS	32.5	36.1	0.85	0.73	-3.56	-11.0	18.6	0.69
80	PAWC8	PRWS	568	620	0.90	0.81	-51.8	-9.11	225	0.80
Median			36.1	36.1	0.90	0.81		-6.26		0.79
Standard deviation					0.04	0.07		7.24		0.09
Minimum					0.81	0.66		1.37		0.59
Maximum					0.93	0.87		-19.1		0.86

(Lott and Hunt, 2001); this finding underscores the problem of insufficient simulated ET loss from wetlands. To circumvent this limitation of inadequate moisture supply to wetlands, it was hypothesized in the Ipswich River Basin HSPF model (Zarriello and Ries, 2000) that the moisture supply to wetlands is from lateral inflows from surrounding upgradient areas in addition to direct precipitation. Simulating this additional moisture supply required treating wetlands as virtual RCHRESs with atmospheric gains and losses plus inflows from adjacent PERLNDs and IMPLNDs. Virtual RCHRES FTABLE characteristics are determined by setting the area equal to the corresponding area of wetlands in the subbasin, estimating storage from area and depth, and empirically adjusting flow to fit simulated flows to observed flows.

The virtual RCHRES concept was evaluated in the upper Pawcatuck River Basin by converting the wetland areas in RCHRESs 34 and 37 to virtual RCHRESs (134 and 137, respectively). The subbasins corresponding to RCHRES 34 and 37 include some of the most expansive area of wetland in the Pawcatuck River Basin (about 30 and 40 percent of their total subbasin areas, respectively). The additional ET loss from wetlands treated as virtual RCHRESs in these subbasins decreased the difference between the mean simulated and observed flows by about half at Pawcatuck River at Kenyon, R.I. (PRBC, RCHRES 37), and resulted in slight improvements of other model-fit statistics. Constructing the model with virtual RCHRES in other areas would likely improve model performance; however, this was not pursued because it was expected to create problems in coupling of HSPF with MODFLOW that was anticipated to come later in the project. Hence, the HSPF model variables were optimized without inclusion of virtual RCHRES for the simulation of wetlands.

Table A2–7. Summary of model-fit statistics for monthly mean discharge, January 2000 through September 2004, simulated by the Hydrologic Simulation Program-FORTRAN (HSPF) and observed at 17 continuous record streamflow-gaging stations, Pawcatuck River Basin, southwestern Rhode Island and southeastern Connecticut.

[Site locations shown in figure A2–4; see table A2–4 for reach names; No., number; RCHRES, model reach; IDLOCN, attribute name for reaches and gages; ft^3/s, cubic feet per second; RMS, Root mean square. Shaded cells indicate stations for which part of the flow record was estimated]

RCHRES		Gage IDLOCN	Mean discharge (ft^3/s)		Correlation coefficient	Coefficient of determination (R^2)	Mean error (ft^3/s)	Percent mean error	RMS error (ft^3/s)	Model fit efficiency (MFE)
No.	IDLOCN		Observed	Simulated						
2	QUEN2	QRPB	7.44	7.68	0.97	0.94	-0.24	-3.26	1.40	0.93
9	QUEN4	QRLY	36.1	35.0	0.96	0.92	1.13	3.12	7.98	0.86
20	QUEN7	USQU	72.0	71.0	0.97	0.95	0.94	1.31	11.6	0.93
32	CHIP2	CRWK	21.5	20.4	0.94	0.89	1.18	5.49	4.95	0.81
36	CHIC2	CBLL	8.76	10.44	0.96	0.92	-1.67	-19.1	2.41	0.82
37	PAWC2	PRBC	131	144	0.97	0.94	-12.8	-9.76	25.8	0.90
42	BEAV2	BRUS	20.0	19.7	0.97	0.95	0.38	1.91	3.09	0.94
43	BEAV3	BRSH	23.2	24.8	0.98	0.95	-1.57	-6.75	3.72	0.94
46	PAWC3	PRWR	197	203	0.97	0.93	-5.82	-2.95	34.0	0.91
47	MEAD1	MBCA	9.76	8.90	0.96	0.93	0.86	8.79	2.70	0.81
53	WOOD2	WRAR	68.6	74.5	0.94	0.87	-5.88	-8.57	17.0	0.86
59	WOOD4	WRHV	150	160	0.96	0.93	-9.46	-6.30	28.4	0.91
50	PAWC4	PRBV	402	430	0.97	0.94	-28.6	-7.13	69.7	0.92
74	PEND1	PHBK	8.44	8.70	0.93	0.86	-0.26	-3.10	2.45	0.81
77	ASHA1	ARAS	53.6	61.0	0.94	0.88	-7.39	-13.8	15.9	0.83
83	SHUN2	SRNS	32.6	36.1	0.94	0.88	-3.56	-10.9	9.49	0.80
80	PAWC8	PRWS	569	621	0.96	0.93	-51.9	-9.12	115	0.90
Median			36.1	36.1	0.96	0.93		-6.30		0.90
Standard deviation					0.01	0.03		7.23		0.05
Minimum					0.93	0.86		1.31		0.80
Maximum					0.98	0.95		-19.1		0.94

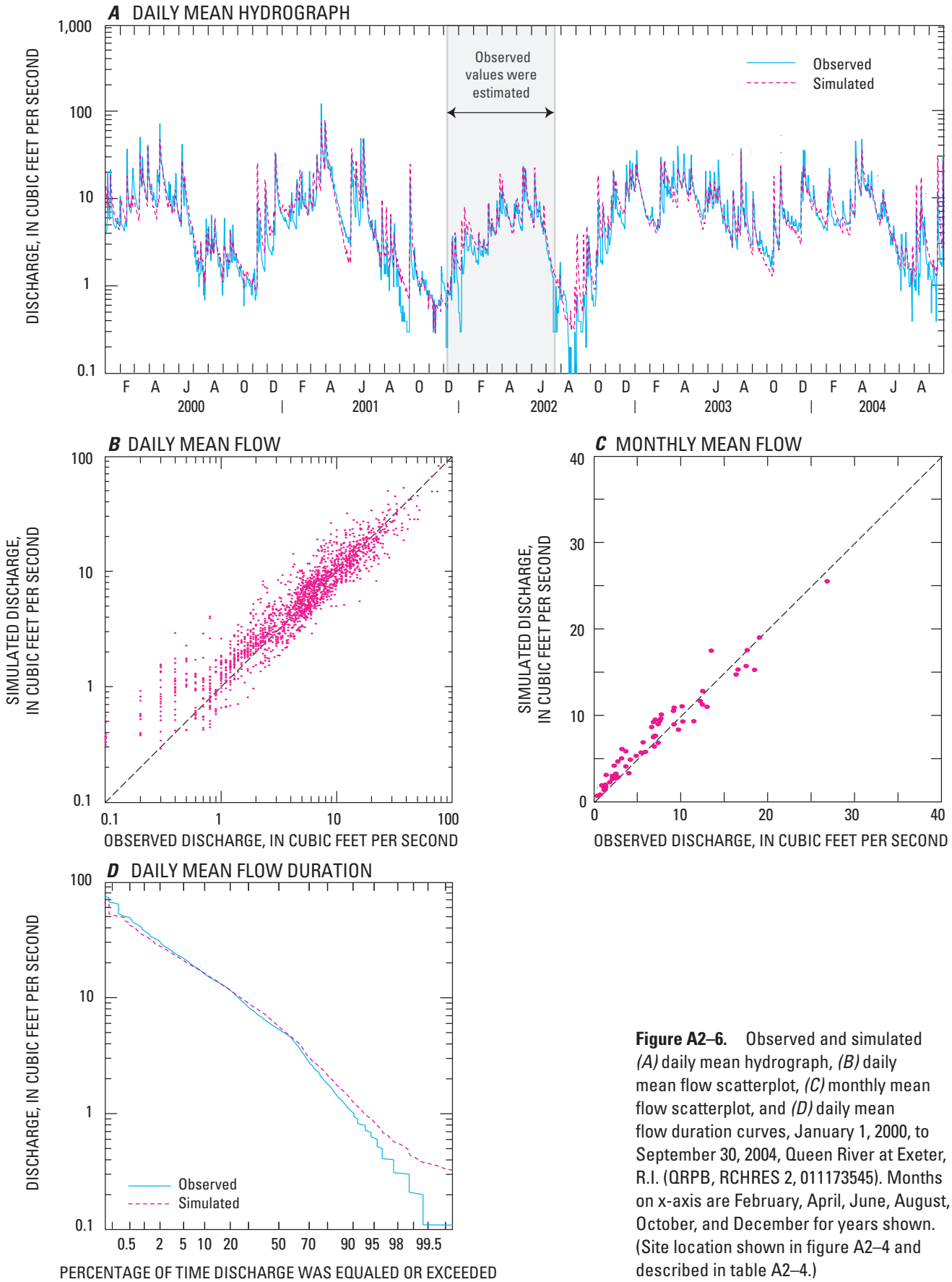

Figure A2–6. Observed and simulated *(A)* daily mean hydrograph, *(B)* daily mean flow scatterplot, *(C)* monthly mean flow scatterplot, and *(D)* daily mean flow duration curves, January 1, 2000, to September 30, 2004, Queen River at Exeter, R.I. (QRPB, RCHRES 2, 011173545). Months on x-axis are February, April, June, August, October, and December for years shown. (Site location shown in figure A2–4 and described in table A2–4.)

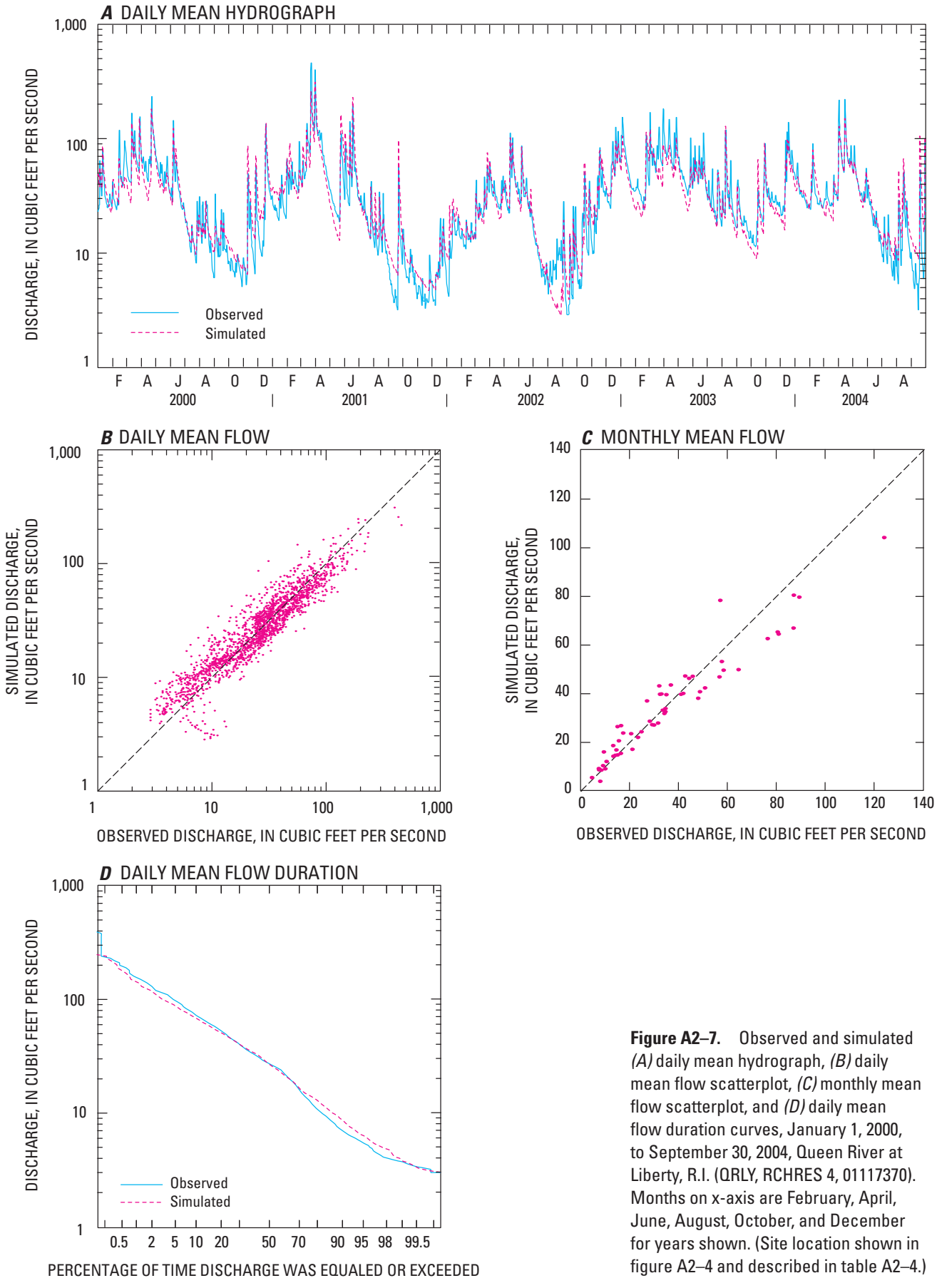

Figure A2–7. Observed and simulated *(A)* daily mean hydrograph, *(B)* daily mean flow scatterplot, *(C)* monthly mean flow scatterplot, and *(D)* daily mean flow duration curves, January 1, 2000, to September 30, 2004, Queen River at Liberty, R.I. (QRLY, RCHRES 4, 01117370). Months on x-axis are February, April, June, August, October, and December for years shown. (Site location shown in figure A2–4 and described in table A2–4.)

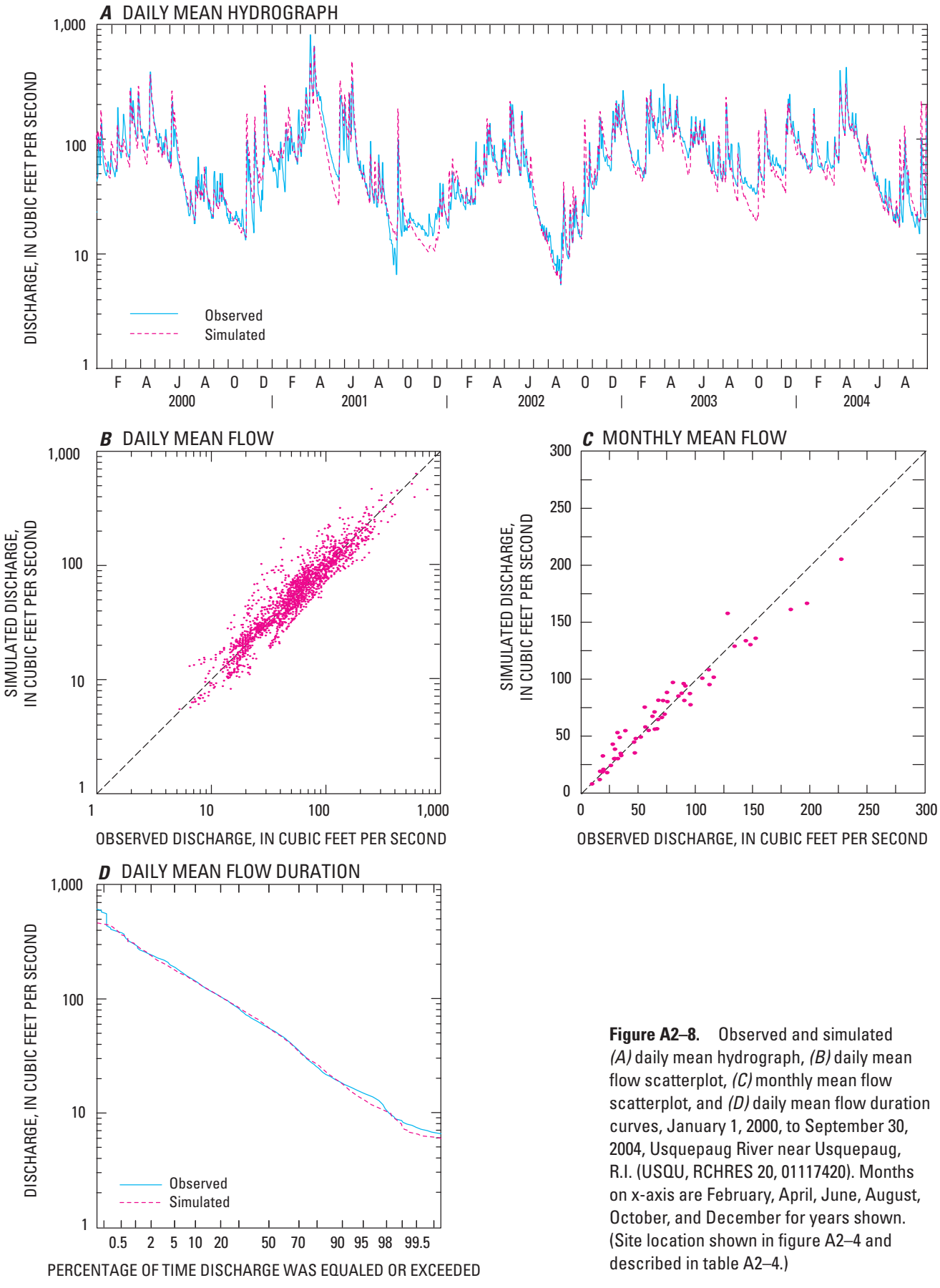

Figure A2–8. Observed and simulated *(A)* daily mean hydrograph, *(B)* daily mean flow scatterplot, *(C)* monthly mean flow scatterplot, and *(D)* daily mean flow duration curves, January 1, 2000, to September 30, 2004, Usquepaug River near Usquepaug, R.I. (USQU, RCHRES 20, 01117420). Months on x-axis are February, April, June, August, October, and December for years shown. (Site location shown in figure A2–4 and described in table A2–4.)

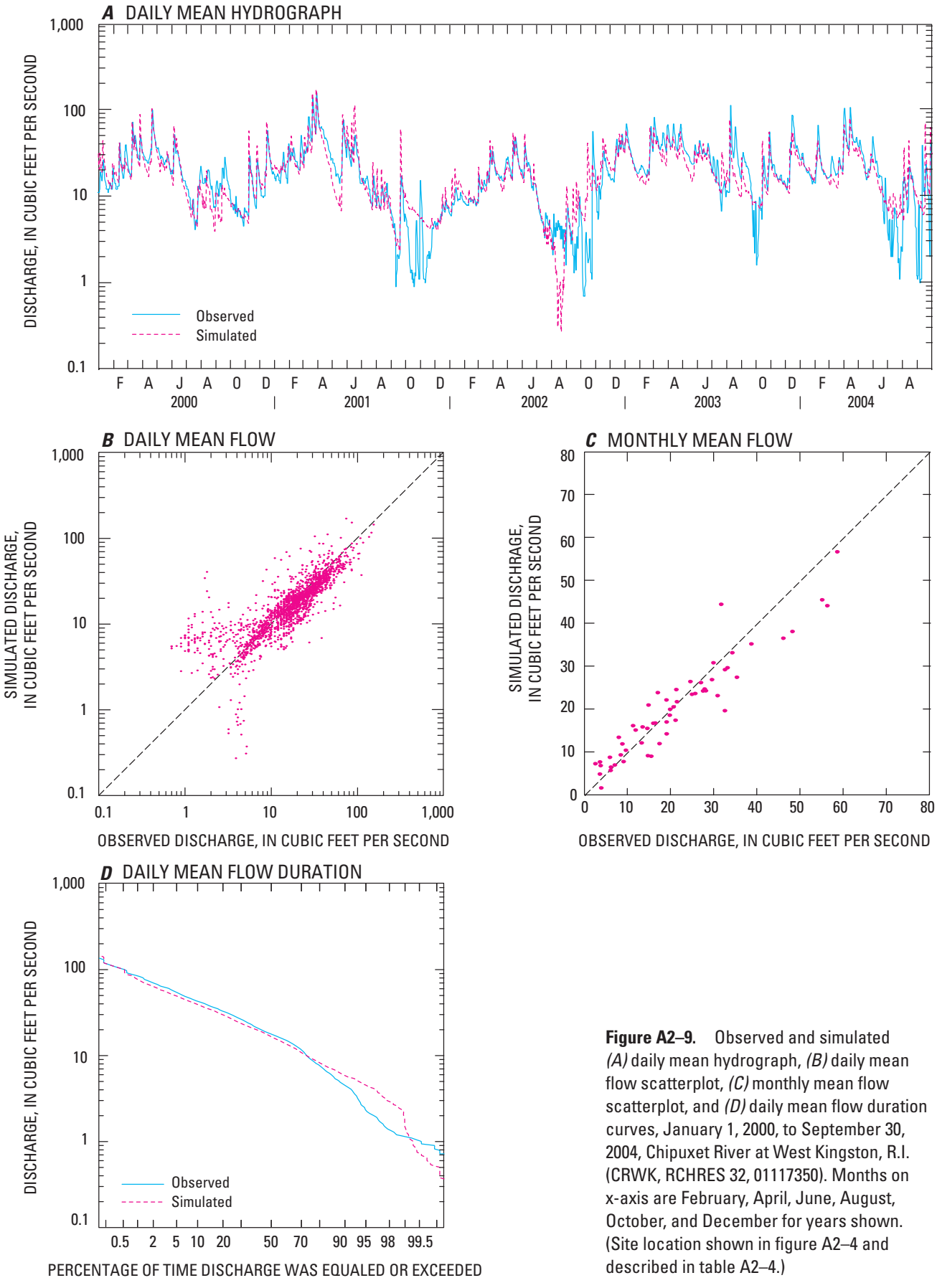

Figure A2–9. Observed and simulated *(A)* daily mean hydrograph, *(B)* daily mean flow scatterplot, *(C)* monthly mean flow scatterplot, and *(D)* daily mean flow duration curves, January 1, 2000, to September 30, 2004, Chipuxet River at West Kingston, R.I. (CRWK, RCHRES 32, 01117350). Months on x-axis are February, April, June, August, October, and December for years shown. (Site location shown in figure A2–4 and described in table A2–4.)

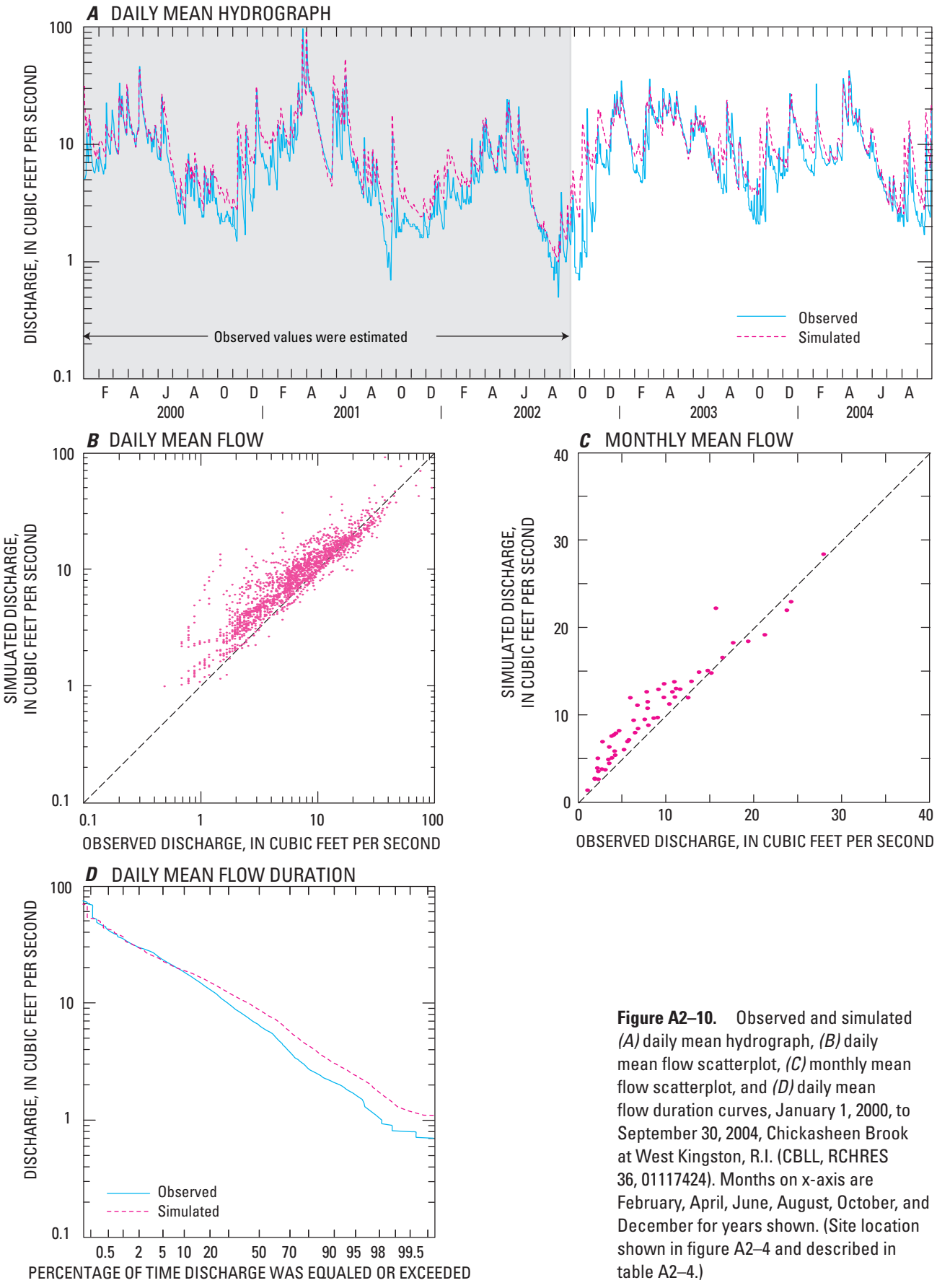

Figure A2–10. Observed and simulated *(A)* daily mean hydrograph, *(B)* daily mean flow scatterplot, *(C)* monthly mean flow scatterplot, and *(D)* daily mean flow duration curves, January 1, 2000, to September 30, 2004, Chickasheen Brook at West Kingston, R.I. (CBLL, RCHRES 36, 01117424). Months on x-axis are February, April, June, August, October, and December for years shown. (Site location shown in figure A2–4 and described in table A2–4.)

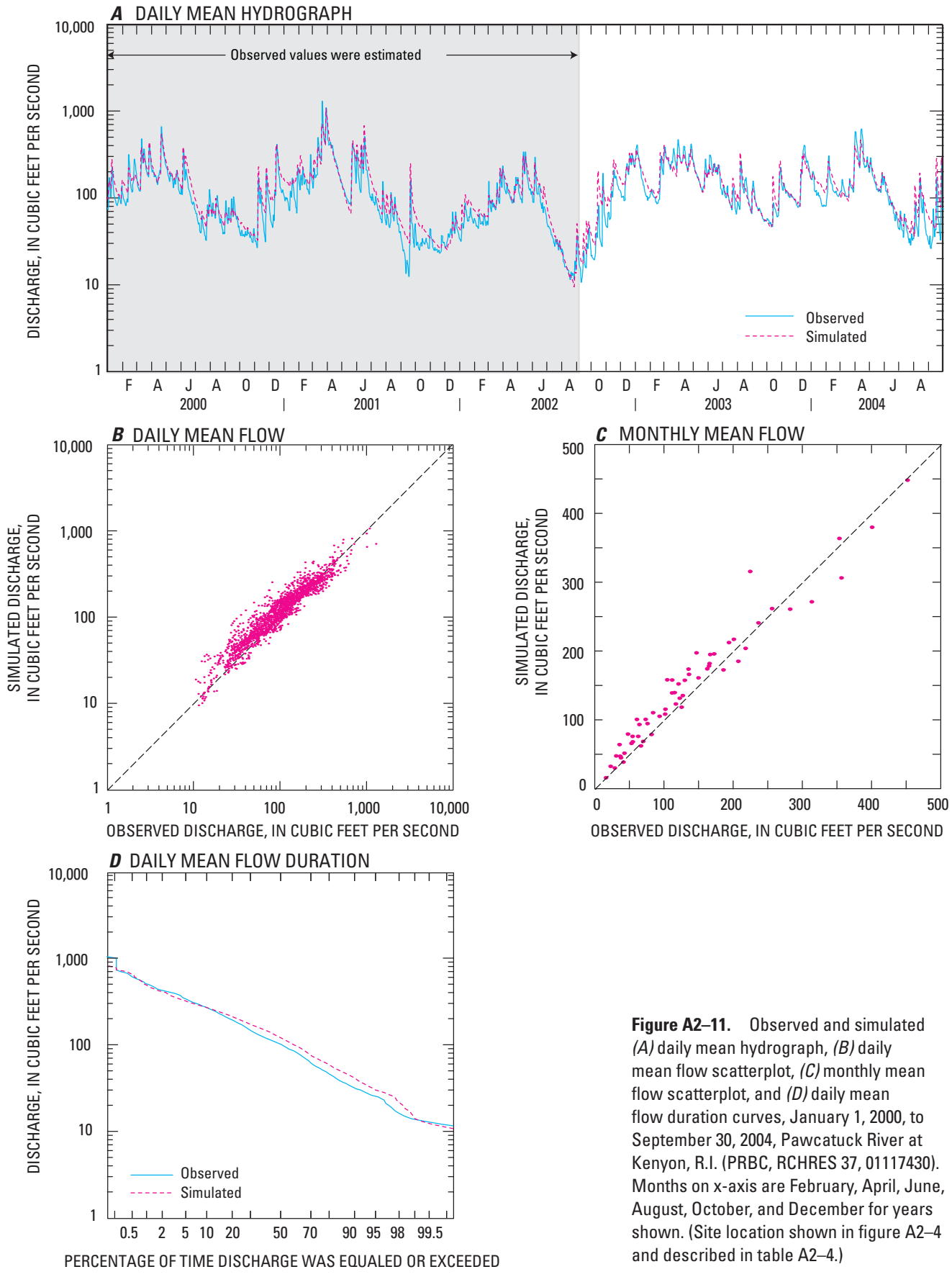

Figure A2–11. Observed and simulated *(A)* daily mean hydrograph, *(B)* daily mean flow scatterplot, *(C)* monthly mean flow scatterplot, and *(D)* daily mean flow duration curves, January 1, 2000, to September 30, 2004, Pawcatuck River at Kenyon, R.I. (PRBC, RCHRES 37, 01117430). Months on x-axis are February, April, June, August, October, and December for years shown. (Site location shown in figure A2–4 and described in table A2–4.)

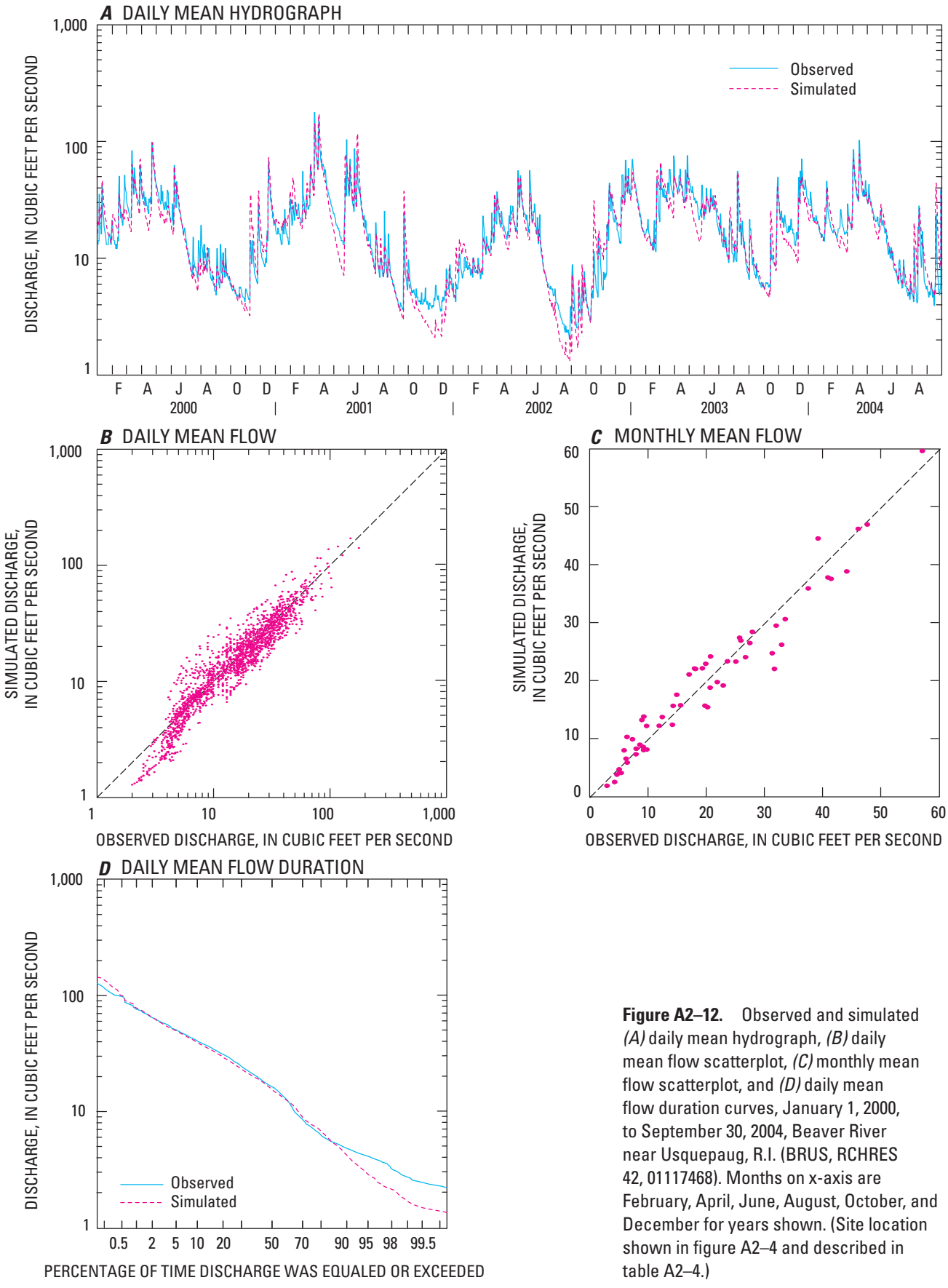

Figure A2–12. Observed and simulated *(A)* daily mean hydrograph, *(B)* daily mean flow scatterplot, *(C)* monthly mean flow scatterplot, and *(D)* daily mean flow duration curves, January 1, 2000, to September 30, 2004, Beaver River near Usquepaug, R.I. (BRUS, RCHRES 42, 01117468). Months on x-axis are February, April, June, August, October, and December for years shown. (Site location shown in figure A2–4 and described in table A2–4.)

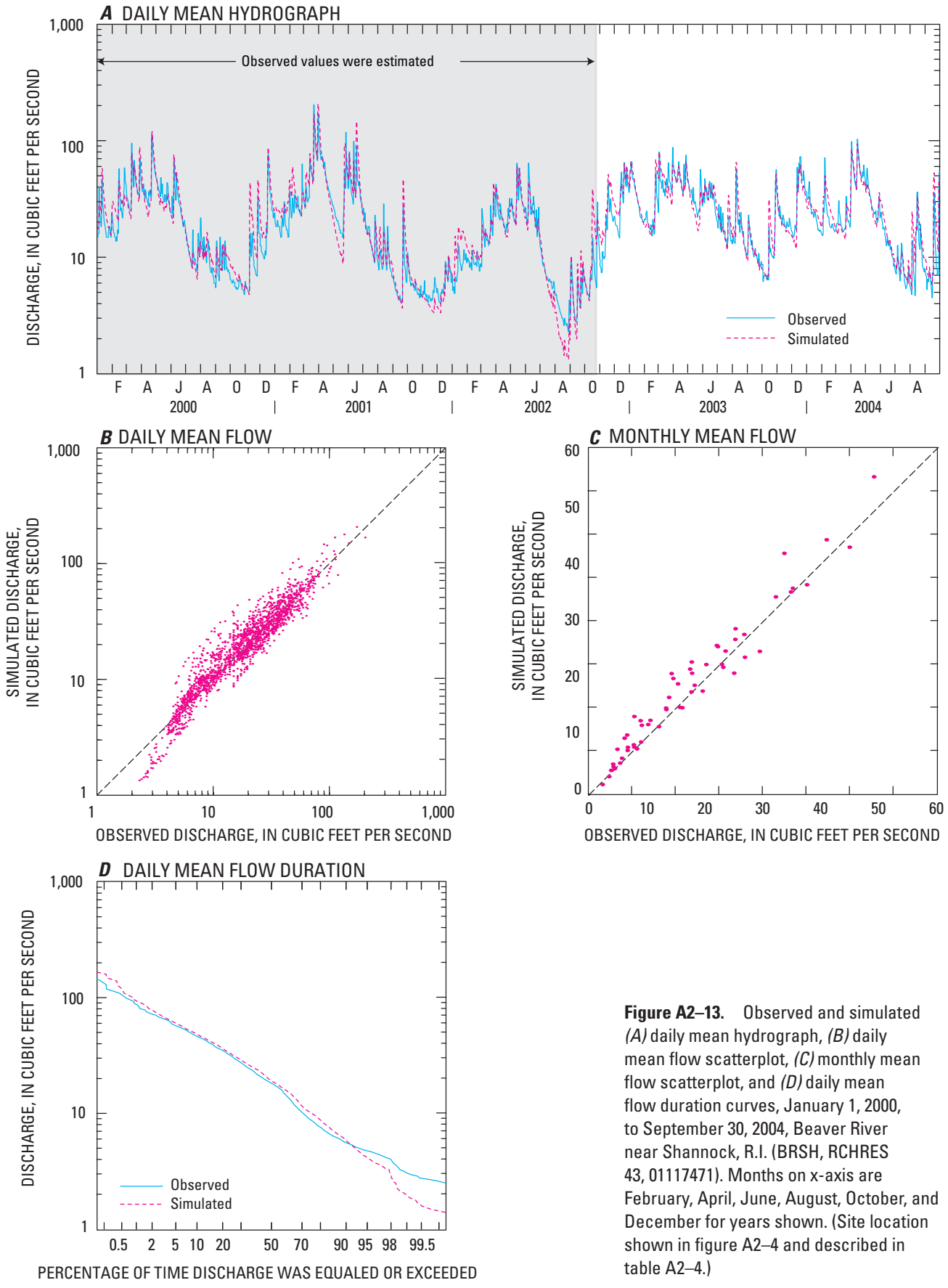

Figure A2–13. Observed and simulated *(A)* daily mean hydrograph, *(B)* daily mean flow scatterplot, *(C)* monthly mean flow scatterplot, and *(D)* daily mean flow duration curves, January 1, 2000, to September 30, 2004, Beaver River near Shannock, R.I. (BRSH, RCHRES 43, 01117471). Months on x-axis are February, April, June, August, October, and December for years shown. (Site location shown in figure A2–4 and described in table A2–4.)

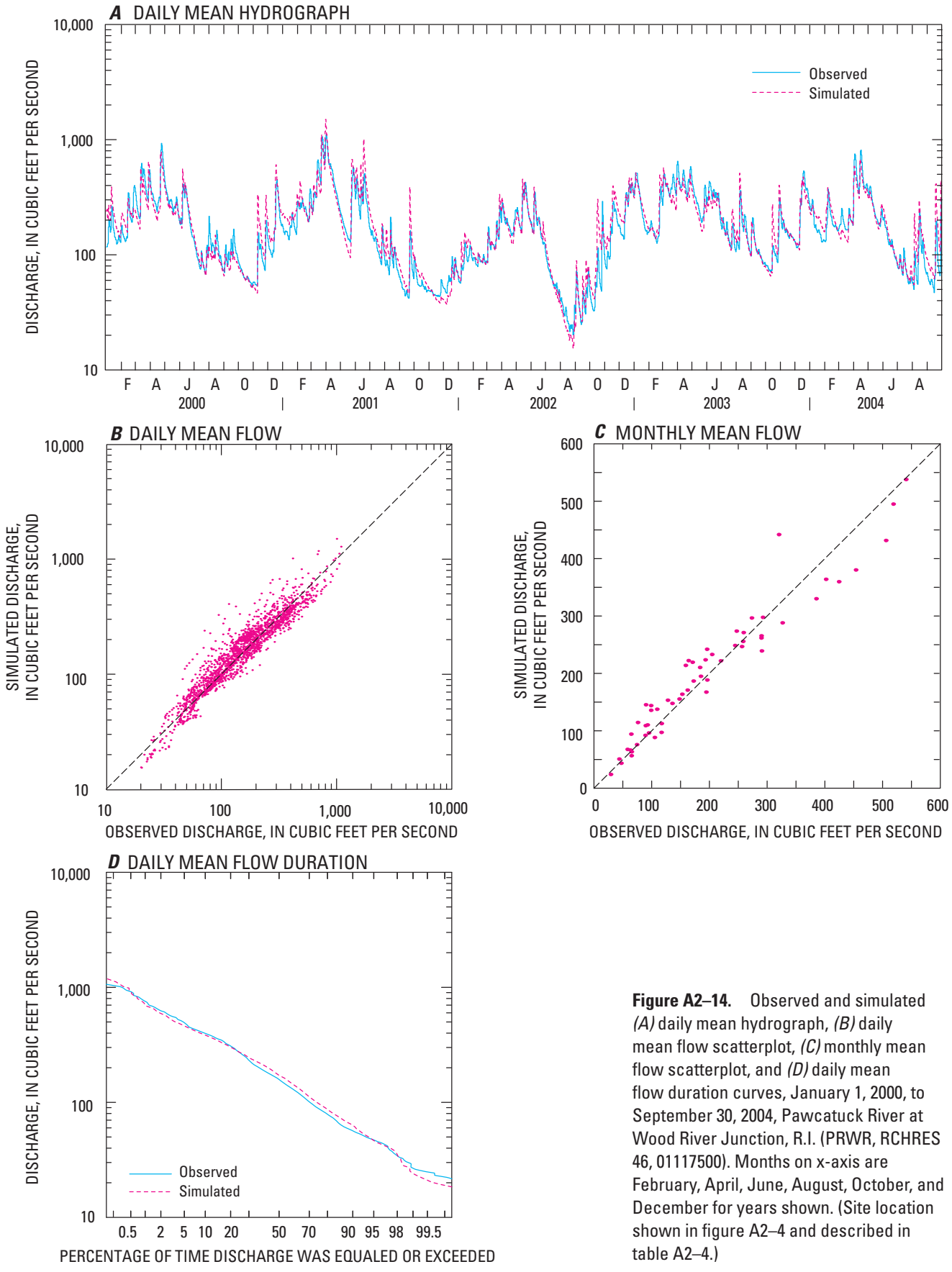

Figure A2–14. Observed and simulated *(A)* daily mean hydrograph, *(B)* daily mean flow scatterplot, *(C)* monthly mean flow scatterplot, and *(D)* daily mean flow duration curves, January 1, 2000, to September 30, 2004, Pawcatuck River at Wood River Junction, R.I. (PRWR, RCHRES 46, 01117500). Months on x-axis are February, April, June, August, October, and December for years shown. (Site location shown in figure A2–4 and described in table A2–4.)

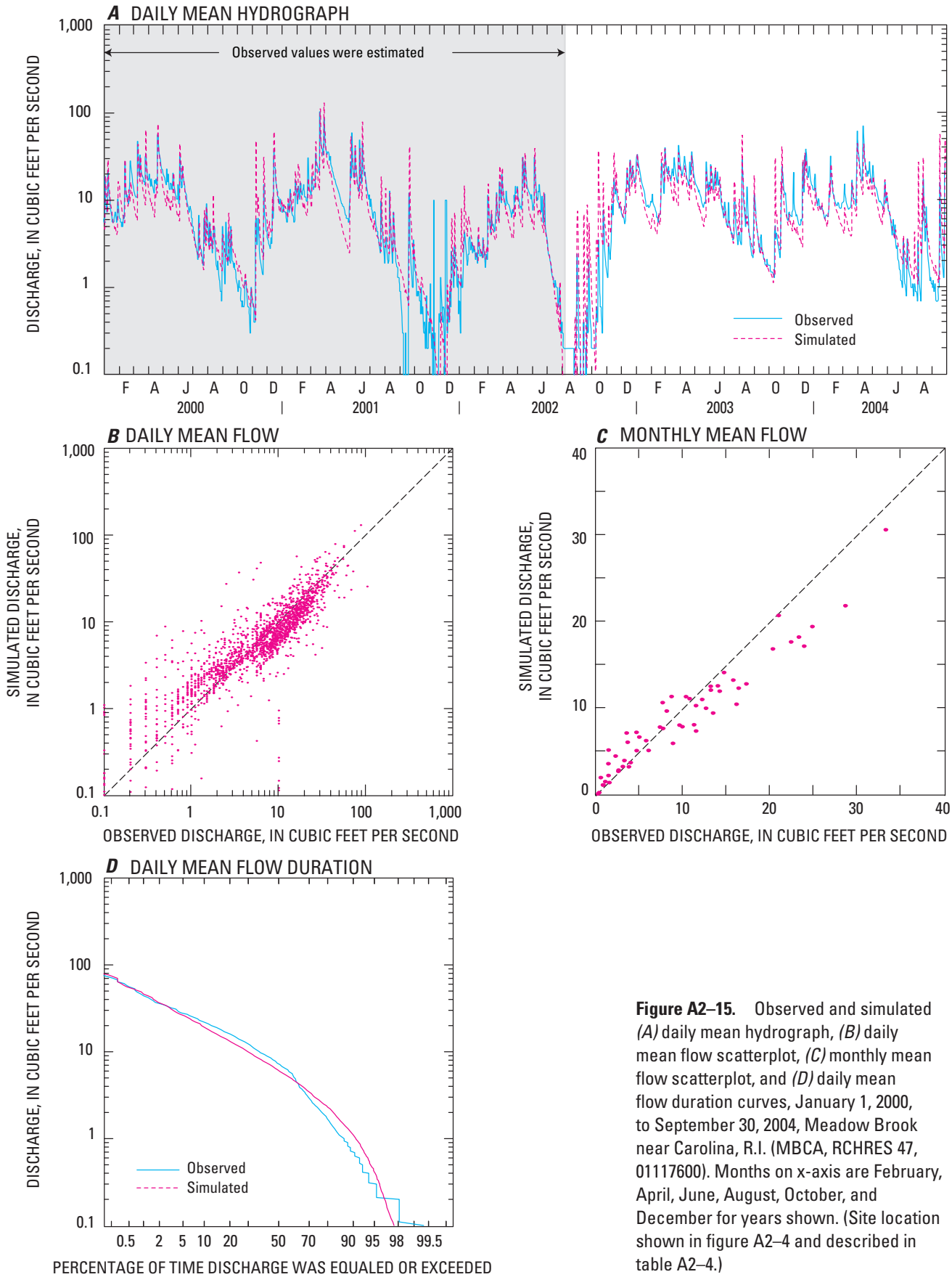

Figure A2–15. Observed and simulated *(A)* daily mean hydrograph, *(B)* daily mean flow scatterplot, *(C)* monthly mean flow scatterplot, and *(D)* daily mean flow duration curves, January 1, 2000, to September 30, 2004, Meadow Brook near Carolina, R.I. (MBCA, RCHRES 47, 01117600). Months on x-axis are February, April, June, August, October, and December for years shown. (Site location shown in figure A2–4 and described in table A2–4.)

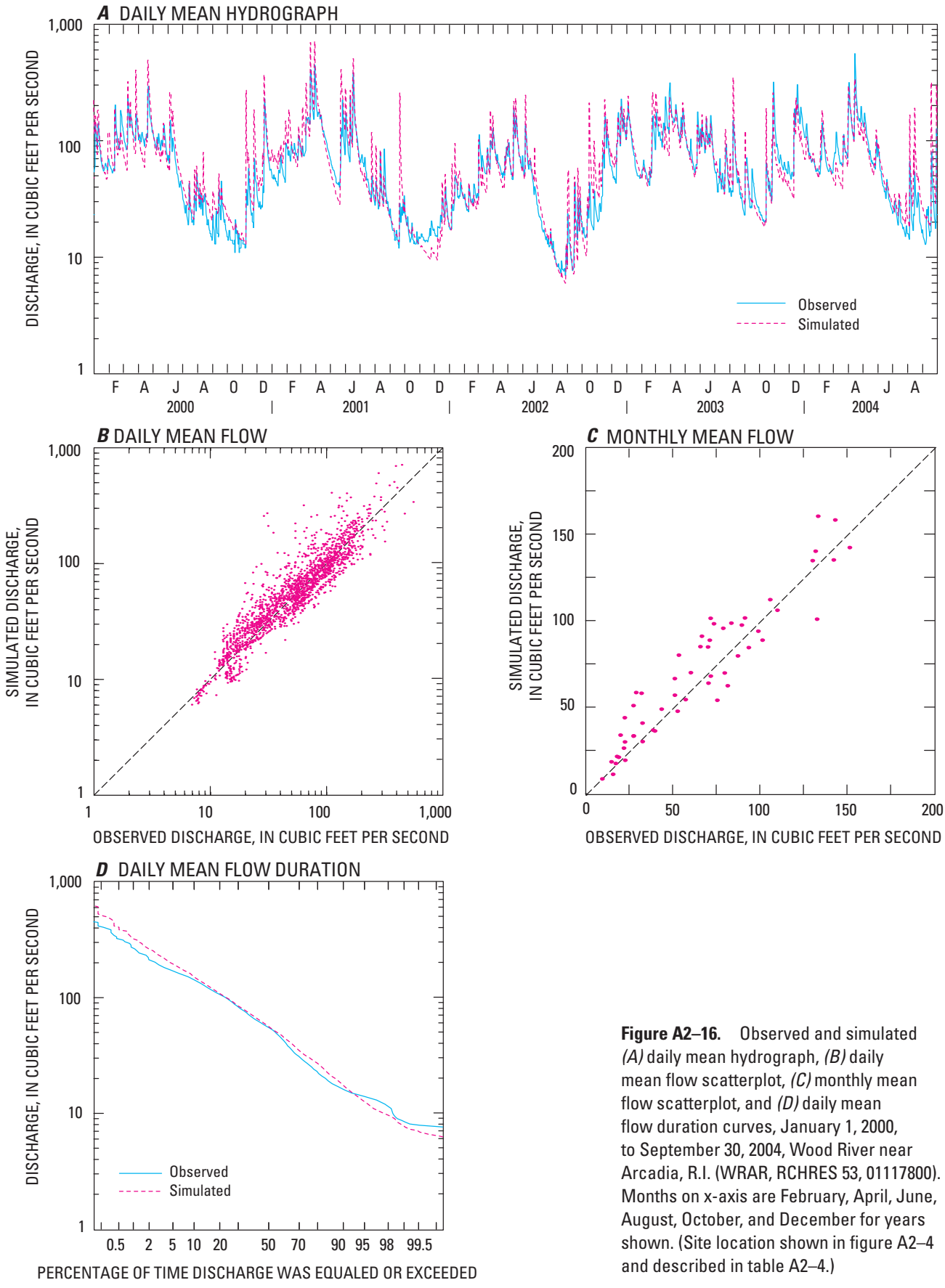

Figure A2–16. Observed and simulated *(A)* daily mean hydrograph, *(B)* daily mean flow scatterplot, *(C)* monthly mean flow scatterplot, and *(D)* daily mean flow duration curves, January 1, 2000, to September 30, 2004, Wood River near Arcadia, R.I. (WRAR, RCHRES 53, 01117800). Months on x-axis are February, April, June, August, October, and December for years shown. (Site location shown in figure A2–4 and described in table A2–4.)

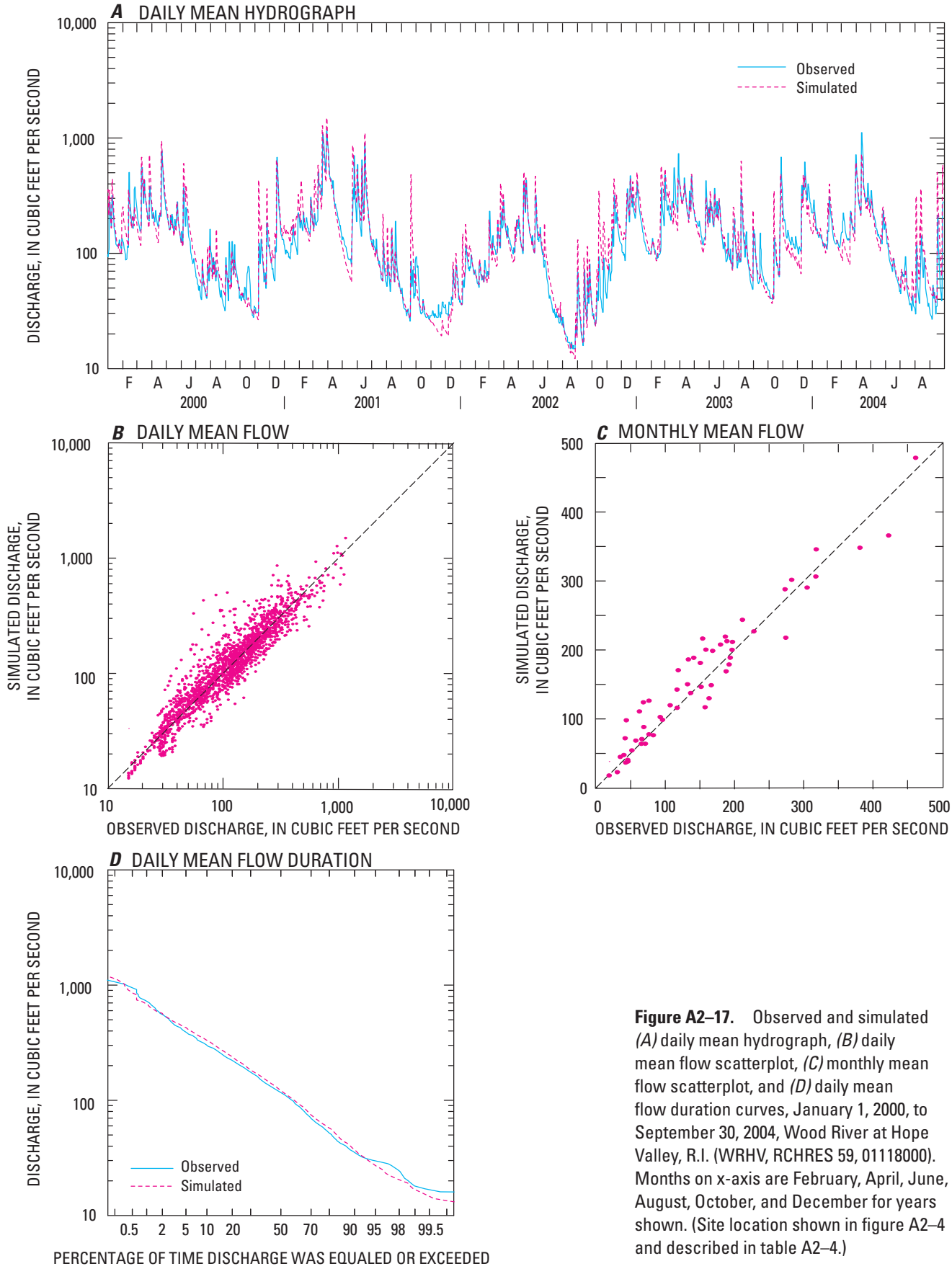

Figure A2–17. Observed and simulated *(A)* daily mean hydrograph, *(B)* daily mean flow scatterplot, *(C)* monthly mean flow scatterplot, and *(D)* daily mean flow duration curves, January 1, 2000, to September 30, 2004, Wood River at Hope Valley, R.I. (WRHV, RCHRES 59, 01118000). Months on x-axis are February, April, June, August, October, and December for years shown. (Site location shown in figure A2–4 and described in table A2–4.)

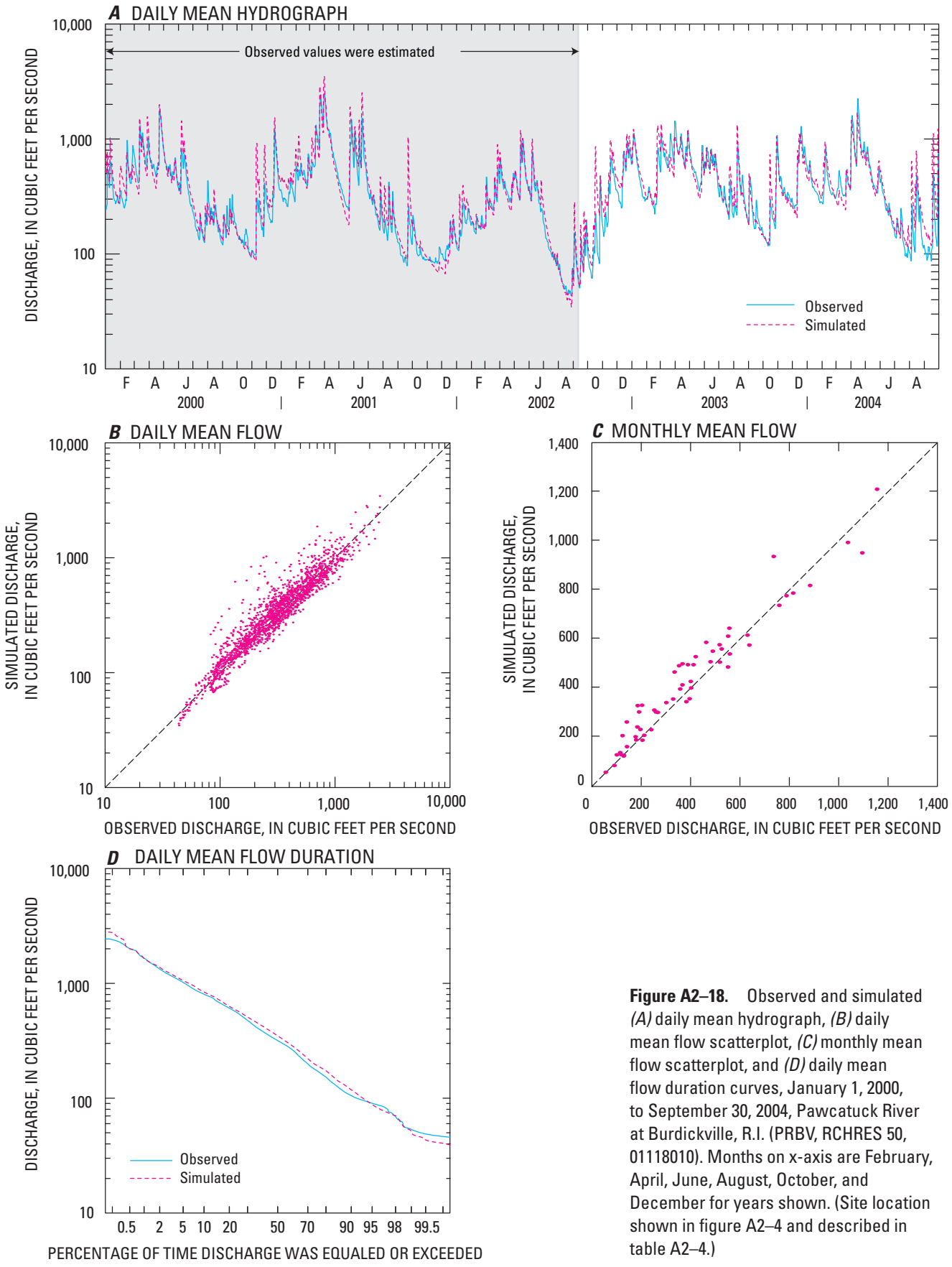

Figure A2–18. Observed and simulated *(A)* daily mean hydrograph, *(B)* daily mean flow scatterplot, *(C)* monthly mean flow scatterplot, and *(D)* daily mean flow duration curves, January 1, 2000, to September 30, 2004, Pawcatuck River at Burdickville, R.I. (PRBV, RCHRES 50, 01118010). Months on x-axis are February, April, June, August, October, and December for years shown. (Site location shown in figure A2–4 and described in table A2–4.)

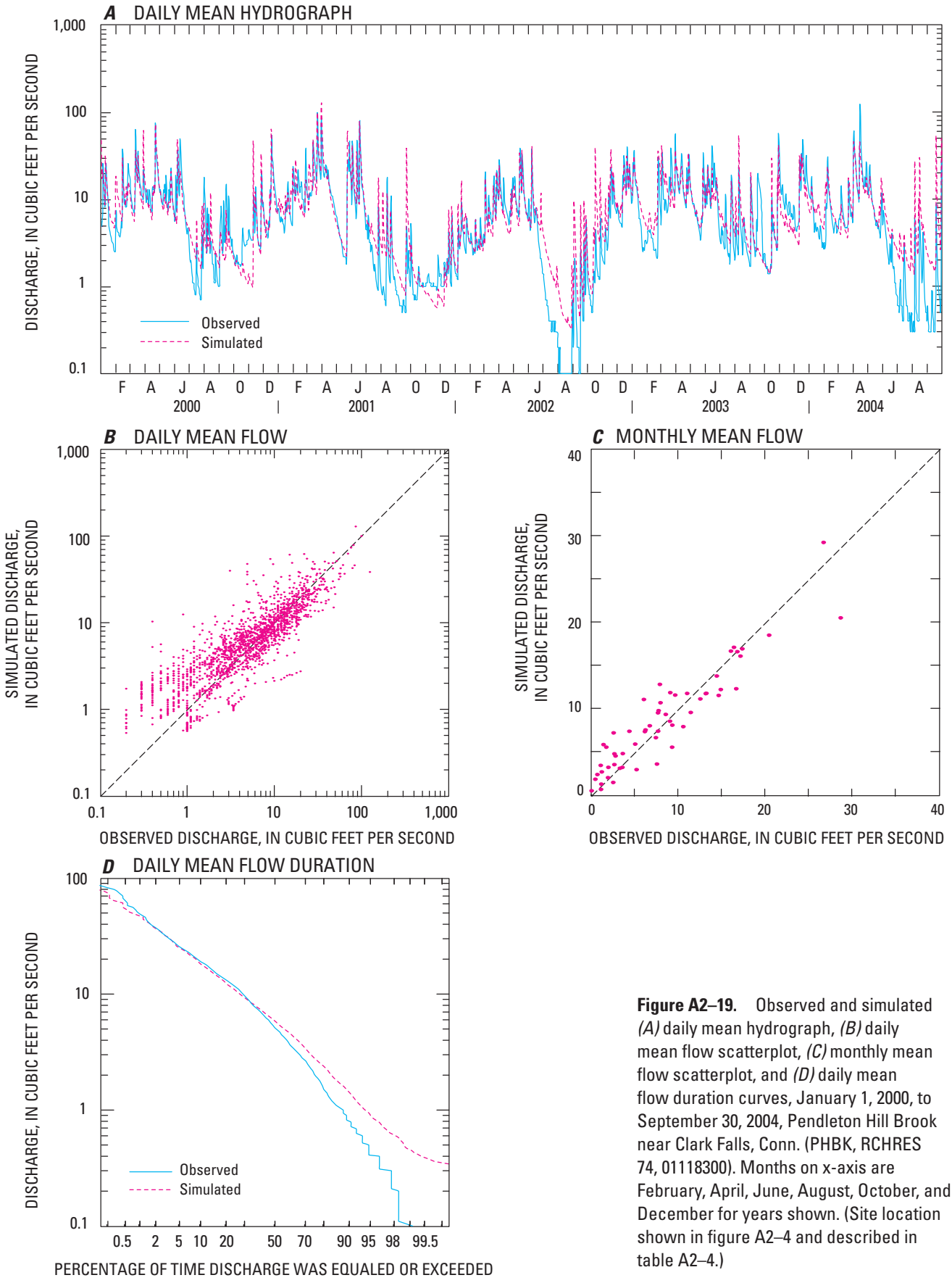

Figure A2–19. Observed and simulated *(A)* daily mean hydrograph, *(B)* daily mean flow scatterplot, *(C)* monthly mean flow scatterplot, and *(D)* daily mean flow duration curves, January 1, 2000, to September 30, 2004, Pendleton Hill Brook near Clark Falls, Conn. (PHBK, RCHRES 74, 01118300). Months on x-axis are February, April, June, August, October, and December for years shown. (Site location shown in figure A2–4 and described in table A2–4.)

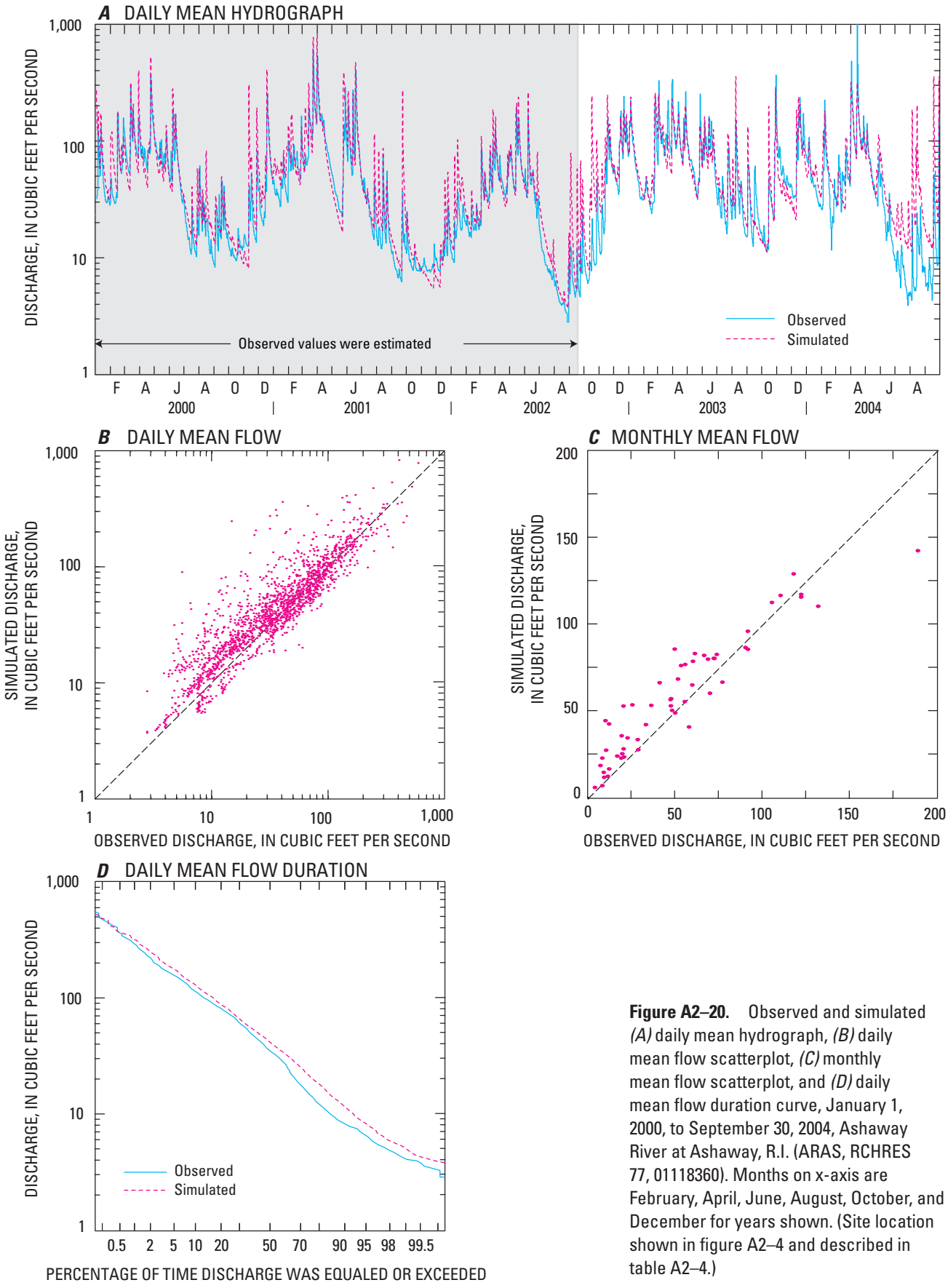

Figure A2–20. Observed and simulated *(A)* daily mean hydrograph, *(B)* daily mean flow scatterplot, *(C)* monthly mean flow scatterplot, and *(D)* daily mean flow duration curve, January 1, 2000, to September 30, 2004, Ashaway River at Ashaway, R.I. (ARAS, RCHRES 77, 01118360). Months on x-axis are February, April, June, August, October, and December for years shown. (Site location shown in figure A2–4 and described in table A2–4.)

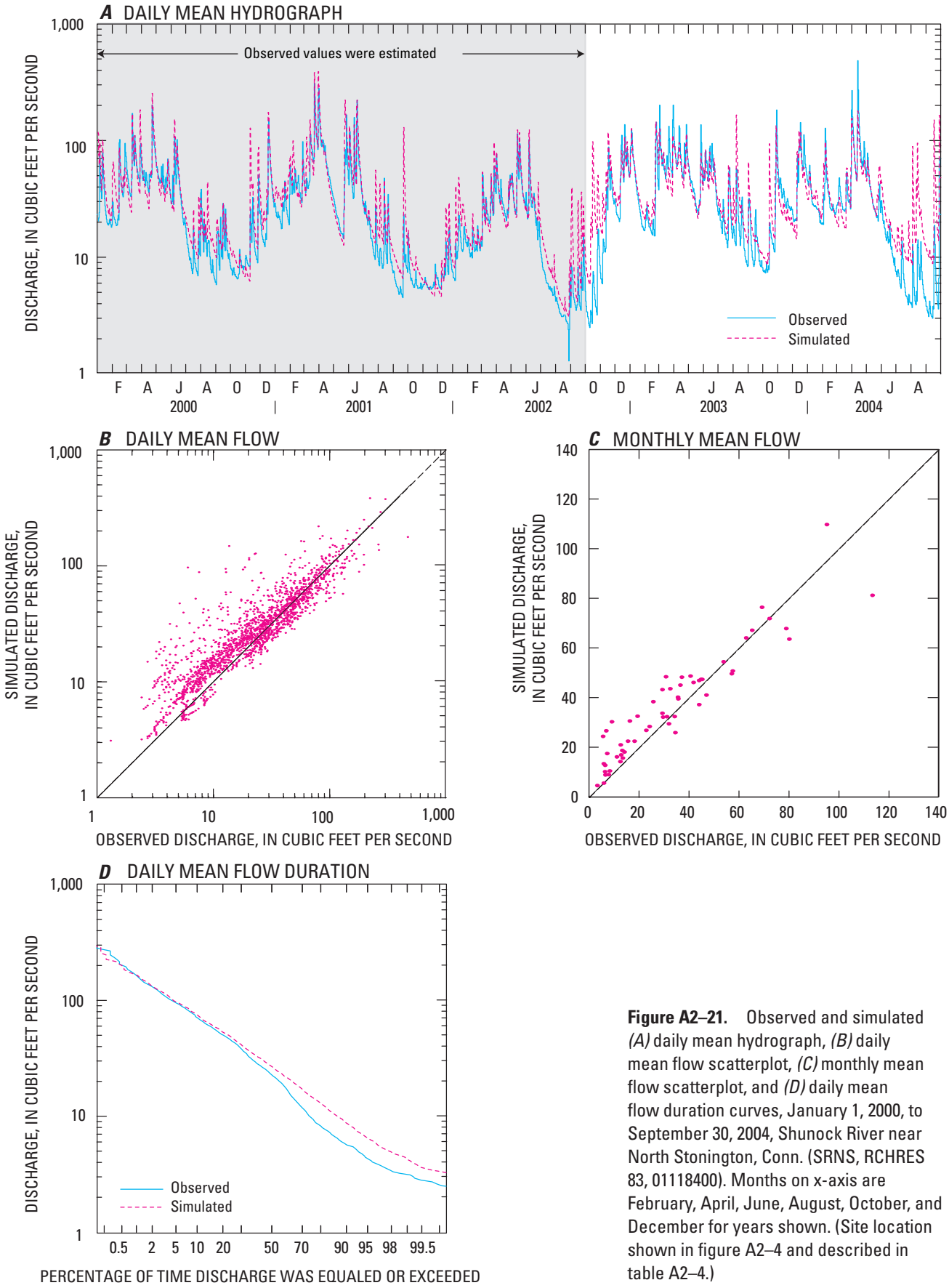

Figure A2–21. Observed and simulated *(A)* daily mean hydrograph, *(B)* daily mean flow scatterplot, *(C)* monthly mean flow scatterplot, and *(D)* daily mean flow duration curves, January 1, 2000, to September 30, 2004, Shunock River near North Stonington, Conn. (SRNS, RCHRES 83, 01118400). Months on x-axis are February, April, June, August, October, and December for years shown. (Site location shown in figure A2–4 and described in table A2–4.)

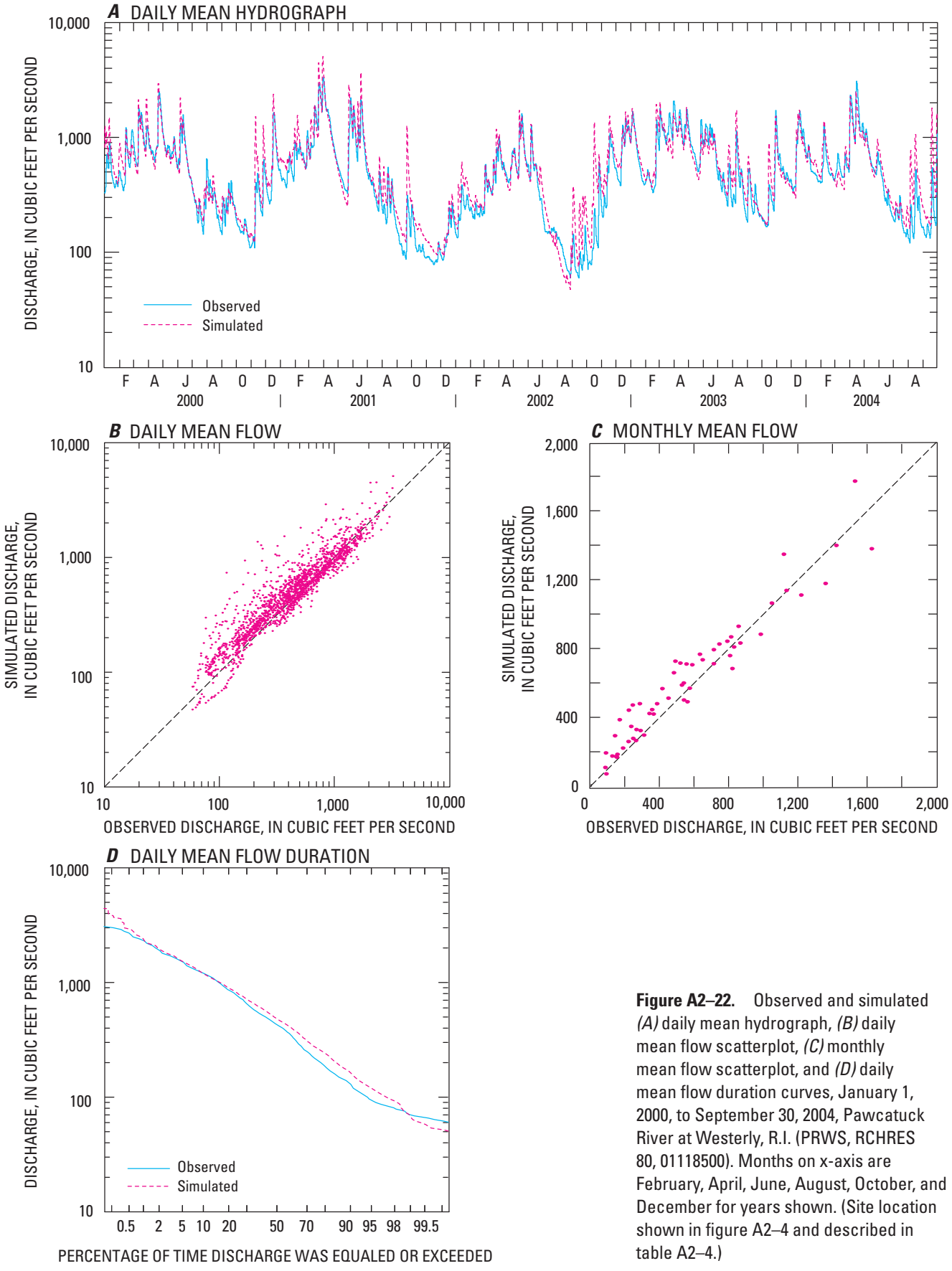

Figure A2–22. Observed and simulated *(A)* daily mean hydrograph, *(B)* daily mean flow scatterplot, *(C)* monthly mean flow scatterplot, and *(D)* daily mean flow duration curves, January 1, 2000, to September 30, 2004, Pawcatuck River at Westerly, R.I. (PRWS, RCHRES 80, 01118500). Months on x-axis are February, April, June, August, October, and December for years shown. (Site location shown in figure A2–4 and described in table A2–4.)

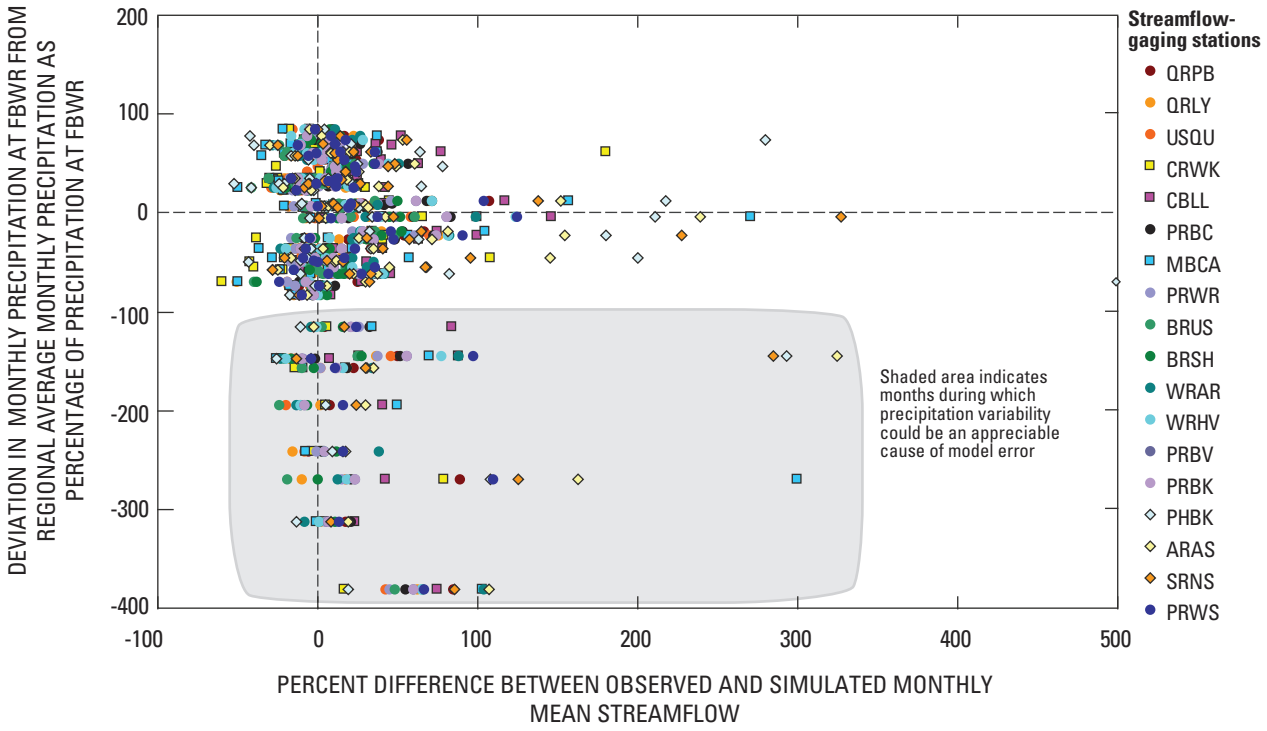

Figure A2–23. Relation of monthly precipitation variability measured as the percent difference between the climate station used for the model calibration (FBWR) and the average of 5 climatic stations in or near the basin to the percent difference between observed and simulated monthly mean streamflow at 17 continuous-record streamflow-gaging stations in the Pawcatuck River Basin, southwestern Rhode Island and southeastern Connecticut, January 2000 through September 2004 (Surface-water site locations shown in figure A2–4 and described in table A2–4). Climatological sites shown in figure 1–1 and described in table 1–1.)

Tributary Streams

Thirty-four partial-record stations established in tributary streams for the purpose of the study were also used to evaluate the model performance. Continuous flow records were estimated for these stations as previously described. The partial-record stations were not used directly in the calibration of the model, but they did provide an independent confirmation of the model performance.

Simulated and observed daily mean flows for the 34 partial-record streamflow-gaging stations have an average R^2 of 0.77 (ranged between 0.53 and 0.84) and an average MFE of 0.67 (ranged between -2.36 and 0.82). Simulated and observed monthly mean flows at the partial-record stations have an average R^2 of 0.91 (ranged between 0.80 and 0.94) and an average MFE of 0.79 (ranged between -1.12 and 0.91). These and other calibration statistics for partial-record streamflow-gaging stations are summarized in tables A2–8 and A2–9.

In general, the model-fit statistics computed for the partial-record stations are comparable to the statistics computed for the continuous-record stations with the exception of some low MFE values. The MFE is more sensitive to differences between the observed and simulated flows; thus, the greater the uncertainty in the estimated discharges at the partial-record station, the greater the likelihood that the MFE value is affected. Five partial-record stations—Queens Fort Brook (QUFB-p; RCHRES 8), Rake Factory Brook (RFBK-p; RCHRES 16), Chickasheen Brook (CBLL-p; RCHRES 35), upper Wood River (WREH-p; RCHRES 51), and Assekonk Brook (ABNS-p; RCHRES 82)—account for the largest source of error in the overall MFE. If these five sites are discarded from the overall fit statistics, the MFE is better than the MFE value obtained for the continuous-record streamflow-gaging stations.

The upper Queens Fort Brook subbasin (QUFB-p; RCHRES 8), has the poorest MFE of any partial-record station. The poor t MFE at this station is attributed to the

Table A2–8. Summary of model-fit statistics for daily mean discharge, January 2000 through September 2004, simulated by the Hydrologic Simulation Program-FORTRAN (HSPF) and estimated for 34 partial-record streamflow-gaging stations, Pawcatuck River Basin, southwestern Rhode Island and southeastern Connecticut.

[Site locations shown in figure A2–4; see table A2–4 for reach names; RCHRES, model reach; IDLOCN, attribute name for reaches and gages; No., number; ft^3/s, cubic feet per second; RMS, root mean square]

RCHRES		Gage IDLOCN	Mean discharge (ft^3/s)		Correlation coefficient	Coefficient of determination	Mean error (ft^3/s)	Percent mean error	RMS error (ft^3/s)	Model fit efficiency
No.	IDLOCN		Observed	Simulated						
1	QUEN1	QECC-p	5.14	5.80	0.89	0.79	-0.65	-12.7	2.89	0.77
5	FISH2	FBEX-p	14.9	16.9	0.92	0.84	-2.06	-13.8	6.18	0.82
8	QUFB2	QUFB-p	2.18	2.71	0.78	0.61	-0.53	-24.2	4.66	-2.36
11	TRIB1	QRTR-p	1.28	2.00	0.90	0.81	-0.73	-56.9	1.04	0.62
14	LOCK1	QRDR-p	8.30	9.56	0.91	0.83	-1.26	-15.2	4.39	0.77
16	RAKE1	RFBK-p	0.23	0.64	0.79	0.62	-0.41	-178	0.60	0.08
17	SHER1	SBGR-p	2.05	2.31	0.86	0.74	-0.26	-12.6	1.31	0.72
18	GLEN1	GRGR-p	4.30	5.96	0.91	0.83	-1.66	-38.7	3.23	0.70
31	CHIP1	CRWK-p	12.8	14.6	0.89	0.80	-1.74	-13.5	5.92	0.67
35	CHIC1	CBLL-p	7.30	6.97	0.88	0.78	0.33	4.51	5.02	0.18
41	BEAV1	BRWR-p	13.5	11.5	0.91	0.82	2.09	15.4	5.21	0.75
44	PASQ1	PBWY-p	8.98	12.71	0.88	0.77	-3.74	-41.6	6.03	0.54
45	TANE1	TBCA-p	2.98	3.50	0.84	0.70	-0.52	-17.3	2.04	0.67
49	CEDA1	CSBK-p	8.21	10.29	0.86	0.74	-2.08	-25.4	5.51	0.67
51	WOOD1	WREH-p	26.8	24.1	0.84	0.70	2.65	9.89	22.3	0.11
52	KELL1	KBEH-p	9.67	9.35	0.89	0.79	0.32	3.31	4.20	0.67
54	FLAT1	FRAR-p	14.4	17.5	0.88	0.77	-3.08	-21.4	9.27	0.69
55	BREA1	BBAR-p	12.2	13.5	0.89	0.80	-1.38	-11.4	6.33	0.77
56	PARR1	PBAR-p	11.5	14.1	0.86	0.74	-2.60	-22.6	7.89	0.68
58	ROAR1	RBAR-p	10.1	10.9	0.89	0.79	-0.83	-8.23	4.59	0.79
60	BRUS1	BBHV-p	7.02	8.04	0.88	0.77	-1.02	-14.6	4.30	0.75
61	MOSC1	MBHV-p	12.7	15.1	0.85	0.73	-2.45	-19.4	9.47	0.68
64	CANO1	CBHV-p	12.0	15.0	0.85	0.72	-3.00	-25.0	9.35	0.67
65	WOOD6	WRAL-p	172	192	0.91	0.82	-19.7	-11.5	74.4	0.81
66	COON1	CHAL-p	3.04	4.35	0.91	0.84	-1.31	-43.2	2.25	0.66
67	PERR1	PHBB-p	4.35	3.64	0.90	0.81	0.71	16.4	1.88	0.77
70	TOMA1	TBBF-p	10.7	12.5	0.91	0.83	-1.80	-16.8	4.83	0.80
73	GREE1	GRLG-p	13.5	15.1	0.73	0.53	-1.67	-12.4	14.7	0.51
75	WYAS1	WBCF-p	22.3	25.1	0.83	0.69	-2.77	-12.4	15.8	0.65
76	GLAD1	GBLG-p	3.20	3.99	0.87	0.75	-0.79	-24.8	2.37	0.72
78	PARM1	PBHK-p	4.06	5.39	0.85	0.73	-1.33	-32.9	3.66	0.54
79	LWPD1	LPPH-p	2.73	3.52	0.87	0.76	-0.79	-28.8	1.51	0.67
81	SHUN1	SRPH-p	13.7	17.3	0.84	0.71	-3.55	-25.9	10.1	0.66
82	ASSE1	ABNS-p	10.1	8.54	0.80	0.64	1.56	15.5	13.9	-1.96

Table A2–9. Summary of model-fit statistics for monthly mean discharge, January 2000 through September 2004, simulated by the Hydrologic Simulation Program-FORTRAN (HSPF) and estimated at 34 partial-record streamflow-gaging stations, Pawcatuck River Basin, southwestern Rhode Island and southeastern Connecticut.

[Site locations shown in figure A2–4; see table A2–4 for reach names; RCHRES, model reach; IDLOCN, attribute name for reaches and gages; No., number; ft^3/s, cubic feet per second; RMS, root mean square]

RCHRES		Gage IDLOCN	Mean discharge (ft^3/s)		Correlation coefficient	Coefficient of determination	Mean error (ft^3/s)	Percent mean error	RMS error (ft^3/s)	Model fit efficiency
No.	IDLOCN		Observed	Simulated						
1	QUEN1	QECC-p	5.15	5.81	0.96	0.92	-0.66	-12.8	1.36	0.89
5	FISH2	FBEX-p	14.9	17.0	0.97	0.94	-2.07	-13.9	3.35	0.90
8	QUFB2	QUFB-p	2.18	2.71	0.90	0.80	-0.53	-24.3	2.10	-1.12
11	TRIB1	QRTR-p	1.28	2.01	0.97	0.93	-0.73	-56.8	0.80	0.57
14	LOCK1	QRDR-p	8.30	9.57	0.96	0.92	-1.27	-15.3	2.58	0.85
16	RAKE1	RFBK-p	0.23	0.64	0.91	0.84	-0.41	-178	0.45	-0.76
17	SHER1	SBGR-p	2.06	2.32	0.95	0.90	-0.26	-12.6	0.55	0.88
18	GLEN1	GRGR-p	4.30	5.97	0.96	0.93	-1.67	-38.8	2.25	0.71
31	CHIP1	CRWK-p	12.9	14.6	0.96	0.92	-1.74	-13.5	3.60	0.75
35	CHIC1	CBLL-p	7.30	6.98	0.96	0.92	0.33	4.48	2.72	0.57
41	BEAV1	BRWR-p	13.56	11.48	0.96	0.92	2.08	15.4	3.24	0.82
44	PASQ1	PBWY-p	8.99	12.73	0.96	0.92	-3.74	-41.6	4.27	0.56
45	TANE1	TBCA-p	2.98	3.50	0.96	0.91	-0.52	-17.4	0.89	0.83
49	CEDA1	CSBK-p	8.22	10.31	0.96	0.92	-2.09	-25.4	2.93	0.76
51	WOOD1	WREH-p	26.8	24.2	0.94	0.89	2.66	9.92	12.0	0.28
52	KELL1	KBEH-p	9.68	9.36	0.95	0.91	0.32	3.32	2.56	0.73
54	FLAT1	FRAR-p	14.4	17.5	0.95	0.91	-3.10	-21.5	4.96	0.80
55	BREA1	BBAR-p	12.2	13.6	0.96	0.91	-1.39	-11.5	3.26	0.88
56	PARR1	PBAR-p	11.6	14.2	0.95	0.91	-2.61	-22.6	3.92	0.84
58	ROAR1	RBAR-p	10.1	10.9	0.96	0.92	-0.84	-8.29	2.26	0.91
60	BRUS1	BBHV-p	7.03	8.05	0.94	0.89	-1.02	-14.6	2.07	0.85
61	MOSC1	MBHV-p	12.7	15.1	0.94	0.89	-2.46	-19.4	4.65	0.80
64	CANO1	CBHV-p	12.0	15.0	0.93	0.86	-3.01	-25.0	4.69	0.75
65	WOOD6	WRAL-p	172	192	0.96	0.93	-19.8	-11.5	36.7	0.90
66	COON1	CHAL-p	3.04	4.36	0.97	0.94	-1.32	-43.3	1.67	0.65
67	PERR1	PHBB-p	3.64	4.36	0.97	0.94	-0.72	-19.7	1.01	0.87
70	TOMA1	TBBF-p	10.7	12.5	0.96	0.93	-1.81	-16.8	2.75	0.88
73	GREE1	GRLG-p	13.5	15.2	0.92	0.84	-1.67	-12.3	4.90	0.77
75	WYAS1	WBCF-p	22.3	25.1	0.94	0.89	-2.78	-12.4	7.14	0.80
76	GLAD1	GBLG-p	3.20	4.00	0.95	0.90	-0.79	-24.8	1.20	0.82
78	PARM1	PBHK-p	4.07	5.40	0.95	0.91	-1.34	-32.9	1.81	0.76
79	LWPD1	LPPH-p	2.73	3.52	0.95	0.91	-0.79	-28.8	0.95	0.72
81	SHUN1	SRPH-p	13.7	17.3	0.94	0.89	-3.56	-25.9	5.27	0.74
82	ASSE1	ABNS-p	10.1	8.6	0.94	0.88	1.56	15.5	6.27	-0.32

complex subsurface-drainage pattern that differs from its surface drainage pattern and likely changes seasonally as the water table responds to recharge. An expanded explanation of the upper Queens Fort Brook drainage issue is given in Zarriello and Bent (2004). During most periods in this study and in a study previously reported by Kliever (1995), the upper Queens Fort Brook rarely flowed. Thus, the water table is likely below the streambed most of the time, and groundwater discharges to the Hunt and Annaquatucket River Basins or flows sublaterally down the Queens Fort Brook valley, or both. Similarly, groundwater in the upper part of the lower Queens Fort Brook subbasin (RCHRES 8) may discharge to the Chipuxet River subbasin (RCHRES 31) if the water-table configuration varies with recharge. As previously described, none of the active-groundwater flow (AGWO) and only 20 percent of the interflow (IFWO) in upper Queens Fort Brook (RCHRES 7) were routed downstream. This routing method provided satisfactory results without the added complexity of seasonally varied loss. Seasonal varied loss, which was simulated through the special action feature in the Usquepaug-Queen HSPF model (Zarriello and Bent, 2004), provided a better model fit at RCHRES 8.

The large errors between simulated and estimated flow at partial-record stations can be attributed to several factors. One is the quality of the estimated flow record. Estimated flows at Rake Factory Brook (RFBK-p) have a large uncertainty because there is no comparable index station for extrapolating the partial-record information for a drainage area of this size (0.26 mi^2). Estimation of the continuous flow at Chickasheen Brook (CBLL-p) is affected by few measurements and poor correlation to index stations; this results in potentially large error in estimated flows. In the upper Wood River (WREH-p) and Assekonk Brook (ABNS-p), partial-record stations that were among those with the lowest MFE, there was no apparent reason the poor model performance. What is known however, is the basin characteristics at these stations are similar to those at Pendleton Hill Brook, which was among the continuous-record stations with the poorest model fit. Thus, the model-variable values may inadequately represent the hydrology in these basins, but it may also be a factor in the estimation of a continuous record at the partial-record stations.

Groundwater Underflow

Another potential source of model error, for both continuous- and partial-record stations, is groundwater underflow that bypasses flow measured or estimated at the streamflow-gaging station. In the HSPF model structure of the Pawcatuck River Basin, with the exception of upper Queens Fort Brook and the upper Meadow Brook subbasins (previously described in the model representation of stream reaches), precipitation that enters active-groundwater eventually discharges to the stream within its subbasin. Thus, if there's a significant downgradient subsurface-flow component in the stream valley, the model could oversimulate flow relative to the measured flow. This discrepancy is typically significant in small basins during low-flow periods when the groundwater underflow is proportionally large relative to the flow in the stream. Groundwater underflow that bypasses a streamflow-gaging station typically discharges to the stream downgradient of the station, and the calculated model error can be attributed to the simulated flow path where groundwater discharges to the stream. The model fit during these conditions may appear poor, but in actuality may better reflect the total flow exiting the basin than that measured at the streamflow-gaging station and should be considered in the evaluation of the model performance.

Sensitivity Analysis

Sensitivity analysis measures the response of the model-simulated discharge to changes in variable values representing the basin. Thus, for the model structure under consideration, the most influential variables are identified, and the range of feasible values is indicated by perturbing model variables. This type of sensitivity analysis is typically an iterative process whereby the value of a given variable is perturbed while all other variable values are held constant, and the response of the model is measured as a change in the model-fit statistics. In the Usquepaug-Queen HSPF model-sensitivity analysis (Zarriello and Bent, 2004) 10 selected PERLND variables were perturbed and the response was measured by four model-fit metrics (relative bias, the relative standard error, the MFE, and the index of agreement). The variable values were uniformly changed (as a percent change from their initial values) across all PERLNDs and included INFILT, LZSN, KVARY, AGWRC, AGWET, MON–LZETP, monthly interception storage (MON–INTERCEP), monthly nominal upper-zone storage (MON–UZSN), monthly interflow (MON–INTERFLW), and monthly interflow-recession rate (MON–IRC).

The results of the Usquepaug-Queen HSPF model-sensitivity analysis are believed to apply to the Pawcatuck HSPF model because the models are similar in structure and range of variable values. The Usquepaug-Queen HSPF model-sensitivity analysis indicated that changes in AGWRC and MON–IRC generally resulted in the largest changes of all measures of the model fit. Decreases in INFILT and MON–INTERFLW also resulted in large changes in the relative standard error and index of agreement for hourly discharge values. Increases in INFILT and MON–INTERFLW indicated a slightly better model fit for hourly discharge, but resulted in a slightly worse model fit for total monthly runoff. Changes in LZSN and MON–LZETP resulted in changes in the model bias relative to most other variables tested, but did not result in corresponding changes in the other fit statistics relative to the other variables tested. For the other variables tested, the model-fit statistics were relatively insensitive to changes in the calibrated (base) values.

This type of analysis provides information about variable values as independent entities, but the approach is not sufficient for identifying variables that interact with each

other (Wagener and others, 2003). The application of PEST in the model calibration facilitated a more complex evaluation of model-variable interactions and their influence on the model performance. The results are more difficult to describe, however, because PEST was used parsimoniously for selected variables as previously described. Thus, the interaction of variables and their influence on model performance can only be compared for variables common to a PEST optimization run. In PEST, sensitivity is measured by the response of the objective function to a change in a model variable.

The composite variable-sensitivity matrix computed by PEST in CASE 5 (fig. A2–24) indicates that infiltration on forested areas overlying till (INFILT–15) was about two or more times more sensitive than the other variables evaluated, including infiltration on forested areas over sand and gravel (INFILT–5), which was one of the least sensitive variables. Although INFILT, in general, was found to be a sensitive variable in the Usquepaug-Queen HSPF model (Zarriello and Bent, 2004), PEST indicates that its importance in the model calibration is largely influenced by the dominance of PERLND 15 in the basin. The importance of INFILT–15 is also underscored by its weak correlation with the other influential variables, most notably monthly lower zone evapotranspiration (LZET) expressed in PEST as a sinusoidal wave function for both forested areas overlying till and overlying sand and gravel, active groundwater evapotranspiration on forested areas overlying till (AGWET–15), the transformed active groundwater recession variable on forested areas overlying till (AGWRCTRANS–15), and the adjustment variable for active groundwater recession on forested areas overlying sand and gravel (KVARY–5).

Eigenvector matrix and eigenvalues calculated by PEST provide a measure of the information content that is obtained during the optimization process. The combination of the paired eigenvector matrix and eigenvalues reflects the interaction between variables (correlation matrix and covariance matrix) not revealed in the composite sensitivity values; the larger the vector value, the less that variable is correlated with other variables. Normalizing the eigenvectors by dividing by the eigenvalues reveals the most influential model variables, which are easily identified by the ranking of values from highest to lowest (fig. A2–25). In other words, the normalized eigenvectors indicate how much of the model performance can be explained by the variable variance. For CASE 5, INFILT–15 was clearly the most influential of the variables tested, followed by AGWET–15 and LZET. Variables AGWRCTRANS–15, KVARY–5, AGWET–5, KVARY–15, and AGWRCTRANS–5 have less influence and have about equal weight in the optimization process. The other variables evaluated (LZSN–15, INFILT–5, UZSN–15, LZSN–5, and UZSN–5) have little influence on the model optimization because they are relatively insensitive, correlated with other variables, or both (fig. A2–25).

The most influential variables in the optimization process are the least correlated with other variables and have the least variance. These variables also exhibit the tightest confidence bands around their optimized value. For example, the 95-percent confidence interval for INFILT–15 was ±0.010 in/hr around an optimized value of 0.117 in/hr. Fortuitously, variables such as LZSN–5 and UZSN–5, whose 95-percent confidence intervals varied widely, were least influential in the optimization process. Thus, although these variables have a high degree of uncertainty, their uncertainty is offset by their lack of influence in the model calibration. The optimized variable values and their confidence limits are provided in table A2–5; PEST was unable to calculate upper and lower confidence limits for CASE 7 because the variables were insensitive, correlated, or both.

The optimization of variables controlling flow from forested areas overlying steep-rocky soil (CASE 6) indicate that infiltration (INFILT–16) was about six times more sensitive than the other variables evaluated (fig. A2–24). The normalized eigenvector matrix (fig. A2–25) also indicates that INFILT–16 dominated the optimization process and the other variables had little effect on the model calibration.

Optimization of the variables that control the amount of surface runoff, upper zone storage, interflow (INTFW), and the recession coefficient for interflow (IRC) for the non-baseflow runoff component (CASE 7) from forested areas overlying sand and gravel, till, or steep-rocky soil produced uncertain results and produce a correlation or covariance matrix. This is because the variables were insensitive, highly correlated, or both and PEST was unable to invert the variable derivatives (Jacobian matrix). Confidence limits could not be determined for the same reasons. Another possible reason why PEST was unable to invert the Jacobian matrix could be that 66 percent of the non-baseflow values were equal to zero; thus, a majority of the matrix values would produce no change in the objective function. The composite sensitivities indicate that IRC from forested areas overlying till (IRC–15) is about three times more sensitive than IRCs for the other two HRUs tested and that INTFW is insensitive (fig. A2–24). INTFW from forested areas overlying sand and gravel (INTFW–5) was insensitive in the model calibration; this is probably because rapid infiltration in this HRU provides little opportunity for precipitation to discharge through surface runoff and interflow.

Optimization of the variables that control baseflow (CASE 8) from forested areas overlying sand and gravel, till, or steep-rocky soil indicate that variable sensitivities (fig. A2–24) and influence on model performance (fig. A2–25) was more evenly divided among the variables examined than in the other optimization runs. This more equitable distribution of variable sensitivity partly results from the insensitivity of the upper-zone soil storage over till (UZSN–15) and was dropped from the optimization analysis.

PEST and its utilities for use in HSPF provide a broad range of possibilities with respect to the types and depth of analysis that can be undertaken. This analysis shows the dominance of infiltration, evaporation loss from active groundwater and lower-zone storage, and the active groundwater-recession variables in the model for forested areas overlying till, the predominant HRU in the basin.

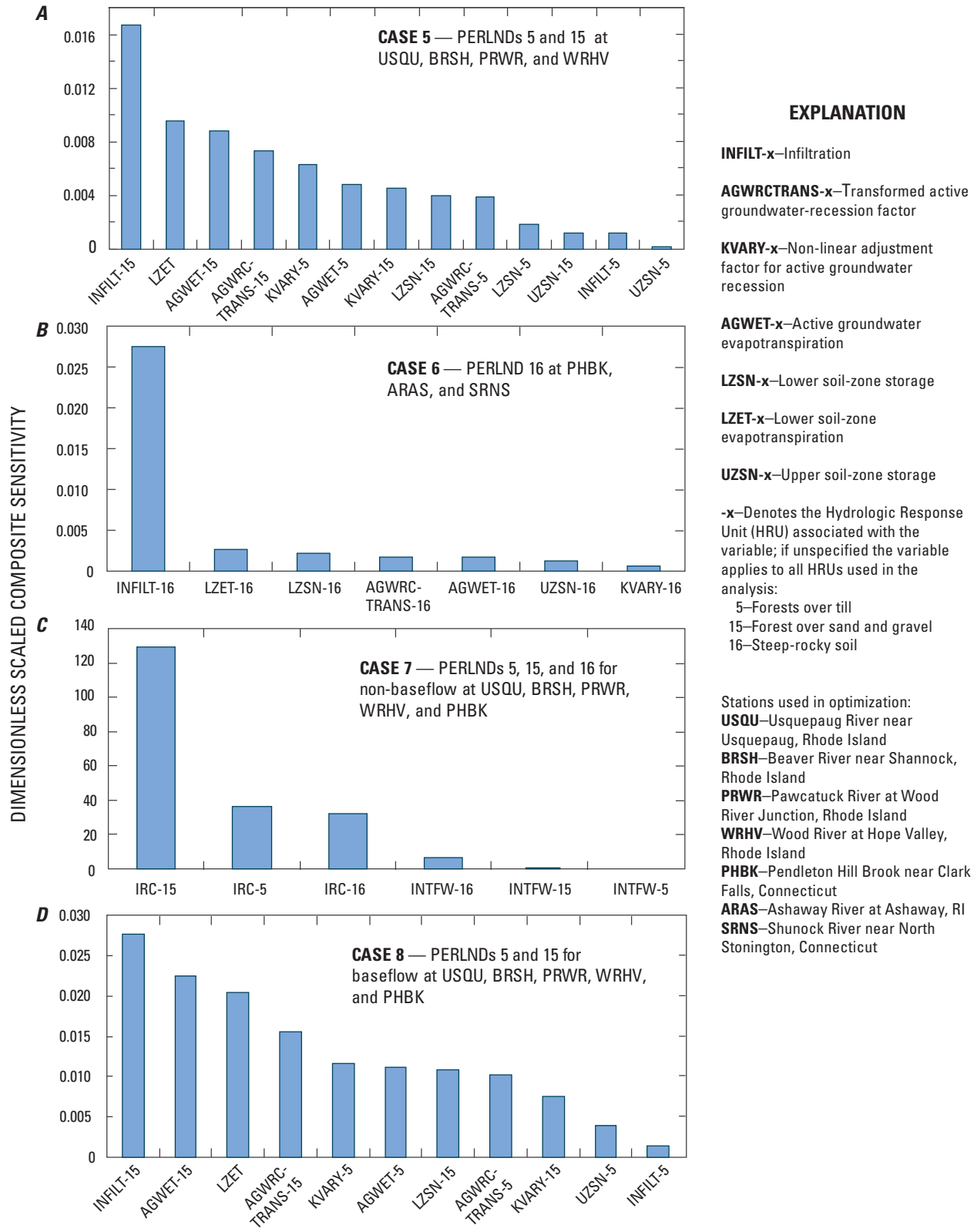

EXPLANATION

INFILT-x–Infiltration

AGWRCTRANS-x–Transformed active groundwater-recession factor

KVARY-x–Non-linear adjustment factor for active groundwater recession

AGWET-x–Active groundwater evapotranspiration

LZSN-x–Lower soil-zone storage

LZET-x–Lower soil-zone evapotranspiration

UZSN-x–Upper soil-zone storage

-x–Denotes the Hydrologic Response Unit (HRU) associated with the variable; if unspecified the variable applies to all HRUs used in the analysis:
5–Forests over till
15–Forest over sand and gravel
16–Steep-rocky soil

Stations used in optimization:
USQU–Usquepaug River near Usquepaug, Rhode Island
BRSH–Beaver River near Shannock, Rhode Island
PRWR–Pawcatuck River at Wood River Junction, Rhode Island
WRHV–Wood River at Hope Valley, Rhode Island
PHBK–Pendleton Hill Brook near Clark Falls, Connecticut
ARAS–Ashaway River at Ashaway, RI
SRNS–Shunock River near North Stonington, Connecticut

Figure A2–24. Composite sensitivity of selected Hydrologic Simulation Program-FORTRAN (HSPF) variables determined by parameter estimation (PEST) for selected model variables and stations, Pawcatuck River Basin, southwestern Rhode Island and southeastern Connecticut. (Site locations shown in figure A2–4 and described in table A2–4.)

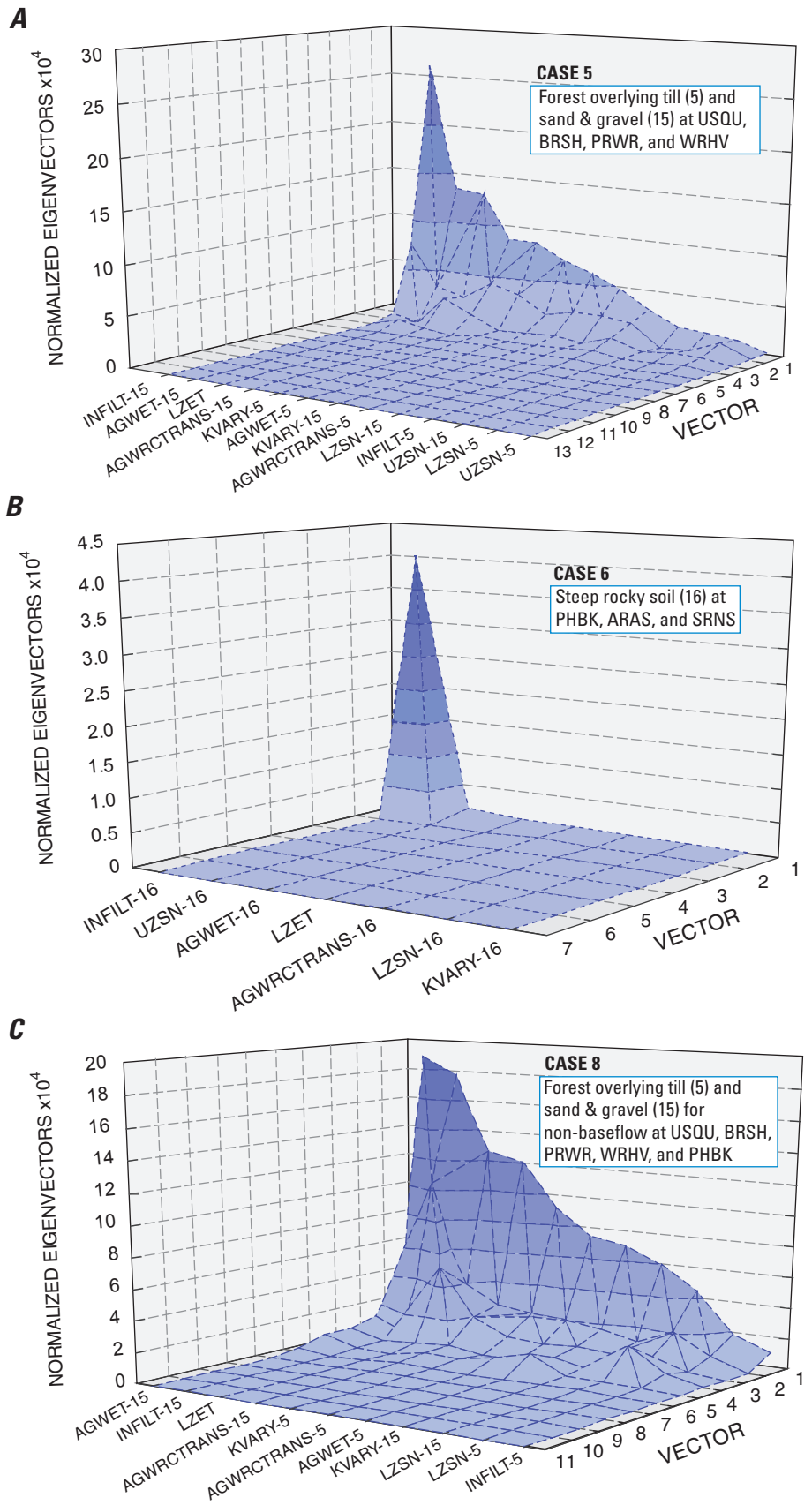

EXPLANATION

INFILT-x—Infiltration

AGWRCTRANS-x—Transformed active groundwater recession factor

KVARY-x—Non-linear adjustment factor for active groundwater recession

AGWET-x—Active groundwater evapotranspiration

LZSN-x—Lower zone storage

LZET-x—Lower zone evapo-transpiration

UZSN-x—Upper soil-zone storage

-x—Denotes the Hydrologic Response Unit (HRU) associated with the variable; if unspecified the variable applies to all HRUs used in the analysis:
5—Forests over till
15—Forest over sand and gravel
16—Steep rocky soil

VECTOR—is the n dimensions in parameter space that the vector is moved in during the optimization process

Stations used in optimization:
USQU—Usquepaug River near Usquepaug, Rhode Island
BRSH—Beaver River near Shannock, Rhode Island
PRWR—Pawcatuck River at Wood River Junction, Rhode Island
WRHV—Wood River at Hope Valley, Rhode Island
PHBK—Pendleton Hill Brook near Clark Falls, Connecticut
ARAS—Ashaway River at Ashaway, Rhode Isalnd
SRNS—Shunock River near North Stonington, Connecticut

Figure A2–25. Relative influence of selected Hydrologic Simulation Program-FORTRAN (HSPF) model variables on minimizing the objective function measured by normalized eigenvectors for three parameter estimation (PEST) runs for *(A)* CASE 5, *(B)* CASE 6, and *(C)* CASE 8 at selected stations in the Pawcatuck River Basin, southwestern Rhode Island and southeastern Connecticut. (Site locations shown in figure A2–4 and described in table A2–4.)

Simulated Hydrologic Budgets and Flow Components

Model-variable values assigned to HRUs control water movement through the hydrologic system, loss to evapotranspiration, and the resulting amount and rate of water discharged to streams. Hydrologic budgets computed for flow components by the model illustrate the hydrologic-response characteristics of different HRUs and the influence of various HRUs in the Pawcatuck River Basin. Hydrologic budgets were examined for the average of the annual budgets from January 1, 2000, through December 31, 2003, a wet month (March 2001), and a dry month (August 2002).

Average annual hydrologic budgets are similar for HRUs with similar surficial materials—sand and gravel, till, steep-rocky soils, and wetlands (fig. A2–26A). Discharge per unit area by component to streams from PERLNDs overlying sand and gravel averaged about 98 percent from active groundwater flow (AGWO), about 2 percent from interflow (IFWO), and a negligible amount from surface runoff (SURO). Discharge to streams from PERLNDs overlying till averaged about 71 percent from AGWO, about 28 percent from IFWO, and about 1 percent from SURO. Discharge components to streams from steep-rocky PERLNDs and wetland PERLNDs were more equally distributed among flow components than discharge from HRUs overlying till or sand and gravel. Discharge to streams per unit area from steep-rocky HRUs was least of any HRU from AGWO (about 22 percent) and greatest from SURO (about 38 percent); discharge from IFWO was about the same as discharge from SURO. Discharge to streams from wetlands was about 43 percent from AGWO, about 39 percent from IFWO, and about 18 percent from SURO. All discharge to streams from IMPLNDs is from SURO.

The simulated annual discharge to streams over the 2000–03 period was 29.3 in., about 50 percent of which was from forested HRUs mostly from AGWO (fig. A2–26B). Discharge to streams from forested HRUs was predominantly from areas overlying till (about 9.9 in.) with about half as much from forested areas overlying sand and gravel (about 4.5 in.). Forested HRUs account for about 59 percent (11.2 in.) of the total annual average evapotranspiration losses from the basin (19.0 in.). Wetlands HRUs account for about 16 percent (3.0 in.) of the total annual average evapotranspiration losses from the basin.

Discharge to streams per unit area during a wet month (March 2001) (fig. A2–27A) was generally proportional to the annual average flow component discharge during the calibration period (fig. A2–26A). Discharge to streams from PERLNDs overlying sand and gravel averaged about 89 percent from AGWO, about 11 percent from IFWO, and a negligible amount from SURO. Discharge to streams from PERLNDs overlying till averaged about 46 percent from AGWO, 50 percent from IFWO, and less than 4 percent from SURO. Discharge to streams from steep-rocky HRUs averaged about 13 percent from AGWO, 27 percent from IFWO, and less than 60 percent from SURO. Discharge to streams from wetland PERLNDs (forested and nonforested) was about evenly distributed between AGWO, IFWO, and SURO (29, 36, and 35 percent, respectively). All discharge to streams from IMPLNDs is from SURO.

During March 2001, the water supply (12.7 in.), mostly from precipitation, was mainly divided between discharge to streams (7.5 in.) and inflow to storage (about 4.9 in.), most of which entered into active groundwater storage; a small amount of the moisture supply was lost to evapotranspiration (about 0.4 in.). About 38 percent of water discharged to streams during March 2001 was from forest PERLNDs overlying till (fig. A2–27B); this PERLND contributed about an equal amount of discharge from AGWO and IFWO. Forests overlying sand and gravel contributed only about 8 percent of discharge to streams because much of the available moisture went into active groundwater storage during this month.

Discharge to streams per unit area during a dry month (August 2002) (fig. A2–28A) was markedly different from the average annual and wet-month water budgets (figs. A2–26A and A2–27A, respectively). Nearly all the discharge to streams was from AGWO during this month and mostly from PERLNDs overlying sand and gravel. Evapotranspiration losses from storage typically exceeded discharge to streams in most HRUs, especially in forested HRUs. Forested PERLNDs have greater losses to evapotranspiration per unit area relative to other PERLNDs because these areas are simulated as having larger losses from lower-zone storage (LZET) and active-groundwater (AGWET) by deep-rooted vegetation. Water lost to evapotranspiration from forested PERLNDs were the dominant part of the basin water budget during August 2002 (fig. A2–28B).

Contrasts in the distribution and magnitude of the simulated outflow components to streams and losses to evapotranspiration for the annual average, a wet month, and a dry month are apparent when summarized for the entire basin (fig. A2–29). For the annual average water budget, about 59 percent (29.3 in.) of the moisture supply (mostly precipitation) to the basin (about 49.5 in.) was discharged to streams and about 38 percent (19.0 in.) was lost to evapotranspiration (fig. A2–29A). The remaining 1.2 in. went into storage; hence, the discharge to streams and evapotranspiration is slightly lower than precipitation.

The average annual discharge to streams (fig. A2–29A) was composed of about 9 percent (2.8 in.) SURO and about 91 percent (27.1 in.) subsurface discharge as IFWO (6.2 in.) and AGWO (20.9 in.). During March 2001, the moisture supply that did not go into storage was mostly discharged to streams and a small amount was lost to evapotranspiration (fig. A2–29B). Discharge to streams during March 2001 was composed of about 20 percent SURO (1.5 in.), 34 percent IFWO (2.6 in.), and 46 percent AGWO (3.5 in.). During August 2002, water loss to evapotranspiration was about 6 times greater than the discharge to streams (fig. A2–29C) and nearly twice the moisture supply to the basin. Nearly all the discharge to streams during this period was from AGWO.

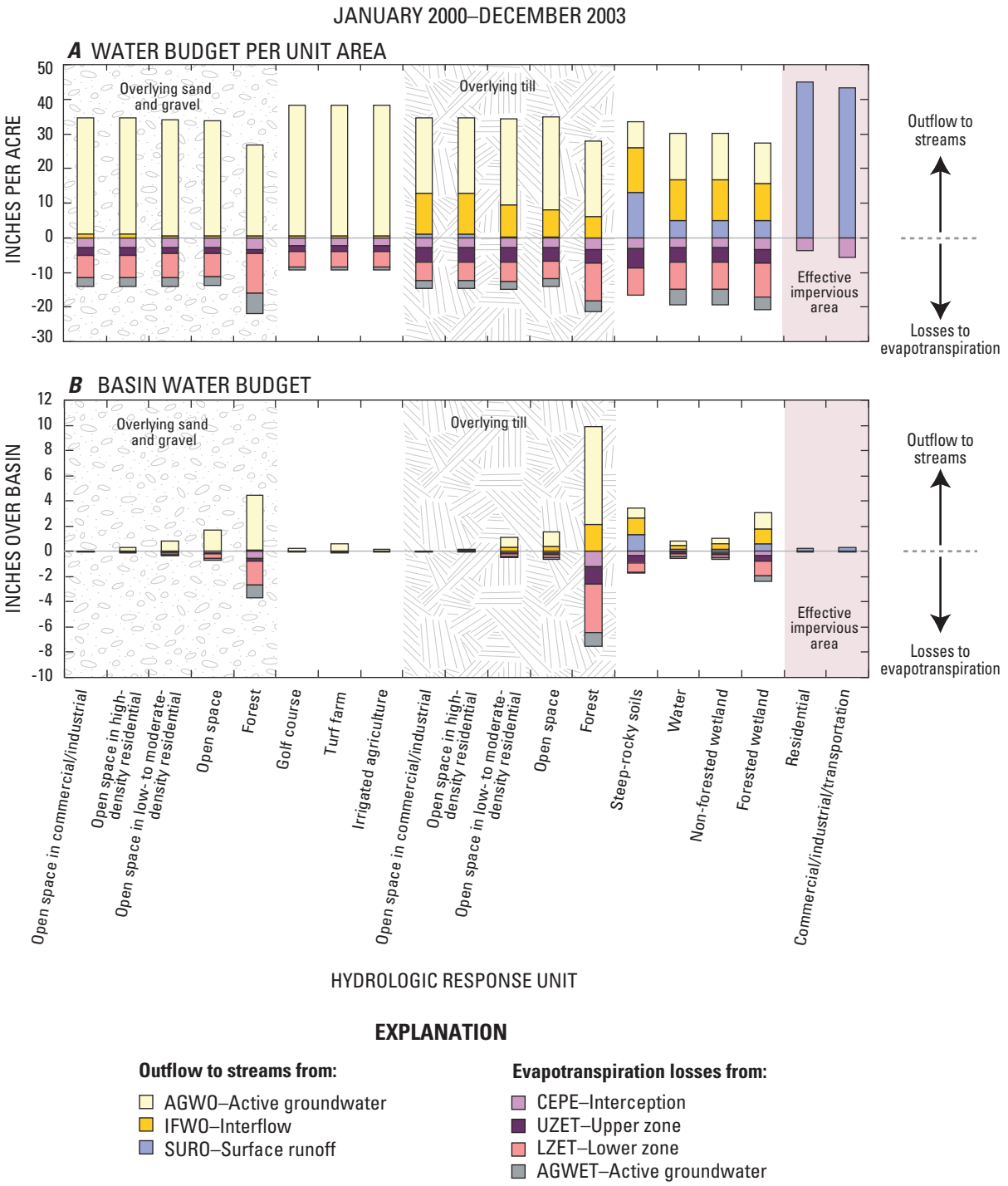

Figure A2–26. Average annual water budget for January 2000 through December 2003 by component in *(A)* inches per acre and *(B)* inches over the entire basin from each hydrologic response unit (HRU) simulated with the Hydrologic Simulation Program-FORTRAN (HSPF) of the Pawcatuck River Basin, southwestern Rhode Island and southeastern Connecticut.

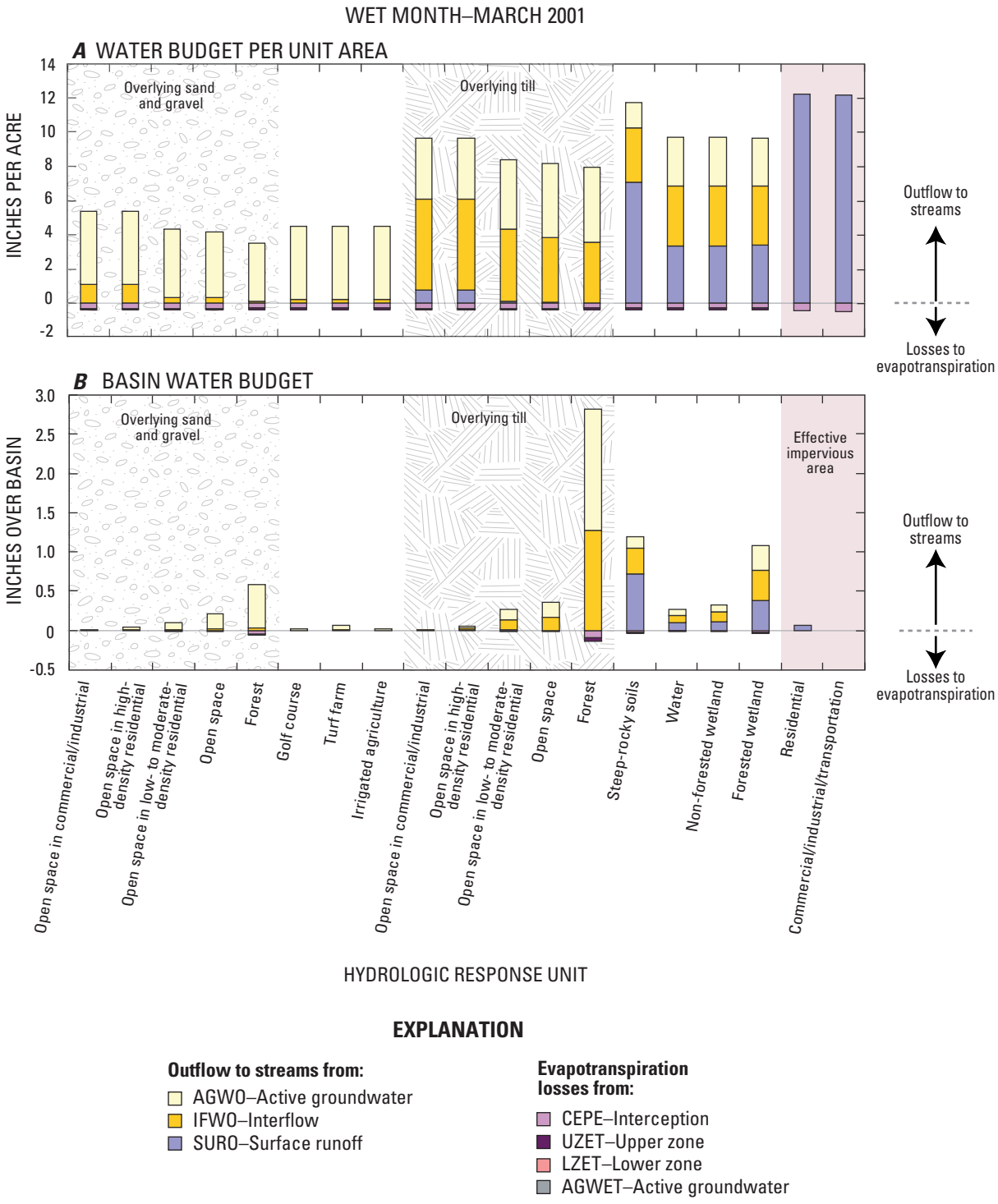

Figure A2–27. Water budget for a wet month, March 2001, by component in *(A)* inches per acre and *(B)* inches over the entire basin from each hydrologic response unit (HRU) simulated with the Hydrologic Simulation Program-FORTRAN (HSPF) of the Pawcatuck River Basin, southwestern Rhode Island and southeastern Connecticut.

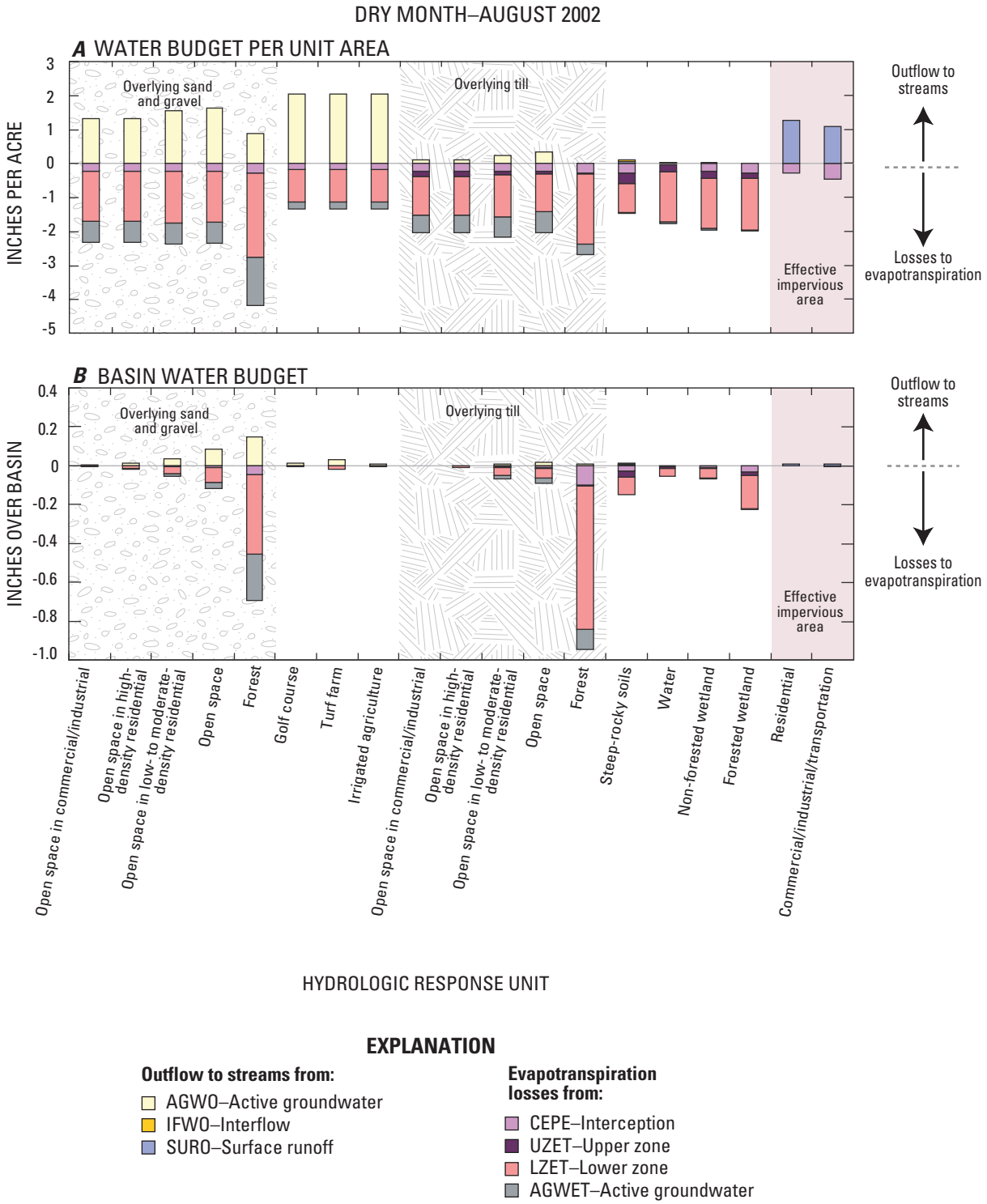

Figure A2–28. Water budget for a dry month, August 2002, by component in *(A)* inches per acre and *(B)* inches over the entire basin from each hydrologic response unit (HRU) simulated with the Hydrologic Simulation Program-FORTRAN (HSPF), Pawcatuck River Basin, southwestern Rhode Island and southeastern Connecticut.

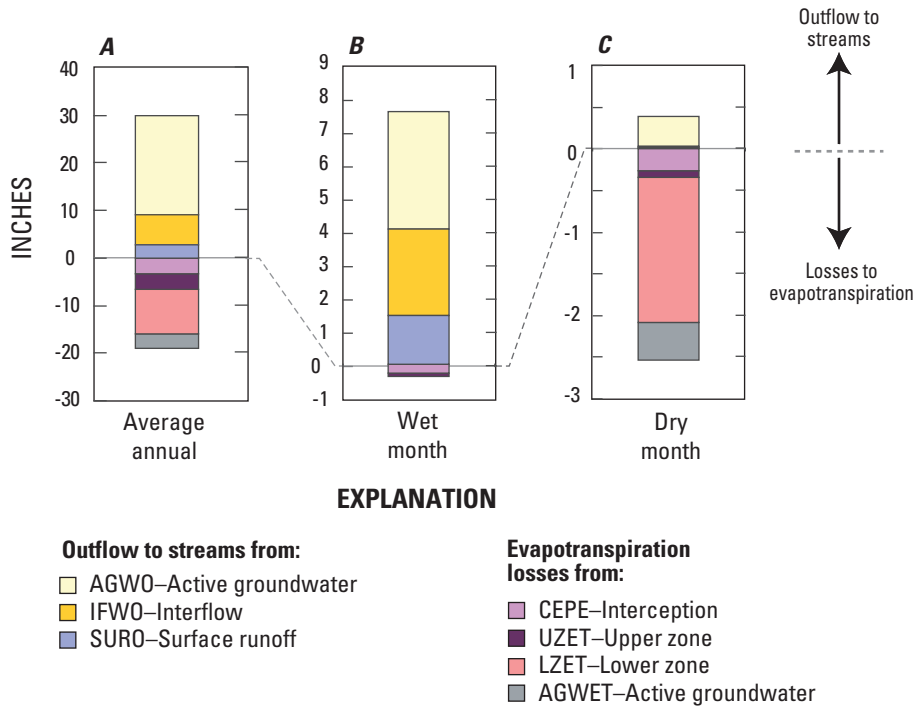

Figure A2–29. Summary of water budgets in inches over the entire basin for *(A)* average annual 2000–03, *(B)* wet month (March 2001), and *(C)* dry month (August 2002) by component simulated with the Hydrologic Simulation Program-FORTRAN (HSPF) of the Pawcatuck River Basin, southwestern Rhode Island and southeastern Connecticut.

Model Uncertainty and Limitations

Numerical simulation models are, at best, approximations of hydrologic systems because of the necessity to simplify the complex processes and physical characteristics of a basin. Despite these limitations, models can be useful tools to evaluate the hydrologic responses of a basin, provided that the model structure and variable values adequately reflect the hydrologic responses of the system to the stresses evaluated. Model uncertainty is associated with input data and the possibility of alternative model structures and variable values that can produce equally acceptable results. The adequacy of the available data to distinguish between alternative models (model structures and variable values), and the realization that alternative structures and variable values can only be rejected as acceptable models is a condition that has been described as equifinality (Beven, 1993; Beven and Binley, 1992).

The HSPF model of the Pawcatuck River Basin was well calibrated to flow records representing a wide range of conditions at 17 continuous-record stations and 34 partial-record stations distributed throughout the basin to a period that spanned about four and half years. The calibration of key model variables and the use of the PEST program to evaluate uncertainties in the variables values provided confidence in the results as being representative of the hydrology of the basin. Yet, despite robust calibration, there are several factors to consider in the use of the model and the interpretation of model results.

Extrapolation of a point measurement to define spatially varied precipitation and potential evapotranspiration over the basin adds uncertainty to the identification of the best-fit variable values. For example, total monthly precipitation can vary widely as indicated by the deviation of total monthly precipitation at the FBWR station (climate data used for the model calibration) from the total average monthly precipitation at the five climate stations in and around the Pawcatuck River Basin (fig. 2–23). Total monthly precipitation at FBWR differed from the combined average precipitation in the region by as much as 400 percent; these differences can be more pronounced during storms periods. Differences in precipitation over the basin, which are not incorporated into the model, result in differences between simulated and observed flows. Although spatially varied climate data can be represented in the model, this modification was not considered necessary because the Pawcatuck River Basin does not have distinctly different climatic regions that affect the simulation of withdrawals or land use change.

Systematic differences between data from stations at FBWR and PROVID could bias simulated flows, however. Data from the PROVID station, which is about 15 mi northeast of the basin, was used to simulate the response of the basin to long-term climatic conditions of the region. From December 1, 1999, through December 30, 2004, total precipitation was 11 percent lower and total potential evapotranspiration was 8 percent greater at the PROVID than at the FBWR station. Total monthly precipitation was less about one-third

of the time, and total monthly potential evapotranspiration was greater about 16 percent of the time at FBWR than at PROVID. Although the differences in total monthly precipitation and evapotranspiration varied between these two stations, the differences were more consistent during the winter months than at other times of year. These differences illustrate the inherent uncertainties of applying a point measurement to represent spatially varied data, regional differences in climate, systematic measurement bias, or a combination of these factors. Although measures were taken to adjust the PROVID data to better match the FBWR data, the differences in the data collected at these two stations underscore that simulations made with the PROVID data may not reproduce the observed day-to-day streamflow in the basin.

Water-use information is another area of data uncertainty. Known major water withdrawals were subtracted directly from simulated streamflow. Once withdrawals were accounted for, the model variable values were adjusted to calibrate the basin's response to precipitation and evapotranspiration. Thus, variable values could have been skewed during the calibration process to compensate for inaccuracies or unknown water withdrawals. Withdrawals for irrigation can vary widely because they depend on climate, plant type and root depth, soil characteristics, and management practices. Although irrigation was measured to the extent allowed, withdrawals for several known irrigation uses could only be estimated. In addition, long-term irrigation was estimated from a logistic-regression equation developed from irrigation patterns observed during 2000–04. These irrigation patterns and rates may not be representative of past or future irrigation withdrawals, however.

The model calibration reflects the combined effects of various HRUs (PERLNDs and IMPLNDs) and RCHRESs. Hydrologic judgment was used to represent the responses of different PERLNDs and IMPLNDs. Although a good fit was obtained between simulated and observed flows over a wide range of conditions, information was not available to explicitly calibrate individual HRUs. Thus, simulation results from ungaged areas or from scenarios that change one type of HRU to another (such as buildout simulations) have a high degree of uncertainty and, therefore, should be viewed as evidence of a relative change instead of an absolute change. Stage, storage, and discharge characteristics of RCHRESs (including wetlands) were determined from measured channel geometry to the extent possible, but many factors, such as channel roughness and changes in channel geometry along a river reach, could not be measured. The stage, storage, and, discharge characteristics of a reach affect the simulated flow and the stream stage.

The Pawcatuck River Basin HSPF model was conceptualized and calibrated to evaluate the effects of withdrawals on streamflow. Many water-resource-management questions can be evaluated by model simulations, but the model may not be appropriate for some analyses. Thus, consideration should be given to the model uncertainties and limitations to ensure that the simulation results do not lead to inaccurate conclusions.

References Cited

Allen, W.B., Hahn, G.W., and Brackley, R.A., 1966, Availability of groundwater, upper Pawcatuck River Basin, Rhode Island: U.S. Geological Survey Water-Supply Paper 1821, 66 p., 3 pls.

Arcement, G.J., Jr., and Schneider, V.R., 1989, Guide for selecting Manning's roughness coefficients for natural channels and flood plains: U.S. Geological Survey Water-Supply Paper 2339, 38 p.

Barlow, P.M., and Dickerman, D.C., 2001, Numerical-simulation and conjunctive-management models of the Hunt-Annaquatucket-Pettaquamscutt stream-aquifer system, Rhode Island: U.S. Geological Survey Professional Paper 1636, 88 p.

Beven, K.J., 1993, Prophecy, reality, and uncertainty in distributed hydrologic modeling: Advances in Water Resources, v. 6, p. 253–254.

Beven, K.J., and Binley, A.M., 1992, The future of distributed models—Model calibration and predictive uncertainty: Hydrological Processes, v. 6, p. 279–298.

Bicknell, B.R., Imhoff, J.C., Kittle, J.L., Jr., Jobes, T.H., and Donigian, A.S., Jr., 2000, Hydrological Simulation Program-Fortran user's manual for release 12: Mountain View, Calif., AQUA TERRA Consultants, variously paged.

Coon, W.F., 1998, Estimation of roughness coefficients for natural stream channels with vegetated banks: U.S. Geological Survey Water-Supply Paper 2441, 133 p.

Dickerman, D.C., Kliever, J.D., and Stone, J.R., 1997, Hydrogeology, water quality, and simulation of ground-water-development alternatives in the Usquepaug-Queen ground-water reservoir, southern Rhode Island: U.S. Geological Survey Water-Resources Investigations Report 97–4126, 48 p.

Doherty, John, 2003, PEST surface water utilities: Watermark Numerical Computing, University of Idaho, unpublished report, variously paged.

Doherty, John, 2004, PEST—Model-independent parameter estimation, 5th ed.: Watermark Numerical Computing, unpublished report, variously paged.

Donigian, A.S., Imhoff, J.C., Bricknell, B.R., and Kittle, J.L., Jr., 1984, Application guide for Hydrologic Simulation Program-Fortran (HSPF): Athens, Ga., U.S. Environmental Protection Agency-600/3-84-065, Environmental Research Laboratory, 177 p.

Duncker, J.J., and Melching C.S., 1998, Regional rainfall-runoff relations for simulations of streamflow for watersheds in DuPage County, Illinois: U.S. Geological Survey Water-Resources Investigations Report 98–4035, 80 p.

Flynn, K.M., Hummel, P.R., Lumb, A.M., and Kittle, J.L. Jr., 1995, User's manual for ANNIE, version 2, a computer program for interactive hydrologic data management: U.S. Geological Survey Water-Resources Investigations Report 95–4085, 211 p.

Kittle, J.L., Jr., Lumb, A.M., Hummel, P.R., Duda, P.A., and Gray, M.H., 1998, A tool for the analysis of model simulation scenarios for watersheds (GenScn): U.S. Geological Survey Water-Resources Investigations Report 98–4134, 152 p.

Kliever, J.D., 1995, Hydrologic data for the Usquepaug-Queen River Basin, Rhode Island: U.S. Geological Survey Open-File Report 95–305, 68 p.

Legates, D.R., and McCabe, G.J., Jr., 1999, Evaluating the use of "goodness-of-fit" measures in hydrologic and hydroclimatic model validation: Water Resources Research, v. 35, no. 1, p. 233–241.

Lott, R.B., and Hunt, R.J., 2001, Estimating evapotranspiration in natural and constructed wetlands: Wetlands, v. 21, no. 4, p. 614–628.

Lumb, A.M., Kittle, J.L., Jr., and Flynn, K.M., 1990, Users manual for ANNIE, a computer program for interactive hydrologic analyses and data management: U.S. Geological Survey Water-Resources Investigations Report 89–4080, 236 p.

Lumb, A.M., McCammon, R.B., and Kittle, J.L., Jr., 1994, User's manual for an expert system (HSPEXP) for calibration of the Hydrological Simulation Program-Fortran: U.S. Geological Survey Water-Resources Investigations Report 94–4168, 102 p.

Regan, R.S., and Schaffranek, R.W., 1985, A computer program for analyzing channel geometry: U.S. Geological Survey Water-Resources Investigations Report 85–4335, 40 p.

Wagener, Thorsten, Wheater, H.S., and Gupta, H.V., 2003, Identification and evaluation of watershed models, *in* Duan, Q., Gupta, H.V., Sorooshian, S., Rousseau, A.N., Turcotte, R., Calibration of Watershed Models, Water Science and Applications: Washington, D.C., American Geophysical Union, p. 29–47.

Zarriello, P.J., and Bent, G.C., 2004, A precipitation-runoff model for the analysis of the effects of water withdrawals and land-use change on streamflow in the Usquepaug–Queen River Basin, Rhode Island: U.S. Geological Survey Scientific Investigations Report 2004–5139, 75 p.

Zarriello, P.J., and Ries, K.G., III, 2000, A precipitation runoff model for the analysis of the effects of water withdrawals on streamflow, Ipswich River Basin, Massachusetts: U.S. Geological Survey Water-Resources Investigations Report 00–4029, 99 p.